

AN ABSTRACT OF THE THESIS OF

Jonathan R. Bristol for the degree of Master of Science in Radiation Health Physics presented on September 13, 2010

Title: Comparison of Eye Plaque Dosimetry Using Deterministic and Monte Carlo Methods

Abstract approved:

Camille J. Lodwick

Eye plaque brachytherapy is an established technique for the treatment of ocular melanoma that allows for the preservation of the affected eye as well as visual function. A common treatment planning system for eye plaque procedures, Plaque Simulator (PS), assists physicists in calculating the radiation dose to the tumor and surrounding eye. The Plaque Simulator software offers a simplistic model of the radiation source-to-eye geometry, along with several case-specific correction factors, that allow for quick estimation of radiation dose without performing a full radiation transport calculation. This research utilizes a deterministic transport code, Attila, to fully model the dosimetry of the Collaborative Ocular Melanoma Study (COMS) eye plaques (12mm, 16mm, and 20mm), fully-loaded with ^{125}I Onco-seed model 6711. A more realistic model of COMS eye plaques, including surrounding bone and an eye-air interface, were simulated in both Attila and MCNPX. Attila results were compared to MCNPX simulations as well as dose predicted from Plaque Simulator. Attila and MCNPX predicted comparable doses at six medically relevant points of interest, with agreement ranging from 1-33% for the 12 mm plaque and within 10% for the 20 mm plaque. However, following normalization to dose at the macula, the percent depth dose of all codes agreed within 2% at the points of interest. Attila calculated the dosimetry for the eye plaque brachytherapy in a fraction of the time required by the Monte Carlo based MCNPX. As a result of this study Attila was proven as an efficient method for modeling complex dosimetry problems without the need of limiting assumptions used by treatment planning software.

©Copyright by Jonathan R. Bristol

September 13, 2010

All Rights Reserved

Comparison of Eye Plaque Dosimetry Using Deterministic
and Monte Carlo Methods

by

Jonathan R. Bristol

A THESIS

submitted to

Oregon State University

in partial fulfillment of
the requirements for the
degree of

Master of Science

Presented September 13, 2010

Commencement June 2011

Master of Science of Jonathan R. Bristol presented on September 13, 2010.

APPROVED:

Major Professor, representing Radiation Health Physics

Head of the Department of Nuclear Engineering and Radiation Health Physics

Dean of the Graduate School

I understand that my thesis will become part of the permanent collection of Oregon State University libraries. My signature below authorizes release of my thesis to any reader upon request.

Jonathan R. Bristol, Author

ACKNOWLEDGEMENTS

The Author Expresses Sincere Appreciation to...

Dr. Camille J. Lodwick for her patience and help in the formation of this thesis

Dr. Todd S. Palmer for providing a wealth of information

Mr. Ian M. Davis for priceless technical support during the use of Attila

In addition, I thank my wife Courtney Bristol for supporting me through the completion of this project.

TABLE OF CONTENTS

	<u>Page</u>
1. Introduction.....	1
2. Literature Review.....	2
2.1. History of Ocular Melanoma Treatments.....	2
2.1.1. Enucleation.....	2
2.1.2. Eye Plaque Brachytherapy.....	3
2.1.3. Collaborative Ocular Melanoma Study.....	3
2.1.3.1. Selection of ¹²⁵ I seeds.....	3
2.1.3.2. Randomized trial of brachytherapy versus enucleation.....	7
2.1.3.3. Quality of life after trial.....	8
2.1.4. AAPM Task Group 43U1 Report.....	8
2.2. Dosimetric Theory used for ¹²⁵ I Seed in Eye Plaque Brachytherapy.....	10
2.2.1. Collaborative Ocular Melanoma Study Manual of Procedures.....	10
2.2.2. Plaque Simulator®.....	10
2.2.3. Effect of eye plaque material on dosimetry.....	10
2.2.3.1. COMS plaque Gold Backing causing Backscatter.....	11
2.2.3.2. COMS silastic seed carrier attenuation of flux.....	11
2.2.3.3. Penumbra effect from seed location and lip of plaque.....	12
2.2.4. Point Source versus Line Source for modeling of ¹²⁵ I seed (model 6711).....	12
2.2.5. Effect of air to eye interface on eye plaque dosimetry.....	13
2.2.6. Inhomogeneity of the eye and surrounding tissue.....	13
3. Project Objectives and Experimental Approach.....	14
3.1. Objectives and Approach.....	14
3.2. Equipment.....	15
3.2.1. MCNPX.....	15
3.2.2. Plaque Simulator.....	16
3.2.3. Attila.....	19
3.3. Dimensions of eye phantom and points of interest.....	19
3.3.1. Plaque and Seeds.....	23
3.3.2. ¹²⁵ I Seed model 6711.....	23
4. Results.....	25
4.1. Formatting Data with Tecplot.....	25
4.2. Calculations for MCNPX and Attila Data.....	25
4.3. 12mm Plaque Normalized Isodose Lines.....	26
4.4. 16mm Plaque Normalized Isodose Lines.....	33
4.5. 20mm Plaque Normalized Isodose Lines.....	39

TABLE OF CONTENTS (continued)

	<u>Page</u>
4.6. 20mm Isodose Line over 100%.....	45
4.7. Plaque’s Central Axis and the Optic Axis Comparison.....	48
4.8. Points of Interest.....	55
4.9. Speed and Ease of Using Attila versus MCNPX and Plaque Simulator.....	57
4.10. Areas for Improvement.....	57
5. Conclusion.....	58
Bibliography.....	59
Appendices.....	62
Appendix A: Dose Values from the plaques Central Axis and the Optic Axis....	62
Appendix B: Points of Interest Dose Values.....	70
Appendix C: MCNPX 12mm Input Deck.....	71
Appendix D: MCNPX 16mm Input Deck.....	86
Appendix E: MCNPX 20mm Input Deck.....	105

LIST OF FIGURES

<u>FIGURE</u>	<u>Page</u>
1. Photon Dose Depth Rate for ^{60}Co , ^{192}Ir , and ^{125}I source ^(adapted from 9)	4
2. Photon Dose Depth Rate for ^{60}Co , ^{192}Ir , and ^{125}I source normalized at 1cm ^(adapted from 9)	5
3. Isodose lines of ^{125}I and ^{60}Co eye plaques demonstrating shielding difference ^(adapted from 9)	6
4. COMS 12mm eye plaque with silastic insert ⁽⁹⁾	6
5. Plaque Simulator's window for tumor definition.....	16
6. Plaque Simulator's menu for plaque setup.....	17
7. Plaque Simulator's menu for patient's eye size.....	17
8. Plaque Simulator's menu for Carrier Attenuation.....	18
9. Plaque Simulator's menu for Shell Collimation.....	18
10. Points of Interest from Thomson's work ^(adapted from 28)	20
11. MCNPX model of Onco-Seed 6711.....	24
12. SolidWork's model of Onco-Seed 6711.....	24
13. X-plane 12mm plaque isodose lines from the Plaque Simulator, 100% at tumor apex	26
14. X-plane 12mm plaque isodose lines from Attila, 100% at tumor apex.....	27
15. X-plane 12mm plaque isodose lines from MCNPX, 100% at tumor apex.....	28
16. Y-plane 12mm plaque isodose lines from the Plaque Simulator, 100% at tumor apex	29
17. Y-plane 12mm plaque isodose lines from Attila, 100% at tumor apex.....	30
18. Y-plane 12mm plaque isodose lines from MCNPX, 100% at tumor apex.....	31
19. X-plane 16mm plaque isodose lines from the Plaque Simulator, 100% at tumor apex	32
20. X-plane 16mm plaque isodose lines from Attila, 100% at tumor apex.....	33
21. X-plane 16mm plaque isodose lines from MCNPX, 100% at tumor apex.....	34

LIST OF FIGURES (continued)

<u>FIGURE</u>	<u>Page</u>
22. Y-plane 16mm plaque isodose lines from the Plaque Simulator, 100% at tumor apex	35
23. Y-plane 16mm plaque isodose lines from Attila, 100% at tumor apex.....	36
24. Y-plane 16mm plaque isodose lines from MCNPX, 100% at tumor apex.....	37
25. X-plane 20mm plaque isodose lines from the Plaque Simulator, 100% at tumor apex	38
26. X-plane 20mm plaque isodose lines from Attila, 100% at tumor apex.....	39
27. X-plane 20mm plaque isodose lines from MCNPX, 100% at tumor apex.....	40
28. Y-plane 20mm plaque isodose lines from the Plaque Simulator, 100% at tumor apex	41
29. Y-plane 20mm plaque isodose lines from Attila, 100% at tumor apex.....	42
30. Y-plane 20mm plaque isodose lines from MCNPX, 100% at tumor apex.....	43
31. +100% Isodose lines of a 20mm plaque from the Plaque Simulator.....	44
32. +100% Isodose lines of a 20mm plaque from Attila.....	45
33. +100% Isodose lines of a 20mm plaque from MCNPX.....	46
34. MCNPX phantom with optic axis and plaque central axis.....	47
35. Plaques central axis dose comparison of the 12mm plaque.....	48
36. Plaques central axis dose comparison of the 16mm plaque.....	48
37. Plaques central axis dose comparison of the 20mm plaque.....	49
38. Optic axis dose comparison of the 12mm plaque.....	50
39. Optic axis dose comparison of the 16mm plaque.....	51
40. Optic axis dose comparison of the 20mm plaque.....	51
41. Optic axis normalized dose comparison of the 12mm plaque.....	52
42. Optic axis normalized dose comparison of the 16mm plaque.....	53
43. Optic axis normalized dose comparison of the 20mm plaque.....	53

LIST OF TABLES

<u>TABLE</u>	<u>Page</u>
1. Dimensions and coordinates of Phantom Eye and Points of Interest ⁽²⁸⁾	21
2. Phantom and COMS Eye Plaque Material Composition ⁽²⁸⁾	22
3. Points of Interest dose difference and percent dose of 12mm plaque.....	54
4. Points of Interest dose difference and percent dose of 16mm plaque.....	55
5. Points of Interest dose difference and percent dose of 20mm plaque.....	55
6. Plaque's central axis dose values for the 12mm plaque.....	61
7. Plaque's central axis dose values for the 16mm plaque.....	62
8. Plaque's central axis dose values for the 20mm plaque.....	63
9. Optic axis dose values for the 12mm plaque.....	64
10. Optic axis dose values for the 16mm plaque.....	65
11. Optic axis dose values for the 20mm plaque.....	66
12. Points of Interest dose values for the 12mm plaque.....	67
13. Points of Interest dose values for the 16mm plaque.....	67
14. Points of Interest dose values for the 20mm plaque.....	68

Introduction

Ocular melanoma is commonly treated with an episcleral plaque brachytherapy. Brachytherapy is a form of radiation therapy that involves placement of sealed radioactive sources in or on a patient's tumor for localized exposure. One of the earliest publications of a medical case involving brachytherapy for the treatment of choroidal sarcoma was in 1929. The patient refused to allow his left eye to be removed as treatment for the choroidal sarcoma because he was blind in the right eye. A radium seed was surgically inserted in the tumor, and later removed. One year following the radium treatment, the choroidal sarcoma had reduced in size and was not visually growing.⁽²⁶⁾ In 1986, the Collaborative Ocular Melanoma Study performed two national clinical trials comparing eye plaque brachytherapy versus enucleation.⁽¹⁰⁾ Following the publication of these trial results, eye plaque brachytherapy became much more widely used for treatment of ocular melanoma. The desired outcome of eye plaque brachytherapy is to eradicate the tumor volume while retaining the affected eye and its vision. However, the optic nerve, lens, retina, eyelids and lashes have dose tolerances below the accepted prescription dose for ocular melanoma, creating the need for carefully planned treatments.⁽²¹⁾ Due to the radiosensitivity of these structures, treatment planning systems for eye plaque brachytherapy need to be accurate and precise. This thesis discusses results of a comparative study of a treatment planning system for eye plaque brachytherapy.

Literature Review

History of Ocular Melanoma Treatments

Enucleation

Enucleation is the surgical removal of the ocular globe from the orbital. It is the common treatment for intraocular malignancy, blind painful eye, and prevention of sympathetic ophthalmia. Prior to recent developments in the understanding and treatment of cancer, enucleation was the primary treatment for intraocular malignancy. The earliest known documentation of modern enucleation was performed by Johannes Lange in 1555. There was no precise account of Lange's operation; however Bartisch, a complementary survivor of Lange's enucleation operation, provided a description of the operation. According to Bartisch, Lange used a hook passed through the globe to provide traction, followed by sharp dissection to sever the globe from the orbit.⁽⁵⁾

The currently accepted method of enucleation is similar. First the eye lids are held back with an instrument, and the Tenon's fascia is opened in all four quadrants. The rectus muscles are secured with suture clamps and transected near their insertion, leaving a 2-3mm stump for a later hold. The oblique muscles are located and transected, along with any residual fibrous attachments on the globe. When the six muscles are transected from the globe, the insertions of the rectus muscles are gripped and pulled by an assistant to meet the resistance of the optic nerve. The optic nerve is clamped and with the use of enucleation scissors it is transected close to the globe. The residual fibrous attachments are dissected with Wescott scissors.⁽²⁰⁾

Eye Plaque Brachytherapy

Although invasive, eye plaque brachytherapy provides an alternative to total removal of the eye. The procedure involves having a gold plaque containing several radioactive seeds sutured directly over the tumorous region. The radiation dose delivered to the tumor is determined by the number and source strength of the radioactive seeds used in the plaque. The total dose also depends on the tumor size, its location, and the length of time that the plaque remains on the treatment area. Eye plaque brachytherapy appears in medical journals as early as 1966 when H. B. Stallard published a comprehensive report on 99 patients treated by a ^{60}Co applicator. The applicator used in Stallard's work looks similar to a current BEBIG ^{106}Ru plaque which has a thin radioactive layer covered by pure silver. In Stallard's study, sixty-nine patients were successes, thirty-eight of these patients suffered poor vision as a side effect of the treatment. ⁽²⁶⁾

Collaborative Ocular Melanoma Study

Selection of ^{125}I seeds

The Collaborative Ocular Melanoma Study (COMS) investigated using ^{125}I radioactive seeds in the ophthalmic plaque. The COMS study considered the following parameters in source selection: distance, time, and shielding. Distance addresses the need for a depth dose of 10,000 rad to the apex of medium sized ocular tumors (2.5-10mm). ⁽⁷⁾ Time addresses the need for a source with a sufficiently long half life for industrial production of source seeds. The ability to shield the radiation emitted by the source allows for the protection of medical staff, and healthy tissue surrounding the cancerous tumor. At the onset of the Collaborative Ocular Melanoma Study, seeds in use for ophthalmic plaque brachytherapy were ^{222}Rn , ^{198}Au , ^{60}Co , ^{192}Ir , ^{182}Ta , ^{125}I , and ^{106}Ru . Of those, ^{106}Ru is the only pure beta emitter of the group. The other radioisotopes are also photon emitters, which affects the radiation interaction mechanisms contributing to dose. ⁽⁹⁾ The alphas and betas emitted by these radioisotopes have very limited range in tissue, so for the most part they can be ignored when choosing the ideal source.

Photons deposit energy in matter by three main interactions (photoelectric absorption, Compton scattering, and pair production). The probabilities of these interactions are influenced

by the energy of the photon and the material through which it is traveling.⁽²⁵⁾ To simplify the dynamics of choosing a source, the Collaborative Ocular Melanoma Study accounted for the fact the human body is 90% water, and defined the eye region as a homogenous material. When a gamma ray passes through a homogenous material, the distance traveled by the gamma ray is a simple function of the gamma ray energy. This can be used to predict the areas of the eye that will receive dose. The Collaborative Ocular Melanoma Study compared dose as a function of distance from 1.0 mCi ^{60}Co , ^{125}I , and ^{192}Ir source seeds (Figure 1). For every disintegration of ^{60}Co , one beta and two high energy gamma rays are emitted. From ^{125}I , an average of 1.5 low energy x-rays are emitted per disintegration.⁽⁹⁾ The difference between the photon energies associated with ^{60}Co and ^{125}I decay is the major contributor to the difference in dose observed in Figure 1. Dose can also be increased by increasing the activity of the source, thus a ^{125}I source with sufficient activity can deposit the same dose as a ^{60}Co source, over the same amount of time. Thus through the use of higher activity, a ^{125}I source can be used to deposit the 10,000 rad prescription dose at the apex of a medium sized tumor.

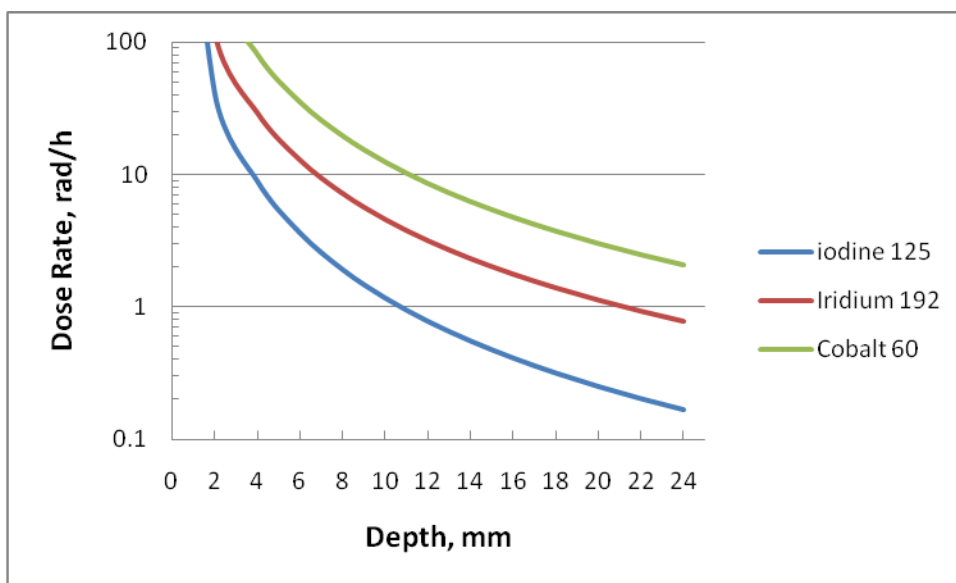


Figure 1: Photon Dose Depth Rate for ^{60}Co , ^{192}Ir , and ^{125}I source ^(adapted from 9)

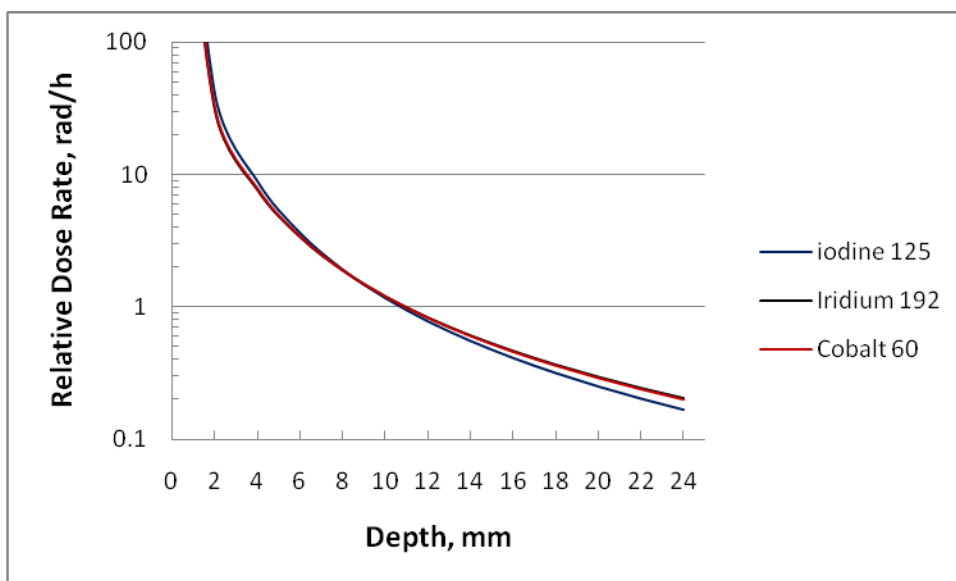


Figure 2: Photon Dose Depth Rate for ^{60}Co , ^{192}Ir , and ^{125}I source normalized at 1cm ^(adapted from 9)

The COMS Eye Plaque (Figure 4) is composed of a silicon seed carrier and a gold backing with suture eyelets for securing the plaque during treatment. The high energy gamma rays produced by a ^{60}Co source penetrate through the gold backing of the COMS Eye Plaque causing an increase in dose to healthy tissue behind the eye plaque. In contrast, the low energy x-rays from ^{125}I are completely shielded by the gold plaque. Figure 3 illustrates the different isodose lines from ^{60}Co and ^{125}I . The Collaborative Ocular Melanoma Study selected ^{125}I source seeds because they provided sufficient dose at the maximum apex depth of 10 mm for medium ocular melanoma tumors while limiting the dose to the healthy tissue surrounding the tumors.⁽⁹⁾ Thus the ^{125}I source seeds allowed medium sized tumors to be treated while protecting healthy tissue from the damage of treatment radiation.

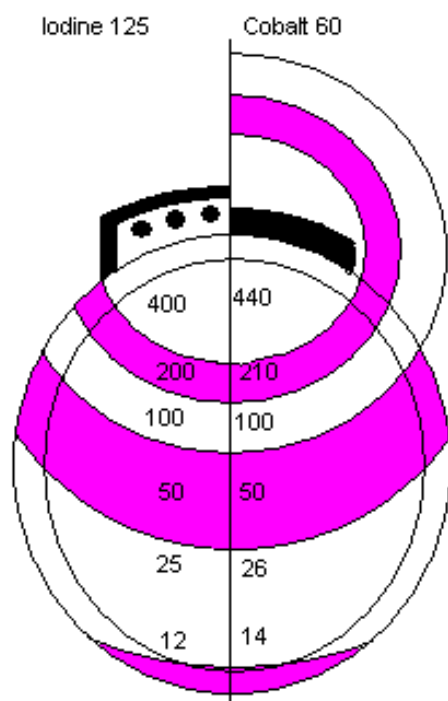


Figure 3: Isodose lines of ^{125}I and ^{60}Co eye plaques demonstrating shielding difference (adapted from 9)

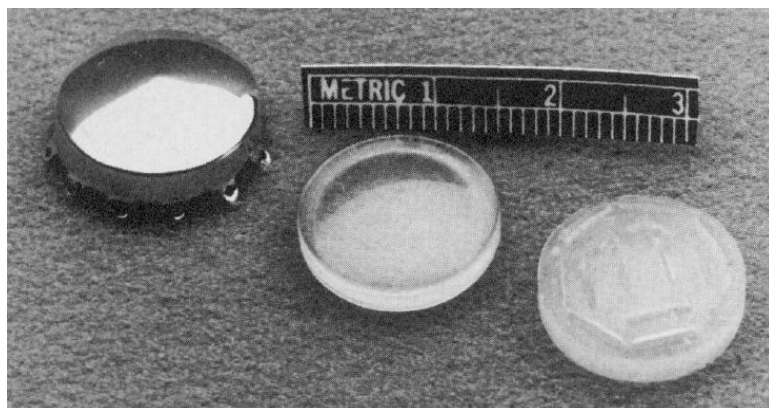


Figure 4: COMS 12mm eye plaque with silastic inserts (9)

Randomized trial of brachytherapy versus enucleation

The Collaborative Ocular Melanoma Study was conducted from 1986 to 2003 with the objective of comparing the long term effects of eye plaque brachytherapy versus enucleation when adhering to the standard protocols of medical studies.⁽¹⁰⁾ Patients were selected for the study using the following considerations: (a) the tumor size and location must be suitable for eye conserving brachytherapy treatment, (b) tumors contiguous with the optic nerve were not eligible, and (c) the patient must not have metastatic melanoma or other cancers other than cancer in situ of the uterine cervix and nonmelanotic, nor noninvasive skin cancer.⁽¹⁰⁾ The patients eligible for the study were asked to sign a contract permitting ten years of follow up visits. Following confirmation of agreement to the terms of the study, the patient was randomly assigned either ¹²⁵I eye plaque treatment or enucleation. The brachytherapy group was prescribed a 10,000 rad apical dose to the tumors. This dose was calculated assuming the ¹²⁵I seeds were point sources in a homogeneous tissue material, without accounting for backscatter off the gold plaque or attenuation through the silastic seed carrier.⁽¹⁵⁾

The collection of data was performed by clinical examinations at six month intervals for five years following the treatment of both patient groups. Following the five years of biannual examination, an annual examination regiment was implemented with an optional 6 month examination for the preceding fifth to tenth year period. After ten years of follow up examinations patients were allowed the option of continuing follow up by Collaborative Ocular Melanoma Study clinical center personnel, or withdrawal from the study. Patients that chose to continue were followed either until death or completion of fifteen year follow up study.

During the COMS study, 1317 patients were treated with either brachytherapy or enucleation. The results indicated there were no statistically significant differences in outcomes between the treatment methods. The combined deaths from both histopathologically confirmed melanoma metastasis and suspected melanoma metastasis provides the following death rates: (a) for the first five years 13% in both study groups, (b) the ten year rates are 21% for enucleation and 22% for the ¹²⁵I brachytherapy group. The study also provided statistically significant evidence that both age and maximum basal tumor diameter (MBTD) influenced the long term outcome of the treatment. Patients over sixty with an MBTD > 11 mm were the group at highest risk of death from any cause, followed by patients over sixty with a MBTD ≤ 11. The MBTD is the greatest influence when comparing deaths with histopathologically confirmed

melanoma metastasis, and as a result the death rate for patients with MBTD ≤ 11 was uninfluenced by age.⁽¹⁰⁾

Quality of life after trial

The COMS Quality Of Life Study (QOLS) started in 1995, 8 years after the first patient was enrolled in the original Collaborative Ocular Melanoma Study, with 209 patients from both treatment groups. The participants answered questionnaires regarding visual function and anxiety for a period of five years. Patients treated with ^{125}I brachytherapy fared better than those treated with enucleation in quality of peripheral vision and the task of driving during the first two years after treatment. This difference in outcome should be expected for eye and vision saving ^{125}I brachytherapy treatment. Following the first two years after treatment, there was no noticeable difference in vision performance between the groups. Anxiety was worse for patients treated with brachytherapy possibly due to continued monitoring of the remaining tumor. Some of this anxiety dissipated after the Collaborative Ocular Melanoma Study released its Medium Tumor Trial results stating no significant difference in treatment outcomes between enucleation and ^{125}I brachytherapy. This study showed that ^{125}I brachytherapy offers the benefit of saving some vision, with no significant physical or psychological drawbacks.⁽⁸⁾

AAPM Task Group 43U1 Report

The American Association of Physicists in Medicine (AAPM) formulated Task Group (TG) 43 in 1988 to review the current literature on dosimetry of interstitial brachytherapy and develop dosimetry protocols. The protocol for source dosimetry calculations recommended by this task group accounts for: anisotropy, dose rate, geometry, radial dose, and air kerma strength.⁽²²⁾ The AAPM equation for dose calculation, revised from the original recommendation, is the currently accepted procedure for calculating dose from an ^{125}I seed, as described by TG-43U1. This provides a two dimensional dose representation in a liquid water phantom representing tissue. TG-43U1 improved upon the previous standard, which offered a one dimensional dose falloff and conversion of a seed-strength calibration in air to tissue/water, assuming a point source distribution.⁽²³⁾ The following equations are those used in the TG-43U1 dose calculation around photon emitting brachytherapy sources:⁽²²⁾

Dose Rate at point (r, θ) :

$$\dot{D}(r, \theta) = S_K \Delta \frac{G(r, \theta)}{G(r_0, \theta_0)} g_L(r) F(r, \theta)$$

Air Kerma Strength (U) at calibration distance 'd' by d squared:

$$S_K = K_S(d)d^2$$

Dose at 1cm on the traverse axis to water per U:

$$\Delta = \frac{\dot{D}(r_0, \theta_0)}{S_K}$$

Geometry Factor for a lines source used for 125I seed:

$$G(r, \theta) = \frac{\beta}{Lr \sin \theta}$$

Where L is the active length of the source, β is the subtended by the active source in reference to the location (r, θ) .

Radial Dose Function (accounts for absorption and scatter in traverse axis):

$$g_L(r) = \frac{\dot{D}(r, \theta_0) G(r_0, \theta_0)}{\dot{D}(r_0, \theta_0) G(r, \theta_0)}$$

Where (r, θ) indicate locations along the traverse axis with the θ_0 equal to $\pi/2$.

Anisotropy Function (for anisotropy around source, absorption, and scatter):

$$F(r, \theta) = \frac{\dot{D}(r, \theta) G(r, \theta_0)}{\dot{D}(r, \theta_0) G(r, \theta)}$$

This anisotropy function calculated the distribution defined by a polar angle to the traverse axis.

The (r, θ_0) of both D and G should be the same as the angle used to define the radial dose function.

Dosimetric Theory used for 125I Seeds in Eye Plaque Therapy

Collaborative Ocular Melanoma Study Manual of Procedures

The Collaborative Ocular Melanoma Study procedure for source calibration calls for an ionization chamber calibrated with a NIST-calibrated ^{125}I seed with a known activity, and recommends the use of a ^{60}Co source for verification of the ion chamber. The dose is to be calculated using the TG 43 equation that assumes a point source, and doesn't account for anisotropy, backscatter from gold backing, composition of the silastic insert (water is assumed), and collimation of the gold lip. A lack of published studies investigating the significance of these effects at the time was the reason for these assumptions. Regions of interest for calculated dose included the radiosensitive structures and the apex of the tumor. ⁽¹¹⁾

Plaque Simulator®

The Plaque Simulator (PS) is a treatment planning system specifically designed for eye plaque radiotherapy, and is distributed by BEBIG GmbH. The most recent version of PS became available in July of 2005, and is designed to operate on the MacOS personal computers. This treatment planning system offers a 3D treatment simulation and modeling package for four different radioisotope sources and many plaque models and sizes. It also allows for the user to add new designs to its plaque library. The PS has been referenced in multiple published documents accrediting its dosimetric theory and assumptions. ^(1, 2, 3, 4, 6, 14, 15, 21, 23, 28)

PS version 5 uses TG-43U1 as a basis for its dosimetric model of the COMS plaque, along with efforts to improve the physics model. Several assumptions have been modified from TG-43U1 in the form of correction factors, including: backscatter from gold backing, penumbra effect of the collimating lip of gold backing, attenuation through silastic insert, and eye to air interface. ⁽⁴⁾

Effect of eye plaque material on dosimetry

In this study the COMS 12mm, 16mm, and 20mm eye plaques, loaded with commercially available 6711 ^{125}I seeds, will be compared using dosimetry simulation software. The COMS eye plaques are made of a gold composite cup with suture eyelets. Inside the gold cup is a seed carrier made of a silastic material with slots on the outer surface used to hold the seeds in a set

location. The 6711 ^{125}I seeds are constructed of ^{125}I absorbed onto a silver wire sealed in a titanium seed.⁽²⁷⁾ The radiation from the brachytherapy source interacts with the material of a COMS eye plaque complicating the calculation of dose to the tumor. The following two sections will briefly discuss the corrections needed to account for this physical behavior.

COMS plaque Gold Backing causing Backscatter

The gold backing of the COMS eye plaque acts as a shield for all radiation emitted away from the choroidal melanoma tumor. Gold has a atomic number (Z) of 79, which is larger than that of tissue (water: Z-eff. = 7.4). This difference in Z is significant because low-energy photons will have a much higher probability of photoelectric absorptions within a much shorter distance in high-Z materials. The gold backing was found to be infinitely thick for the low energy photons emitted from ^{125}I seeds.^(12, 16, 29, 30) However, these photoelectric interactions with gold result in the release of 10 keV x-rays, some of which will be emitted back towards the tumor tissue. Due to their low energy, all gold x-rays will be attenuated 7 mm from the gold backing, minimizing their impact to the eye⁽¹²⁾. The backscatter of gold x-rays will cause an increase in dose to the eye up to a depth of 1mm.⁽³⁰⁾ However, tissue depths beyond 1 cm show a reduction in dose to the tumor due to the loss of scatter from tissue behind the plaque.^(12, 16, 29, 30) When the gold backing is absent, radiation emitted away from the tumor has the potential to scatter back into the tumor region. The presence of the gold plaque eliminates this dose from scattered photons causing a 10% reduction in dose at distances greater than 1 cm.

COMS silastic seed carrier attenuation of flux

The early assumption used in the Collaborative Ocular Melanoma Study was that the silastic seed carrier was water equivalent for treatment dose calculations of a Choroidal Melanoma tumor. Further studies have looked into the impact of the silastic seed carrier on the attenuation of the photons reaching the tumor region. The effect of the silastic seed carrier has been shown to reduce dose as a function of the distance from the plaque in the plaques central axis as well as the off-axis direction. Chiu-Tsao suggests that the silastic insert alone [has approximately the same quantitative effect on] the dose as the insert with gold backing.⁽⁶⁾ Thomson, using BrachyDose (an EGSnrc user code) suggests that the silastic insert accounts for

an additional 10% reduction in dose, and that the combination of gold backing and insert causes a reduction of 16% - 17% near the seeds and 20% on the opposing side of the eye.⁽²⁸⁾ In Thomson's study, the Plaque Simulator was shown to overestimate dose near the seeds and underestimate dose away from the seeds.

Penumbra effect from seed location and lip of plaque

The lip surrounding the gold backing of the COMS eye plaques was first assumed to have no significant effect on the dose distribution when ^{125}I seeds are used. However, because it is much thicker than the half-value layer for ^{125}I photons, the gold lip has a similar impact as the backing.^(28, 31) Therefore, a penumbra effect shows in the resulting isodose lines, indicating a reduction in dose to tissue outside the radius of the plaque. The penumbra effect has been found to vary with location of the seed and size of the plaque due to the additional high-Z material resulting in significant attenuation of the photon energy off axis. The penumbra effect, when accounted for, allows oncologists to maintain treatment dose prescriptions while reducing dose to sensitive tissues outside the treatment region.

Point Source versus Line Source for modeling of 125I seed (model 6711)

The configuration of the 6711 ^{125}I seed is a silver wire with ^{125}I absorbed to the surface, encased in titanium.⁽²⁷⁾ The radioactive source of this seed model is ^{125}I absorbed on the surface of the wire producing a cylindrical source shape. To simplify the dose distribution calculation, the seed is approximated as 2D line source. This is different from the original point source used to perform dose distribution calculations for the Collaborative Ocular Melanoma Study. The Plaque Simulator uses the AAPM TG 43 line source dose distribution equation referenced earlier, for the base of its dose distribution calculations when modeling the model 6711 Onco seed.⁽¹⁾

Effect of air to eye interface on eye plaque dosimetry

The air interface at the cornea of the eye creates a local dose reduction due to the difference between the attenuation coefficient of air and eye tissue. The mean free path of a photon is the

inverse of the attenuation coefficient, which means that the mean distance a photon travels between interactions will increase with less attenuation. The attenuation coefficient of dry air is approximately $1.278 \times 10^{-3} \text{ cm}^{-1}$ for the average energy of an ^{125}I photon, while for homogenous tissue it is approximately 0.3153 cm^{-1} . This means that the mean free path increases approximately by a factor of 200 in that region. The increased mean free path also reduces the geometric probability of a scattered photon returning to the eye.⁽²⁵⁾ Alberto de la Zerda used TLDs to determine the effect of an air-to-eye interface on the dose distribution of a COMS eye plaque.⁽²¹⁾ The results were then compared to Monte Carlo MORSE data published by Chiu-Tsao, one of the participating physicists.⁽⁶⁾ Experimentally, the off-axis dose reduction as a function of depth into the eye was determined to increase up to 13% at 2.5 cm. The Monte Carlo calculation indicated a similar reduction of 10% for a point source. The plaque in the experiment and calculation was located at the posterior of the eye such that the flux would be lowest at the air interface. This plaque location would cause poor resolution at the air-to-eye-interface because of the low dose rate due to attenuation through the eye. Following this experiment Astrahan developed a new correction factor in the Plaque Simulator dose calculation which accounted for dose reduction due to an air interface.⁽⁴⁾ The resulting correction factor attributed 11% of the absorbed dose from ^{125}I to backscatter from the neighboring hemisphere. However, if the neighboring hemisphere is air then this backscatter is absent. Astrahan's correction factor has been tested by Thomson using BrachyDose, an EGSnrc user code.⁽²⁸⁾ Thomson's calculations modeled fully loaded 12mm and 20mm COMS eye plaques with both the ^{125}I seed and ^{103}Pd seed. Thomson found that for a fully loaded 20mm plaque centered on the equator (i.e. axis running top to bottom of eye) the Plaque Simulator overestimates the dose reduction due to an air interface at a point opposite the plaque.⁽²²⁾

Inhomogeneity of the eye and surrounding tissue

The eye consists of many different tissues, all with slightly different properties. The variation in tissue properties effects both the attenuation and the mass absorption coefficient of low energy photons. The change in the interaction probabilities of low energy photons causes variations in the fluence and absorbed dose rates within these tissues. The Plaque Simulator currently calculates dose distribution through the eye assuming the tissue within the eye and surrounding it is water equivalent. Thomson's simulation with BrachyDose investigated the dose distribution

for ^{125}I photons accounting for the tissues in the eye and bone outside the eye.⁽²⁸⁾ Bone surrounding the phantom eye caused a dose reduction of 5% for ^{125}I photons to a point opposite the plaque. The assumption of homogenous tissue of the eye causes a dose reduction of ~2-3% and tissue of the lens causes a reduction of ~9% when compared to water.

Project Objectives and Experimental Approach

Objectives and Approach

The objective of this research is to use a Monte Carlo code, MCNPX, and a deterministic code, Attila, to compare against the dose generated with the clinically used Plaque Simulator program. Although several of the assumptions implemented in Plaque Simulator have been compared with Monte Carlo codes^(3, 4, 6, 28), this research will compare these assumptions with the result from a deterministic transport code. The advantage of using a deterministic code is the time reduction to obtain the solution of the transport equation, compared with statistically simulating each photon interaction as in Monte Carlo.

Transpire Inc. has developed the deterministic transport code Attila, designed for quickly calculating the solution to a discretized Boltzmann transport equation for neutrons, photons and/or electrons. Attila simulations will be compared to the dose calculations of the Plaque Simulator and MCNPX. These dose calculations will account for the air-to-eye interface, bone surrounding the eye, a homogeneous eye tissue, silastic plaque insert, and the gold plaque, assessing the suitability of the Plaque Simulator correction factors. The plaques used in this comparison are the 12mm, 16mm, and 20mm COMS eye plaques fully loaded with ^{125}I Onco-seeds model 6711.

Equipment

MCNPX

The MCNPX2.5.0 Monte Carlo code used in this project is a superset of MCNP4C and MCNPX2.4.0 released in 2005 by Los Alamos National Laboratory. It is a general purpose

statistical radiation transport code capable of tracking nearly any particle with nearly any energy. The difference between a deterministic transport code like Attila and a Monte Carlo code is that Monte Carlo tracks individual particles from birth to death. Characteristics of the events are defined by statistical sampling of the probability distributions of the governing physics. The statistical sampling is done through random number generation.

MCNPX2.5.0 is operated through an input text file in which the geometry, source, tallies, and variance reduction are defined. The geometry definition in the text file is difficult to write without creating errors. These geometry errors can result in particles being lost, causing the tally information to be false. Visual Editor is a program offered by Los Alamos to provide help with troubleshooting errors in the geometry definition.

The Visual Editor project was started in 1992 to aid MCNP users in viewing the input geometry of an MCNP input deck. It was first released to RSICC in 1997, and was added to the MCNP package with the release of version 5 of MCNP. This software has a windows based user interface that allows users to view their geometry input in two-dimensional windows. It also allows the user to edit the text lines of the input file, which is helpful in debugging.

The input file of this project was coded with a combination of text file writing and proofing with the use of MCNP Visual Editor. The first stage of coding was to writing the geometry specifications. Once the geometry was correctly defined for the three COMS eye plaques, text file writing was used to define the source, photon importance, and tally specifications. In this project, MCNPX was operated in photon mode only, with a rectangular mesh tally to track dose through a voxelized representation of the geometry. The tally used was an rmesh type three with mesh cells 0.1 cm^3 in volume.

Plaque Simulator

Plaque Simulator version 5.3.6 copyright from 1991 to 2005 by Melvin A. Astrahan, Ph. D was used for this project. The Plaque Simulator allows users to upload CT and MRI images for defining patient and tumor dimensions. It also allows the user to specify corrections to include in the dose calculation from the available options. The Basic Tutorial found in the Plaque Simulator User Manual was referenced for the problem definitions used to compare to the calculation of MCNPX and Attila. The tumor, plaque, eye sizes, and locations were entered using the interactive windows displayed in Figures 5, 6, and 7.

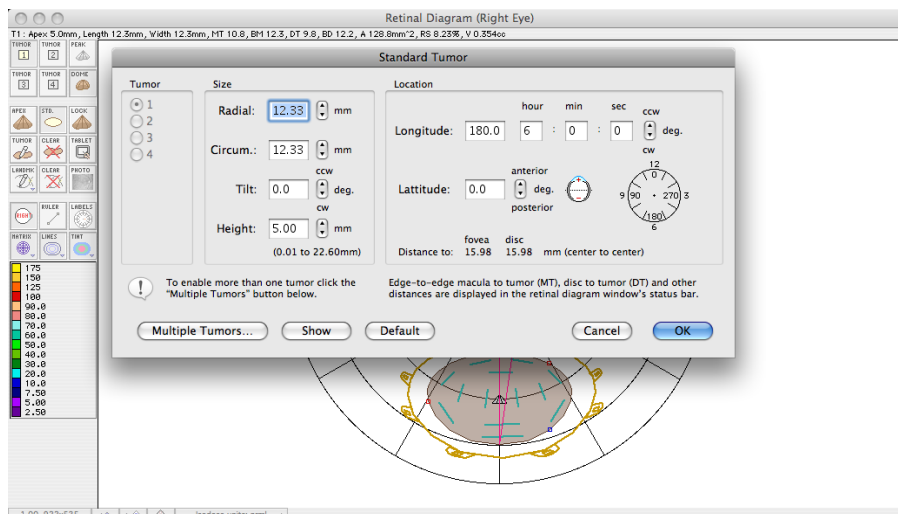


Figure 5: Plaque Simulator's window for tumor definition

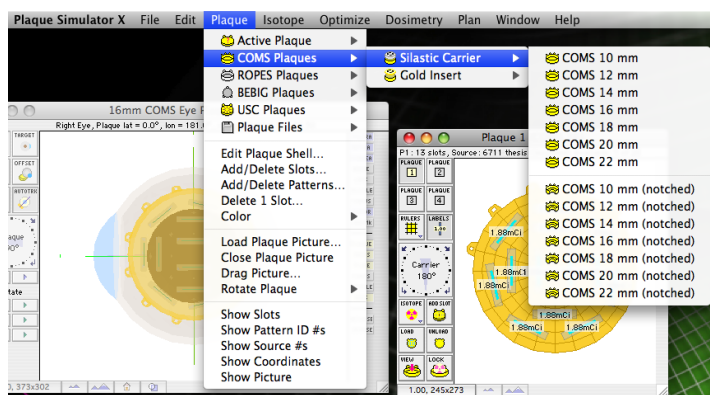


Figure 6: Plaque Simulator's menu for plaque setup

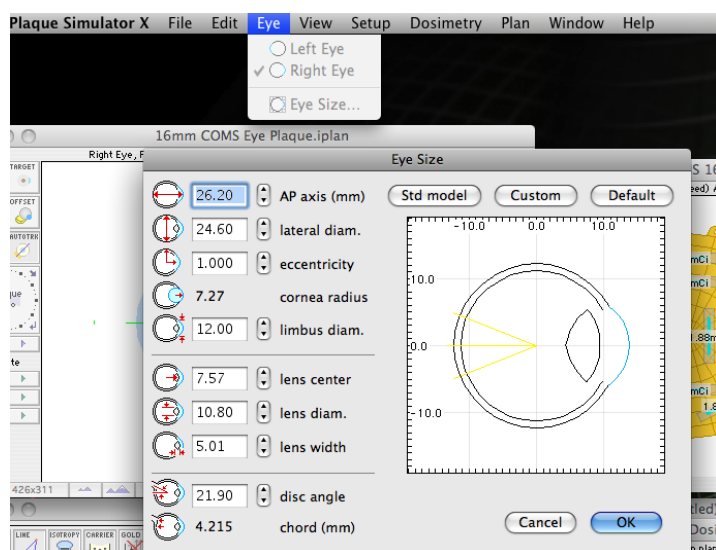


Figure 7: Plaque Simulator’s menu for patient’s eye size

From the Plaque window menu, the source seed inventory was updated to contain forty-five¹²⁵I seeds (model 6711) with activities of 1.98, and 2 mCi. The plaque type and size was defined using the same menu option and aligned to match the setup used in the other programs. The Points of Interest were defined for the dose calculation using the Prescription window menu RX>User Points. The Prescription window was used to specify the dosimetry calculation options. The dose was calculated using the following options: CALC. “USC”, Line source, Isotropy, Carrier, Air interface, Shell gold collimation, and normal instead of slotted gold plaque. The plaque scatter option “Gold” was left off because the carrier correction accounts for this back scatter. The calculation options were further defined using the menu Dosimetry displayed in the Figures 8 and 9.

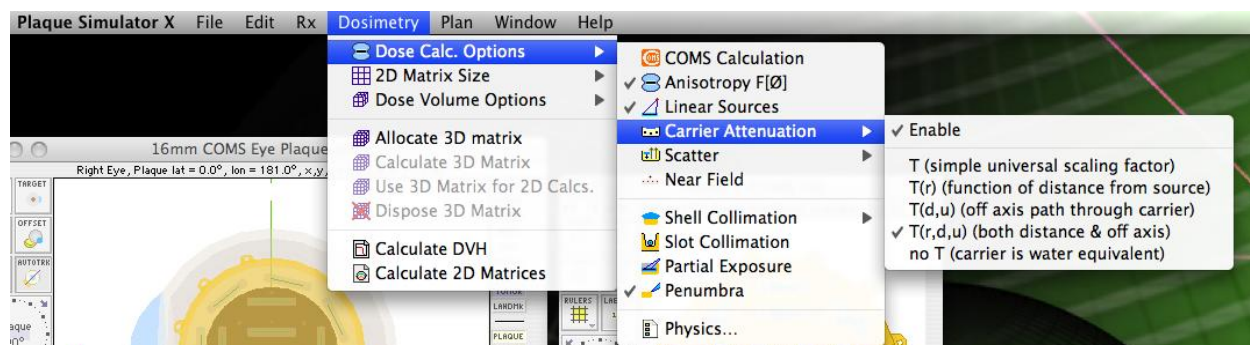


Figure 8: Plaque Simulator’s menu for Carrier Attenuation

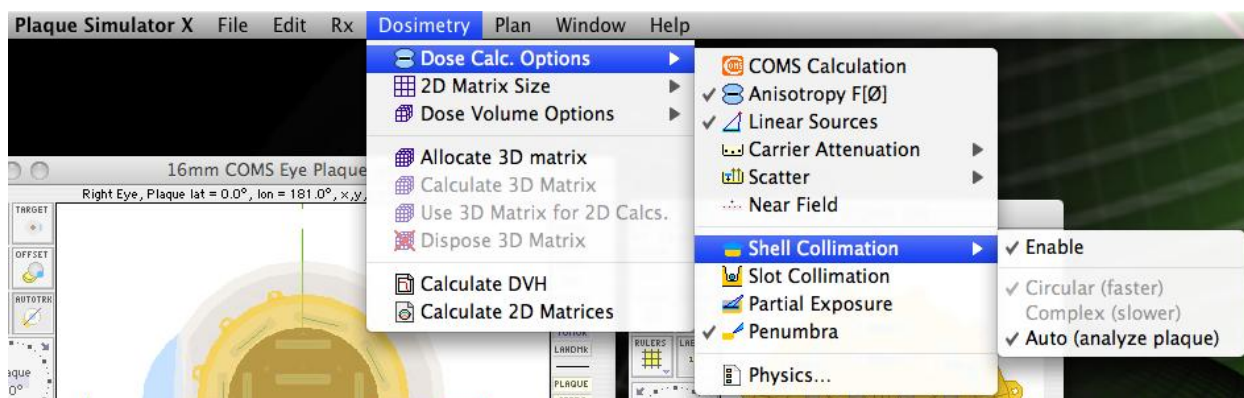


Figure 9: Plaque Simulator’s menu for Shell Collimation

The CALC. option USC versus COMS allows the user to select between the TG 43U1 dosimetry calculation “USC” and the calculation use in the COM Study. Using the Prescription window, the prescription time was defined as 169 hours and the points of interest were individually defined for comparable dose calculations.

Attila

Attila7.0 was used for this project. In the spring of 1995 a research and development prototype of Attila was developed at Los Alamos National Laboratory. Attila was validated in 2007 as a code for neutronics analyses of the International Thermonuclear Experimental Reactor. This program is a deterministic code designed to solve the linear Boltzmann transport equation for many radiation transport problems. Attila can operate from a 64 bit Window (XP or Vista) operating system, allowing the user install it on most desktop PCs. The geometry input for Attila was from a Computer Aided Design (CAD) program. The CAD-based geometry input offers a user-friendly system for the geometry definition. The user interface of Attila allows for 3-D viewing of the problem geometry, which is useful when assigning material specifications to regions of the problem, and assigning source locations.

Solid Works was the CAD program used for generating the geometry input file for the Attila portion of this project. This program allows the user to draw two-dimensional sketches, and

with the use of extrude, revolve, and mold cavity functions, the user can generate 3-D objects. It also offers an assembly function the user can use to build complex multipart designs. The mold cavity function was particularly useful for the Attila input geometry, because it allows the user to fill geometry voids in complex multipart assemblies. Similar to the MCNPX program, any voids or other geometry errors can result in transport calculation errors.

For the calculations of this project the transport code setting in Attila based off the Venus Reactor Tutorial. [This is not relevant – why would the settings for a reactor be useful for a dose calculation?] The S_N value was set to 2 and the P_N value was set to 16. The convergence floor was defined as 1.0×10^{-10} .

Dimensions of eye phantom and points of interest

The phantom head was simulated as a box 30cm on a side containing liquid water. The phantom eye was modeled a 1.23 cm radius sphere centered within the box. The eye model also incorporated a cornea consisting of a second sphere centered on the x-axis at 0.663 cm from the origin of the eye with a radius of 0.727cm. The plaques were positioned inferior to the eye, centered on the equatorial axis. The plaque was modeled to match the specifications of 12mm, 16mm, and 20mm COMS eye plaques without the suture eyelets. Outside of the plaque, a skull bone was modeled as a hollow sphere 0.545 cm thick. The region between the eye and bone and outside the plaque was filled with liquid water to model the muscle and other tissue supporting the eye. The air interface was a box 13.77 cm in depth on the x-axis, and 30 cm by 30 cm in the y and z dimensions. The phantom was designed with the same dimensions and material specifications used by Thomson.⁽²⁸⁾ The points of interest compared in this project are those used in Thomson's research as depicted in Figure 10 and Table 1.⁽²⁸⁾

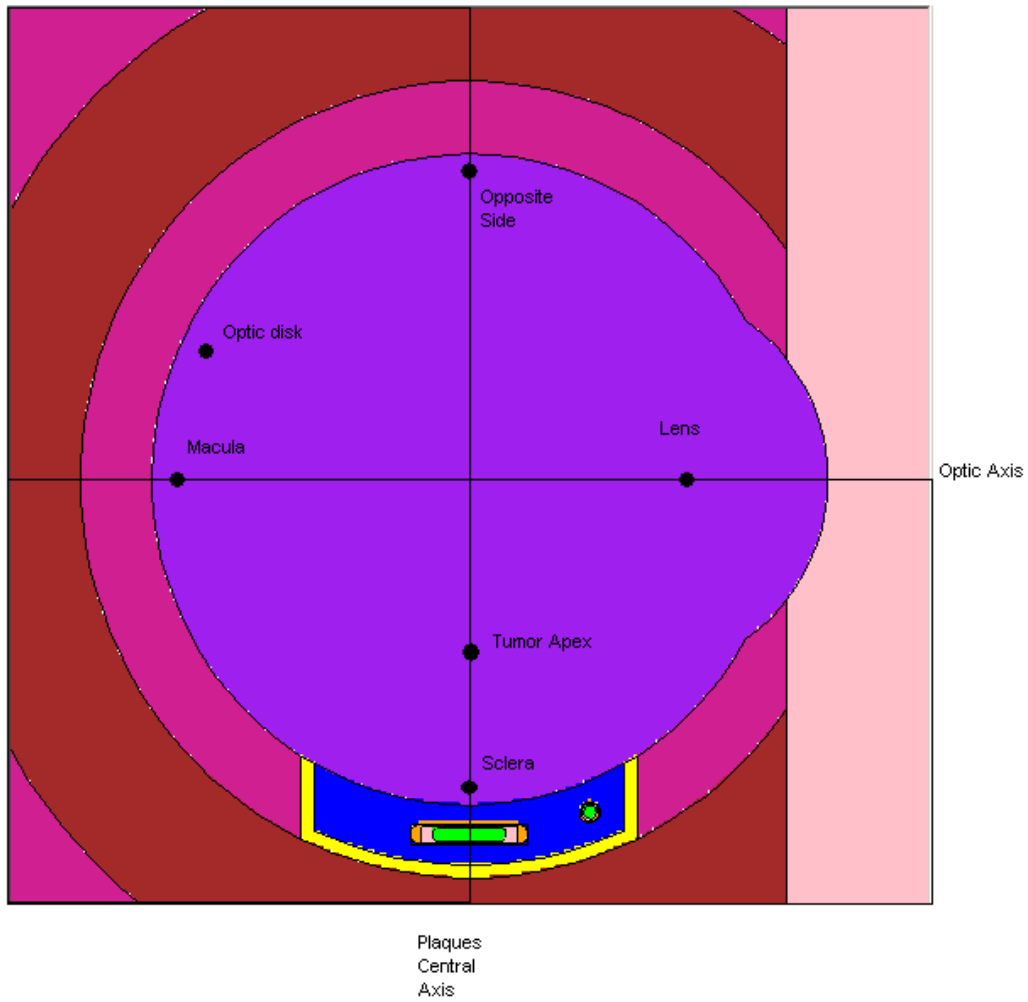


Figure 10: Points of interest from Thomson's work (adapted from 28)

Table 1: Dimensions and coordinates of Phantom Eye and Points of Interest ⁽²⁸⁾

Eye Phantom and Points of Interest for Plaque Simulator				
Locations	cm	center (x)	center (y)	Center (z)
AP axis	2.620	---	---	---
Lateral Diameter	2.460	0	0	0
Eccentricity	1.000	---	---	---
Cornea Radius	0.727	0.583	0	0
Limbus Diameter	1.200	---	---	---
Macula	--	-1.31	0	0
Optical Disk	---	-1.06	0.4	0
Center of Lens	---	0.73	0	0
Sclera	---	0	0	-1.13
Opposite Side	---	0	0	1.13
Tumor Apex	---	0	0	-0.63

Table 2: Phantom and COMS Eye Plaque Material Composition ⁽²⁸⁾

Material Elemental Composition (% by Mass)												
Material	H	C	N	O	Na	Mg	P	S	Ca	Ar	--	g/ cm ³
Water	11.11901	---	---	88.8099	---	---	---	---	---	---	---	0.9980
Dry Air	---	0.012425	75.52673	23.17812	---	---	---	---	---	1.282725	---	0.0012
Homogenized Eye	10.70	3.80	1.20	84.30	---	---	---	---	---	---	---	1.030
Bone	5.00	21.10	4.00	43.50	0.10	0.20	8.10	0.30	17.60	---	---	1.600
Material Elemental Composition (% by Mass)												
Material	Ag	H	C	O	Si	Pt	Pd	Au	Br	I	Ti	g/ cm ³
Silastic	---	6.00	25.00	29.00	40.00	0.01	---	---	---	---	---	1.120
Modulay	14.00	---	---	---	---	---	1.00	77.00	---	---	---	15.800
Ag-I	54.00	---	---	---	---	---	---	---	28.00	18.00	---	6.200
Silver	100.00	---	---	---	---	---	---	---	---	---	---	10.500
Titanium	---	---	---	---	---	---	---	---	---	---	100	4.540

Plaques and Seeds

The episcleral plaques modeled in this project were 12mm, 16mm, and 20mm COMS eye plaques with silastic inserts loaded with ¹²⁵I Amersham Oncoseed 6711. The plaque was designed to the specifications defined by Thomson.⁽²⁸⁾ All the plaques had the same outer and inner curvature radius of 1.505cm and 1.455 cm respectively. The top and collimating lip of the plaques were 0.05 cm thick, and the edges of the lips were extended to meet the outer surface of the eye. The locations of the seeds were taken from the center coordinates of seed locations in the Plaque Simulator COMS eye plaque models. These locations were chosen instead of the locations defined by Thomson to reduce any geometric error affecting the comparison between

the programs' dose calculations. The MCNPX simulation of the multiple sources was simplified by running a simulation for each seed location, with the other seeds inactive. This allowed the source to be modeled as thin plating on the source wire inside the seed capsule. To account for the total dose distribution of all seeds being radioactive the tally results were summed for each seed.

125I seed model 6711

The ¹²⁵I seed was modeled after the Amersham Oncoseed Model 6711, as specified by Dolan, which was also the basis of Thomson's seed specifications.⁽¹³⁾ The source is a mixture of AgBr and AgI at a molecular ratio of 2.5:1. The source mixture is coated on a silver wire with a coating thickness of 1.0-1.5 μm. The silver wire dimensions including the radioactive coating is 0.395 cm long with a radius of 0.025 cm with ends tapered at a 45° angle. The silver wire is encapsulated in a titanium cylinder having an outer radius of 0.04 cm, walls 0.006 cm thick, and an inner length of 0.375 cm. The titanium was enclosed with welded spherical caps resulting in total length of 0.455 cm. The cavity inside the capsule allows the source wire to slide approximately 0.04 cm. The simulation models the source wire as centered within the air-filled capsule. The Solid Works model slightly varies from the MCNP model in order to make the smooth surfaces more efficient to mesh. The silver wire was defined as an eight-sided polyhedral bar, and the radioactive coating was defined as an eight-side polyhedral tube. The titanium capsule is an eight-side polyhedral tube with caps tapered at 45° to the side faces. Substituting polyhedral shapes for the round surfaces causes the seeds to be slightly larger in cell volume because the previous radii values were used to define the radius to the center of the polyhedral faces. The difference in volume should be insignificant to the attenuation calculations because it is on the order of 1-3 μm. Figures 11, and 12 show the ¹²⁵I Onco-seed models in MCNPX and Attila.

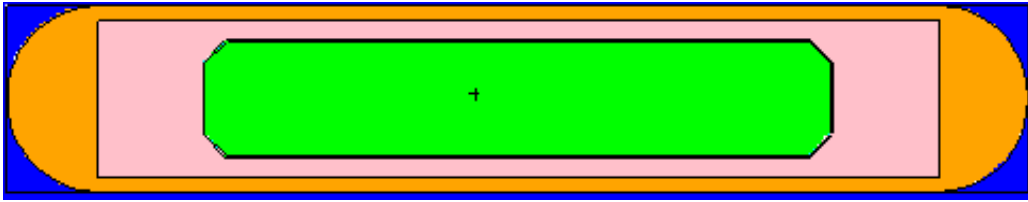


Figure 11: MCNPX model of Onco-Seed 6711

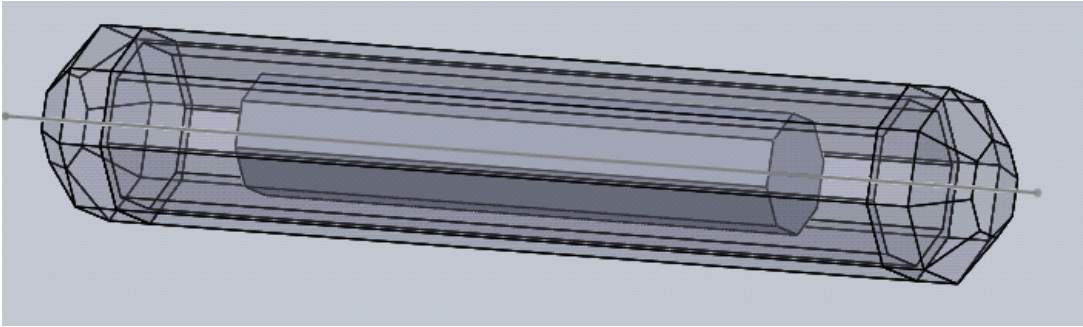


Figure 12: SolidWork's model of Onco-Seed 6711

Results

Formatting Data with Tecplot

The absorbed energy values determined in MCNPX were tabulated in a file called 'mctal.' The mctal file was in a FORTRAN format that had to be reformatted to be read into a plotting program. The plotting software used is called Tecplot, and Palmer PhD wrote a FORTRAN program to read the mctal file and produce a file readable by Tecplot. Using Tecplot the MCNPX tally values were displayed in 2D plots on the x, y, or z planes.

Calculations for MCNPX and Attila data

The RMESH tally used in MCNPX produces absorbed energy values for the mesh cells, or voxel volumes, in units of MeV/(cm³-γ). With absorbed energy values for each seed, the total plaque dose was calculated by totaling the values from each seed:

Absorbed Energy value Total Equation:

$$Dose_{plaque} = [x_{seed1} + x_{seed2} + x_{seed3} + x_{seed4} + \dots]$$

Error for the Total Absorbed Energy Equation:

$$\sigma_{plaque} = \sqrt{[\sigma_{x1}^2 + \sigma_{x2}^2 + \sigma_{x3}^2 + \sigma_{x4}^2 + \dots]}$$

Tecplot was used to view the data and extract values for comparison between the programs.

Following extraction of data from both MCNPX and Attila, some unit conversion was done so that data from all three programs could be compared in units of Gy. The dose values taken from the Plaque Simulator were for the total dose absorbed over the length of treatment, in units of Gy. Thus the absorbed energy values per photon from MCNPX and Attila were multiplied by the total photons emitted during the treatment time, and the resulting dose was converted to units of Gy. The following equations were used to convert the values from MCNPX and Attila to units of Gy for the total treatment:

Unit Conversion equation for MCNPX calculation:

$$\frac{[MeV/cc] 1.602177E - 10 [J * g / MeV * Kg] * \left(\frac{A_0(1 - e^{-\lambda t})}{\lambda} \right)}{1.03 [g/cc]} = Gy$$

Unit Conversion equation for Attila calculation:

$$[MeV/g] * 1.602177E - 10 [J * g / MeV * Kg] * \left(\frac{A_0(1 - e^{-\lambda t})}{\lambda} \right) = Gy$$

12 mm Plaque Normalized Isodose Lines

Isodose plots of percent depth dose (Figures 13-33) were generated in both the X and Y plane for the three plaques from Plaque Simulator, MCNPX and Attila. In these plots, 100% depth dose is equal to the dose found at the tumor apex in each case. This allows for a comparison of the dose distribution produced for each plaque by the three different programs.

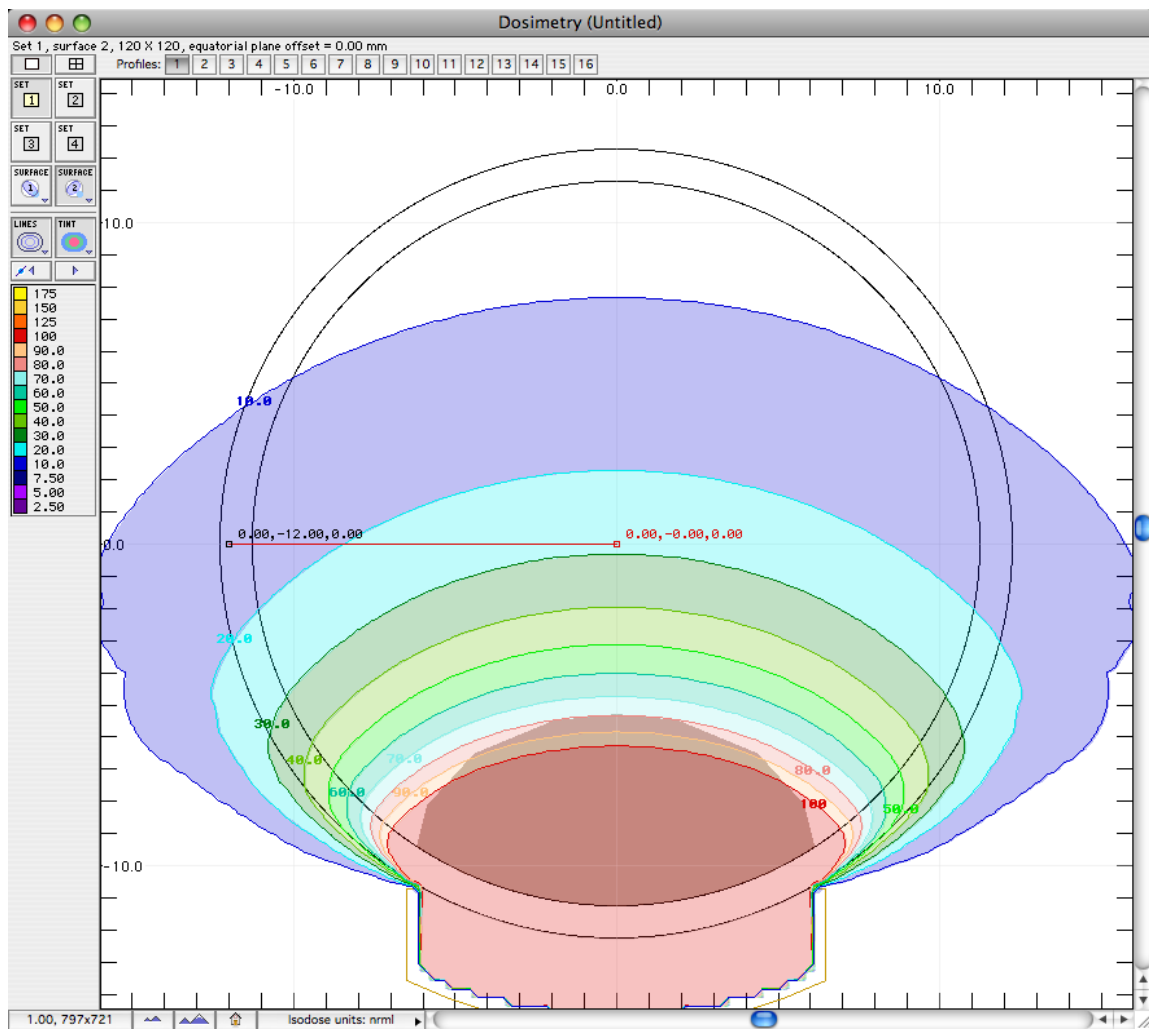


Figure 13: X-plane 12mm plaque isodose lines from the Plaque Simulator, 100% at tumor apex

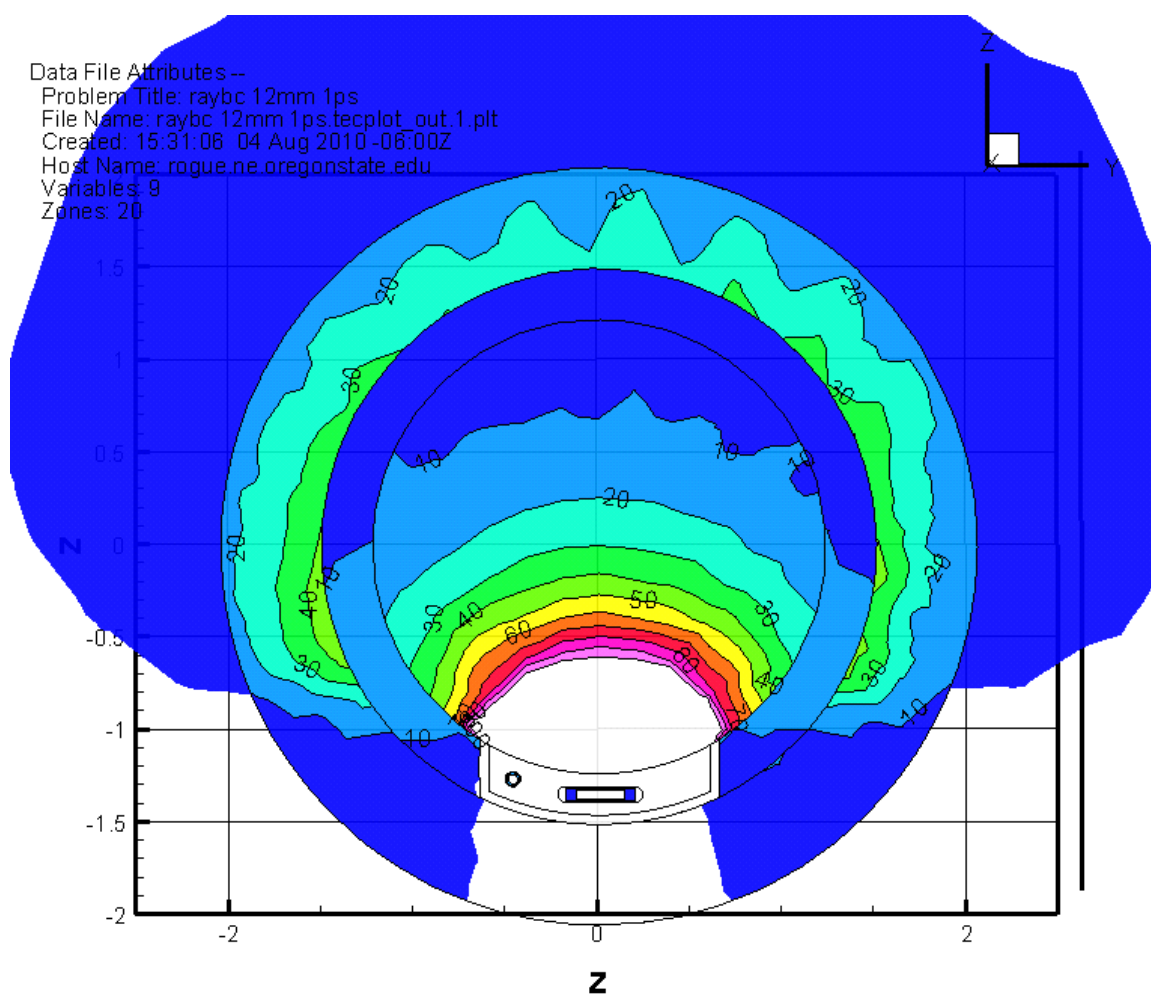


Figure 14: X-plane 12mm plaque isodose lines from Attila, 100% at tumor apex

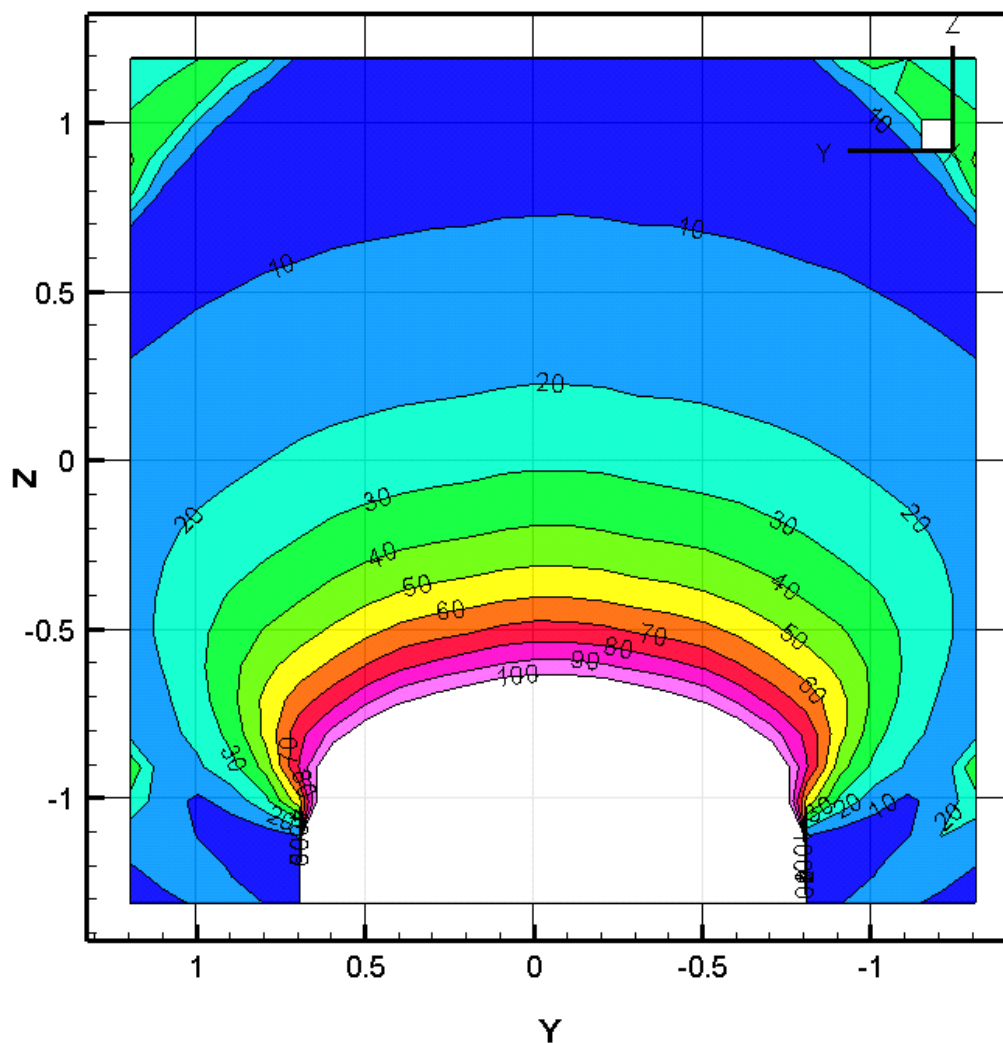


Figure 15: X-plane 12mm plaque isodose lines from MCNPX, 100% at tumor apex

Comparing Figures 13-15, the percent depth dose from all three programs are relatively similar. The Plaque Simulator's percent depth dose doesn't include the surrounding tissue and bone, and fails to indicate areas of higher dose outside the eye. In Figure 14, the 10% isodose line from Attila indicates a more non-uniform dose distribution than the other codes. This variation in the 10% isodose line may be due to poor angular resolution in the calculation, and may be mitigated with higher order angular quadratures.

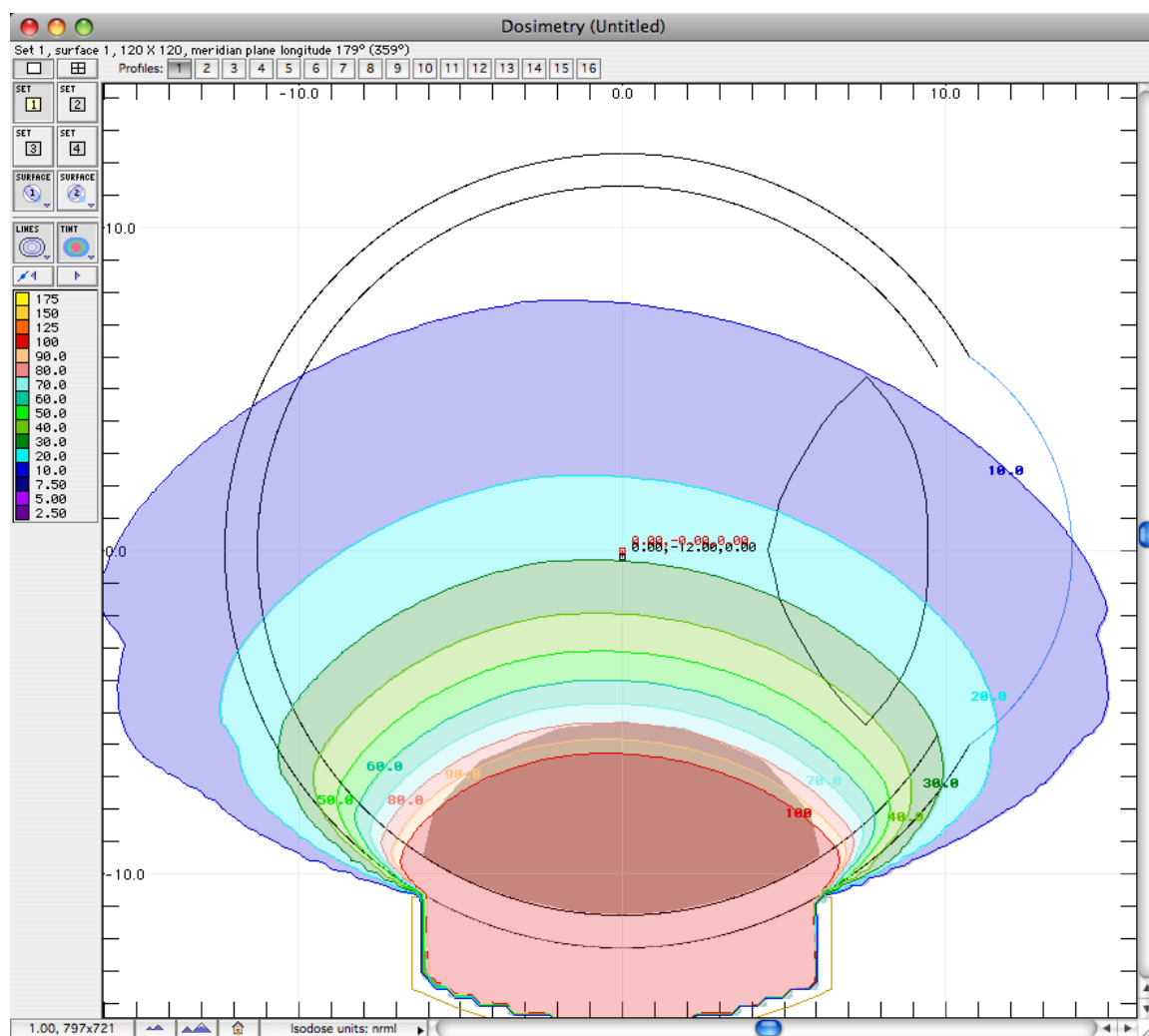


Figure 16: Y-plane 12mm plaque isodose lines from the Plaque Simulator, 100% at tumor apex

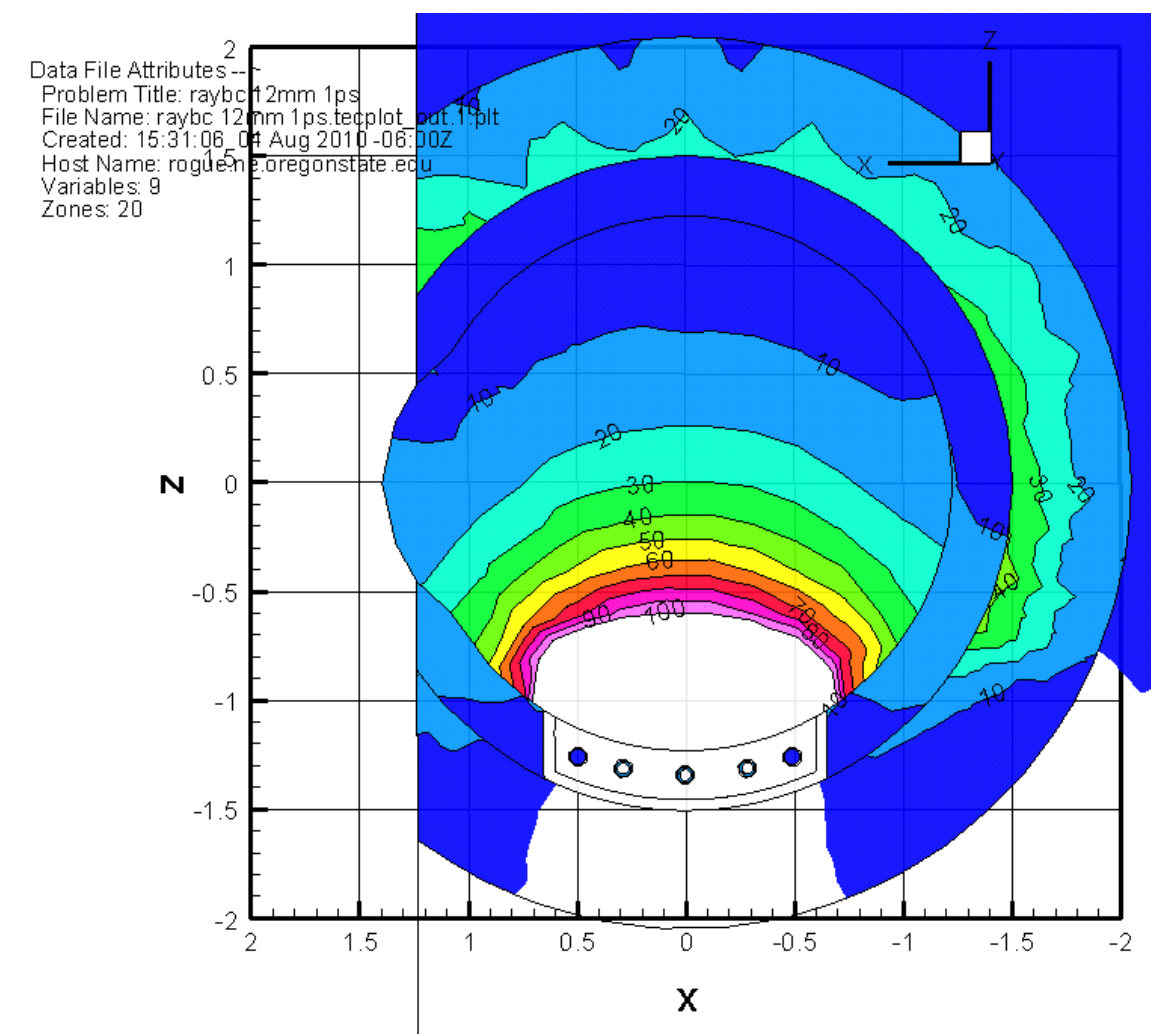


Figure 17: Y-plane 12mm plaque isodose lines from Attila, 100% at tumor apex

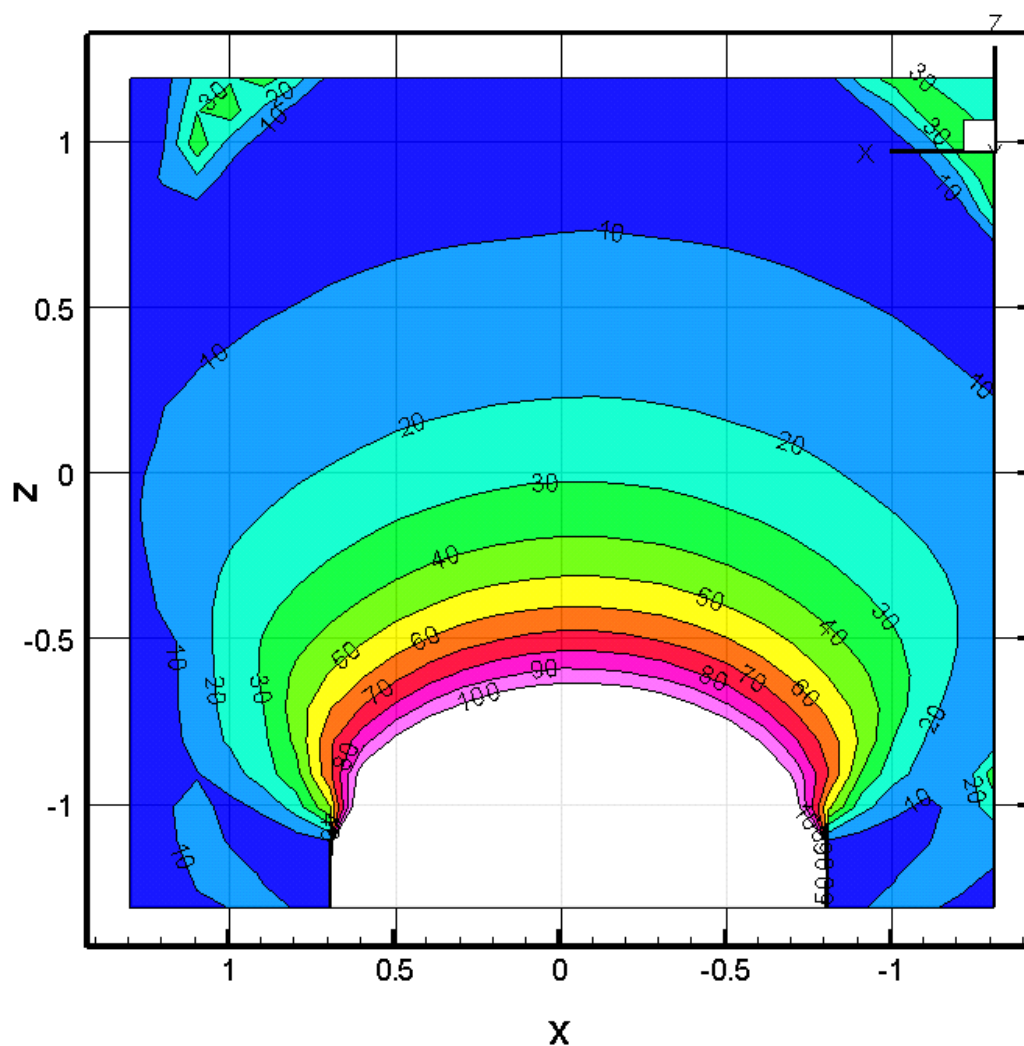


Figure 18: Y-plane 12mm plaque isodose lines from MCNPX, 100% at tumor apex

The Figures 16- 18 indicate that the Plaque Simulator may be overestimating the reduction in dose at the eye to air interface. The 10% isodose line from MCNPX has a very slight negative arch, while the same isodose line from the Plaque Simulator is steeper. The shape of the 10% isodose line as it moves toward the bone suggests that the Plaque Simulator is overestimating the backscatter off the bone and surrounding tissue. As before, the Attila percent depth isodose lines show a more non-uniform dose distribution.

16 mm Plaque Normalized Isodose Lines

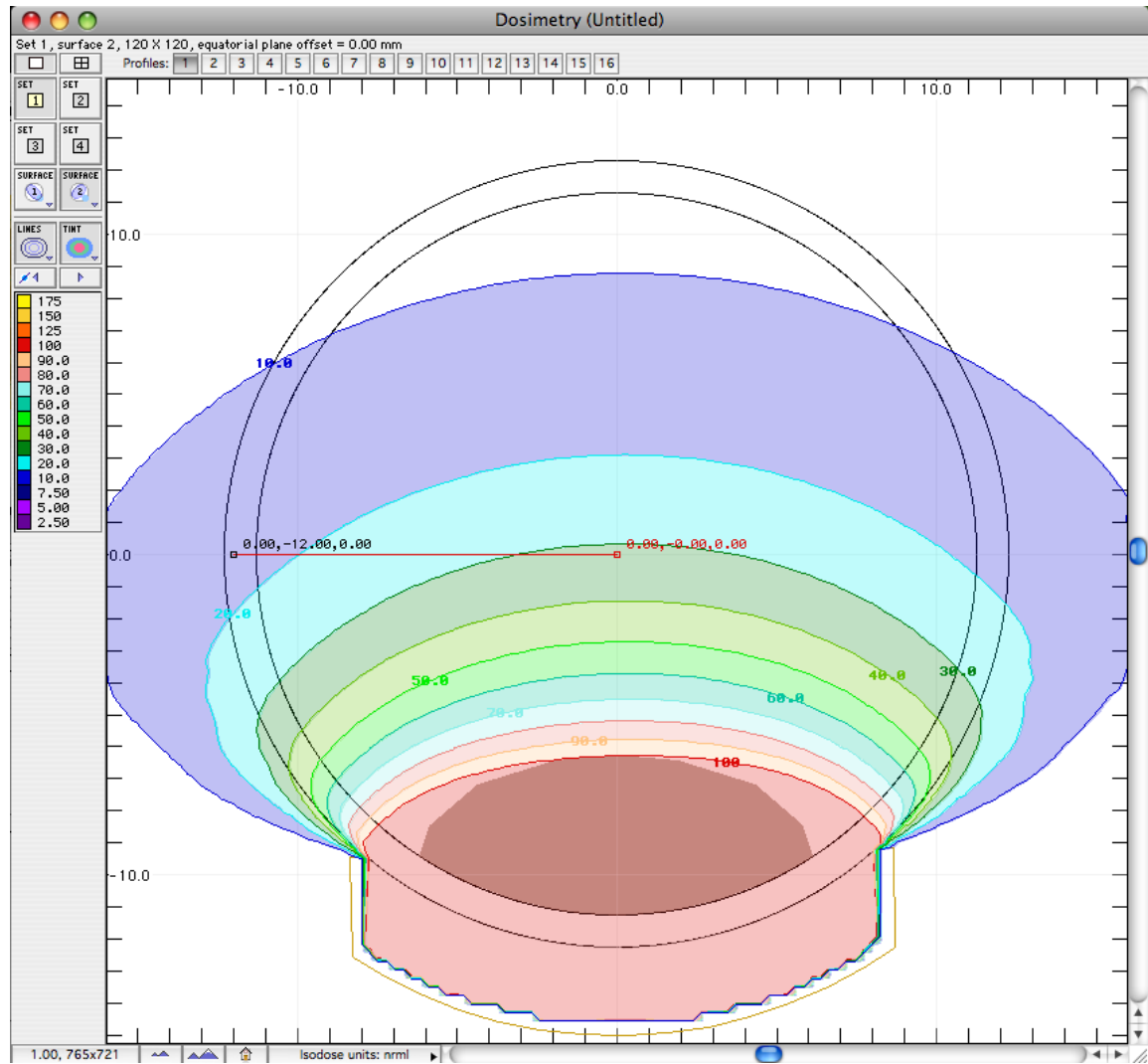


Figure 19: X-plane 16mm plaque isodose lines from the Plaque Simulator, 100% at tumor apex

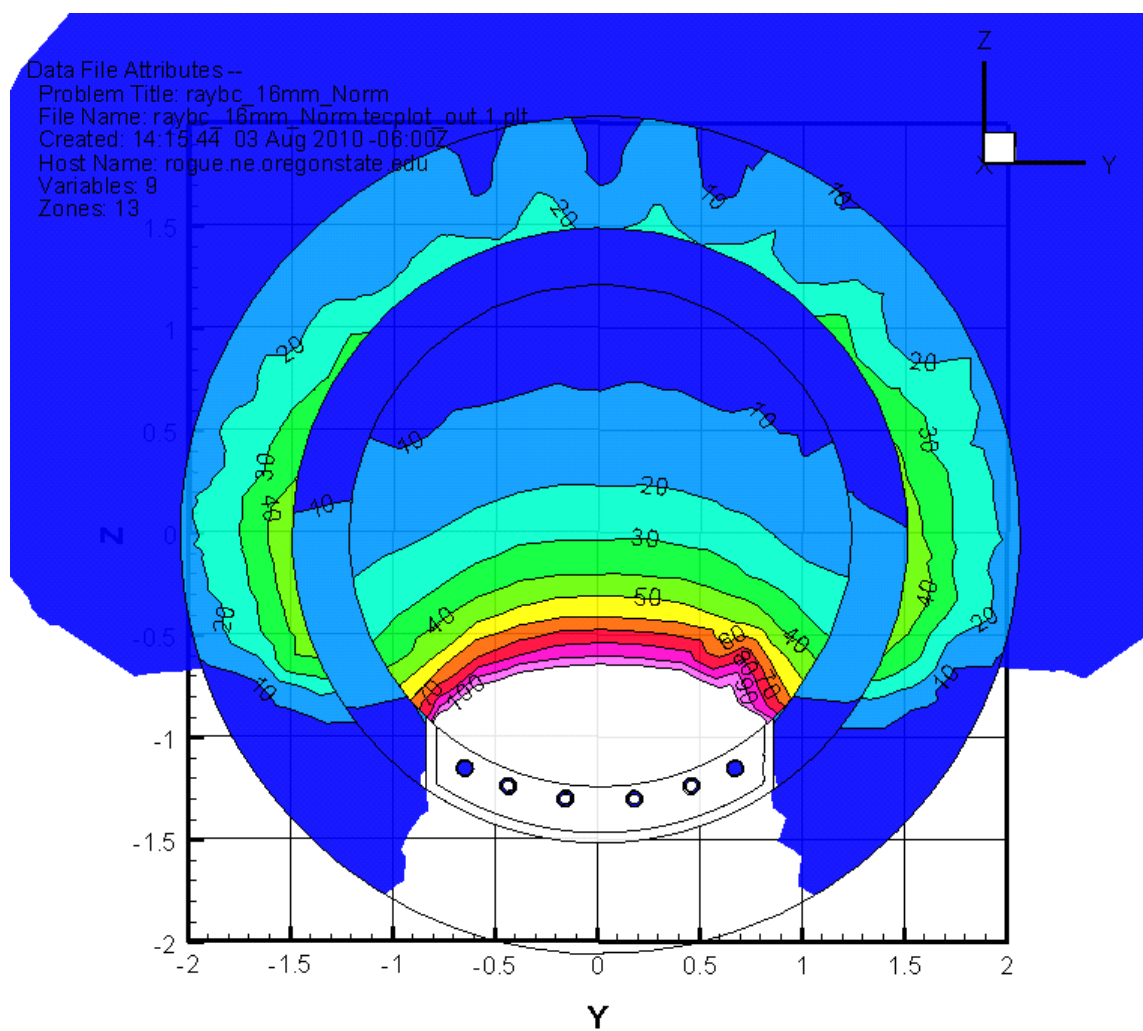


Figure 20: X-plane 16mm plaque isodose lines from Attila, 100% at tumor apex

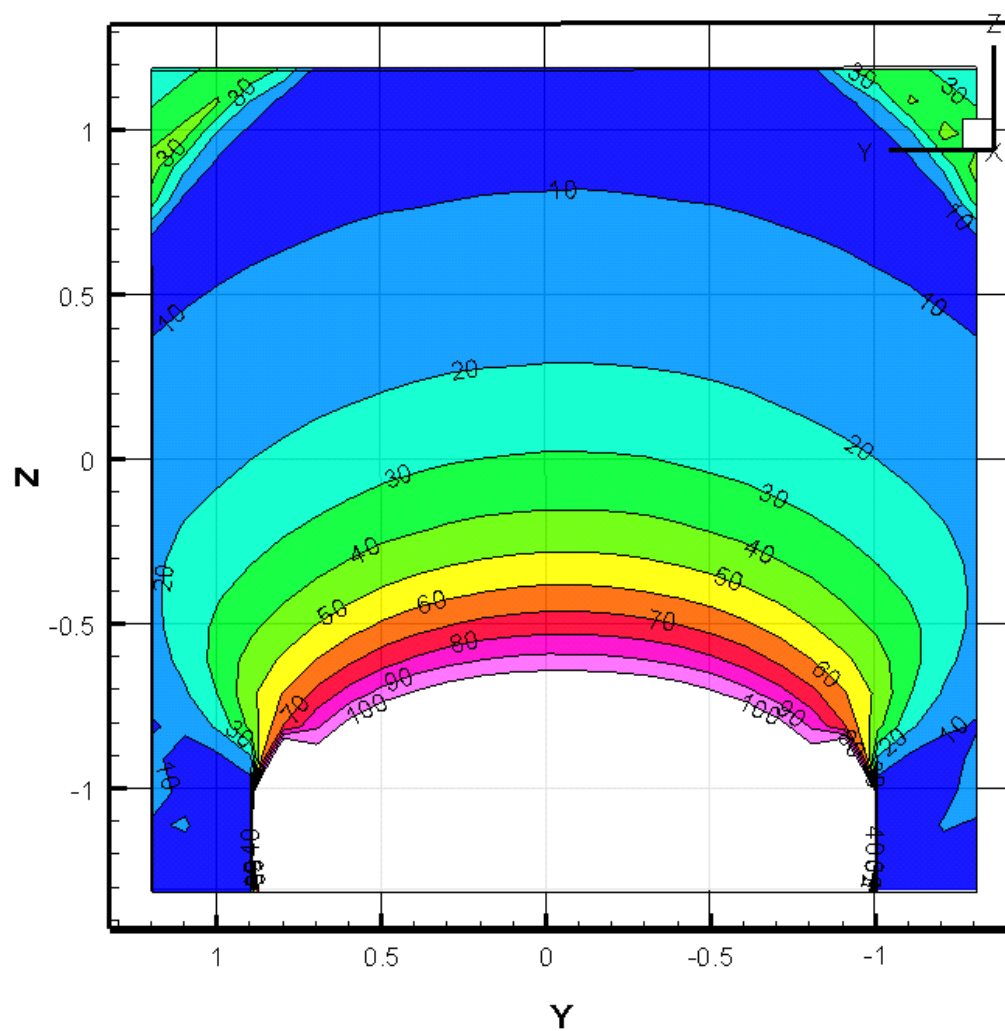


Figure 21: X-plane 16mm plaque isodose lines from MCNPX, 100% at tumor apex

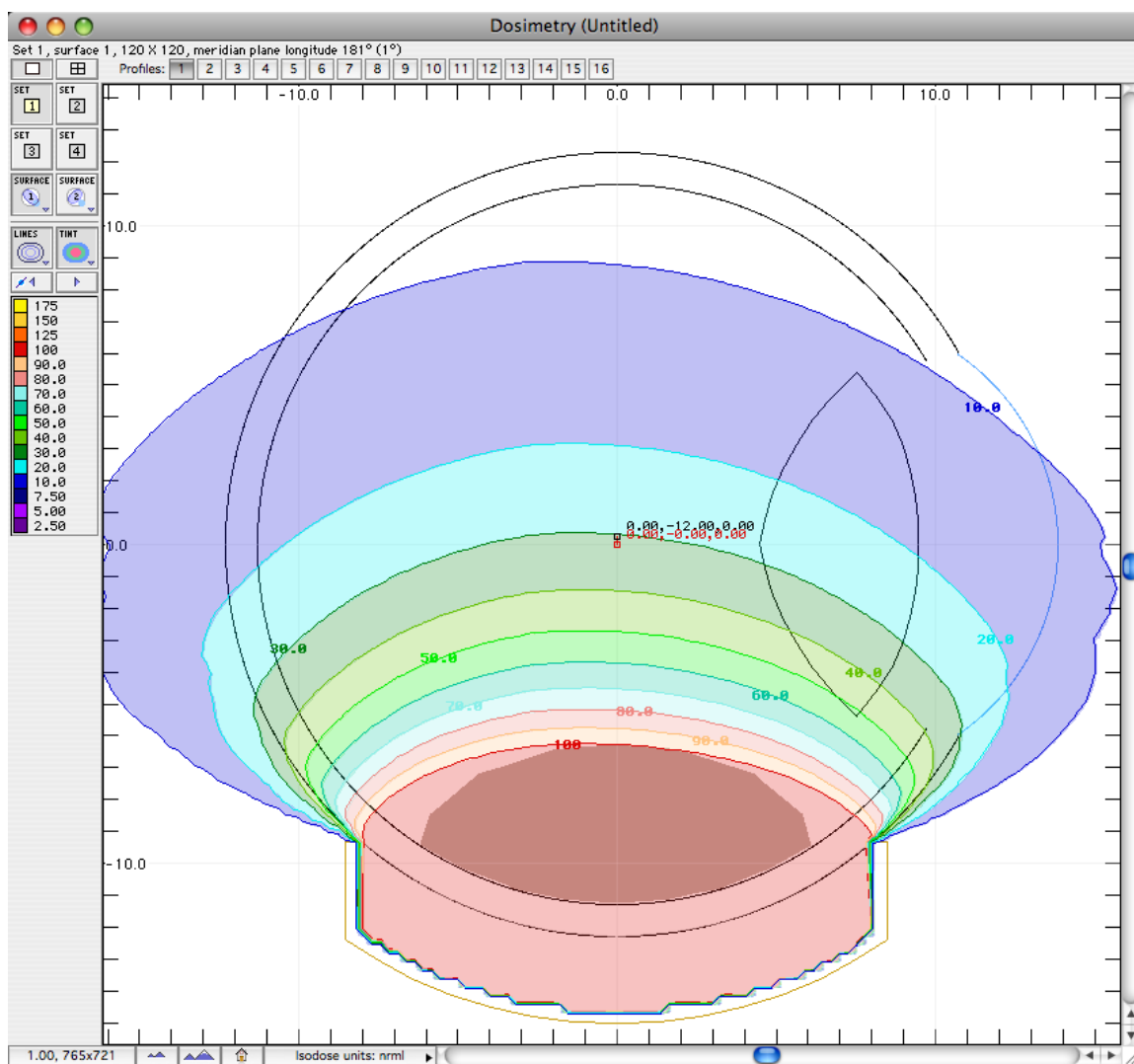


Figure 22: Y-plane 16mm plaque isodose lines from the Plaque Simulator, 100% at tumor apex

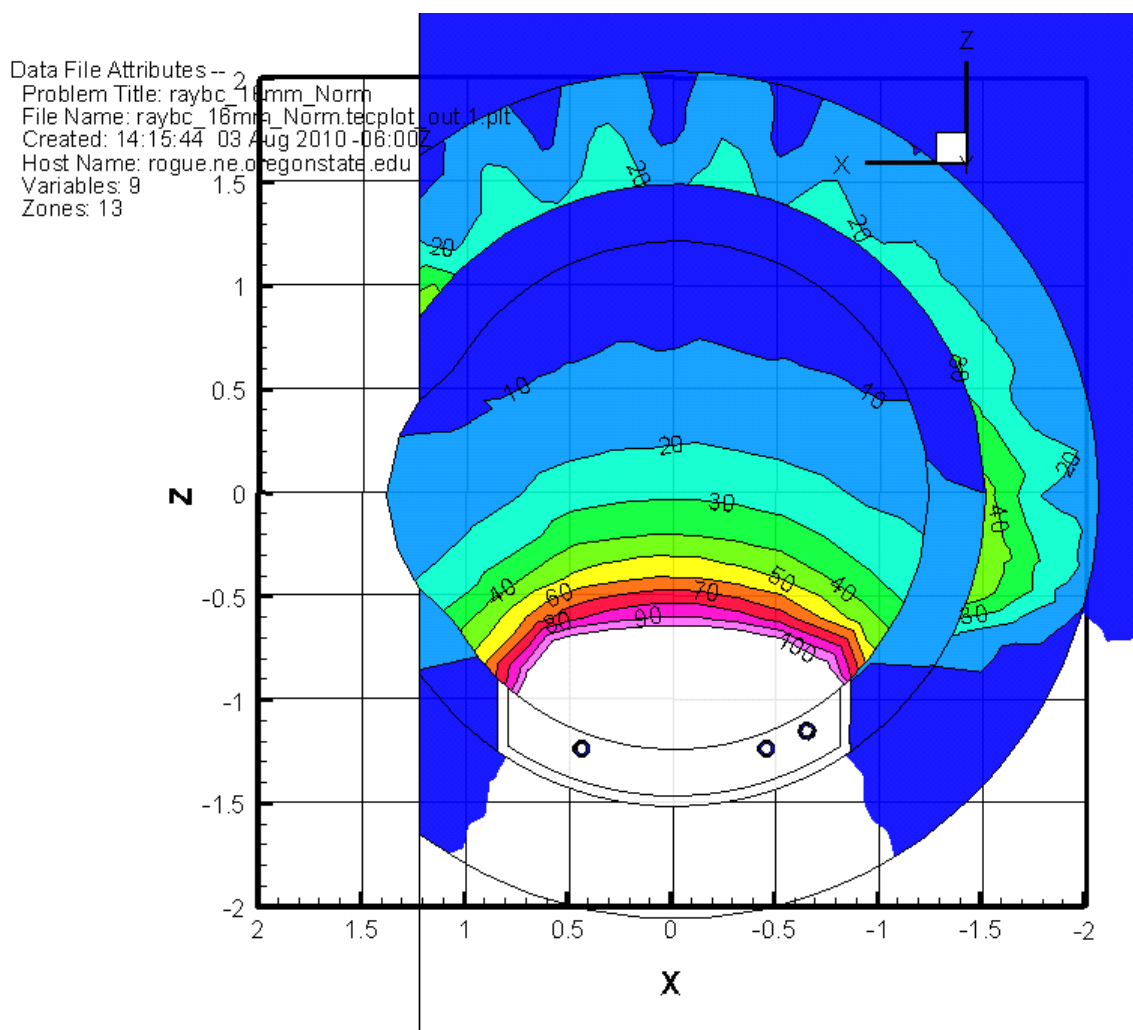


Figure 23 Y-plane 16mm plaque isodose lines from Attila, 100% at tumor apex

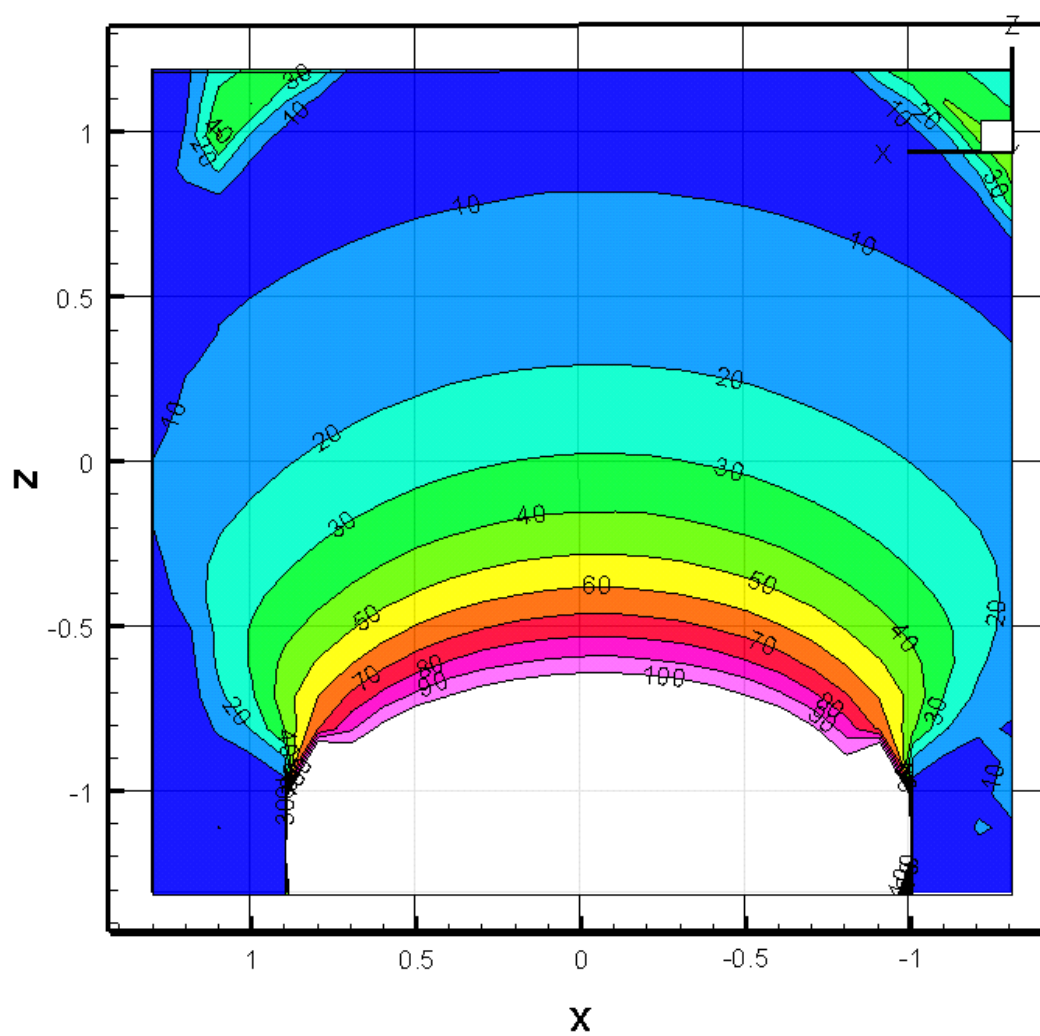


Figure 24: Y-plane 16mm plaque isodose lines from MCNPX, 100% at tumor apex

20 mm Plaque Normalized Isodose Lines

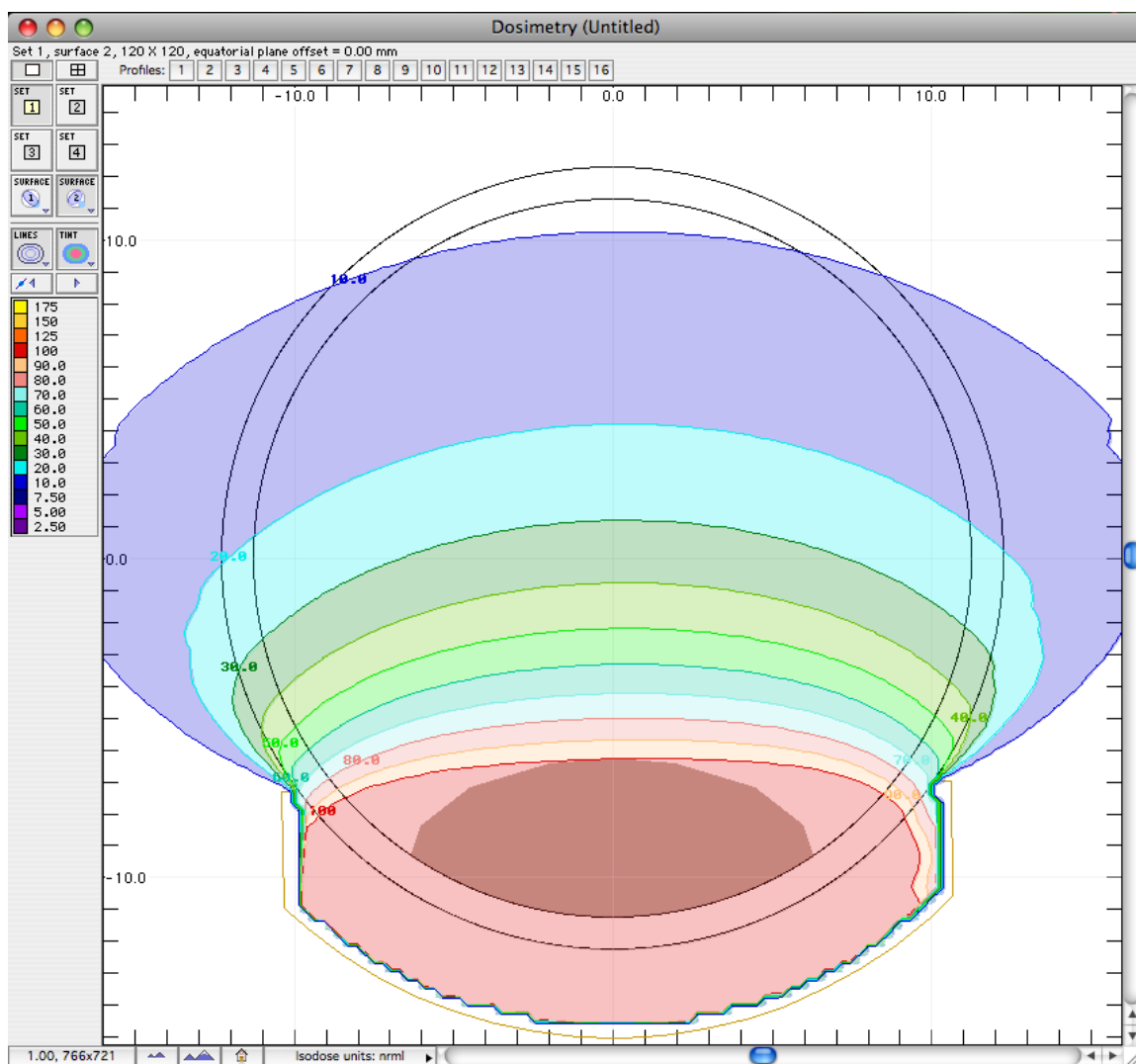


Figure 25: X-plane 20mm plaque isodose lines from the Plaque Simulator, 100% at tumor apex

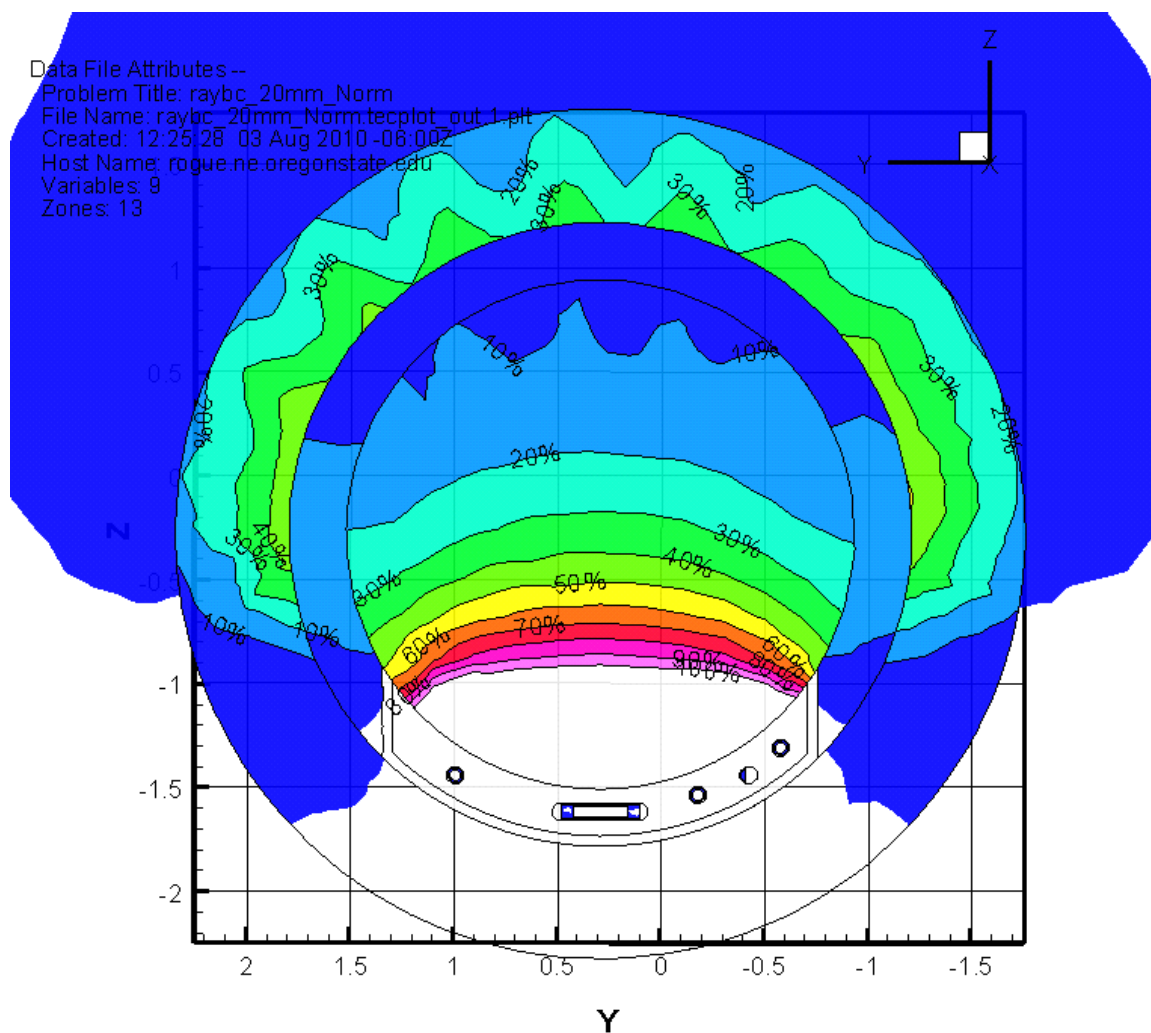


Figure 26: X-plane 20mm plaque isodose lines from Attila, 100% at tumor apex

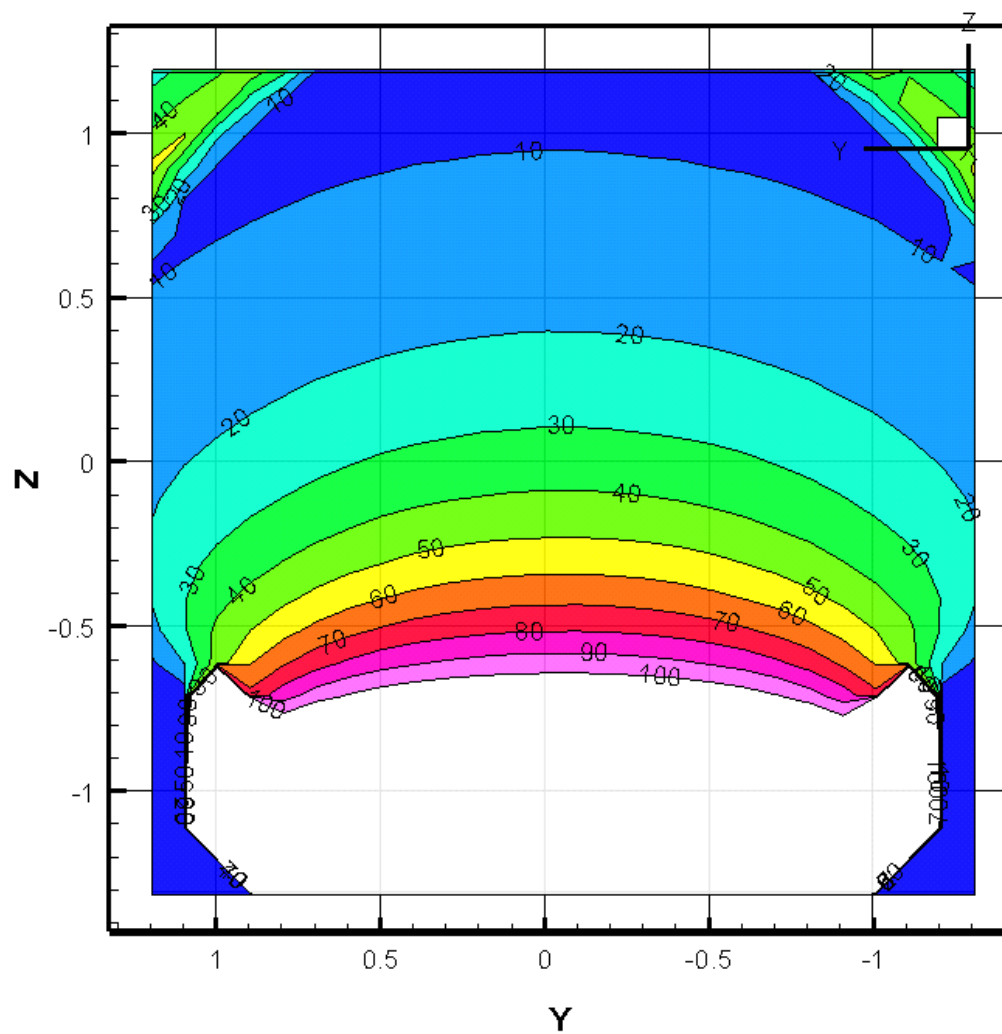


Figure 27: X-plane 20mm plaque isodose lines from MCNPX, 100% at tumor apex

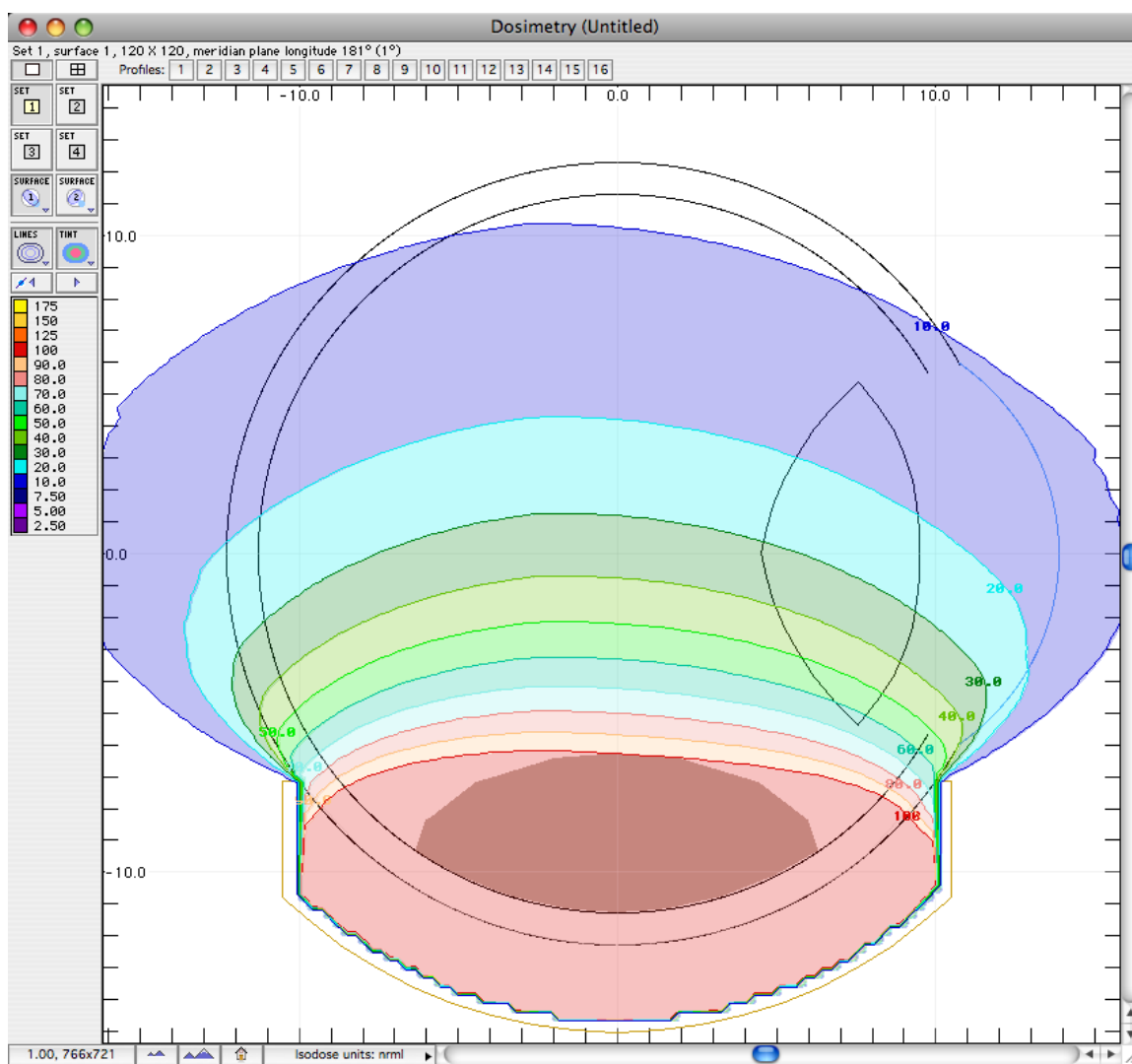


Figure 28: Y-plane 20mm plaque isodose lines from the Plaque Simulator, 100% at tumor apex

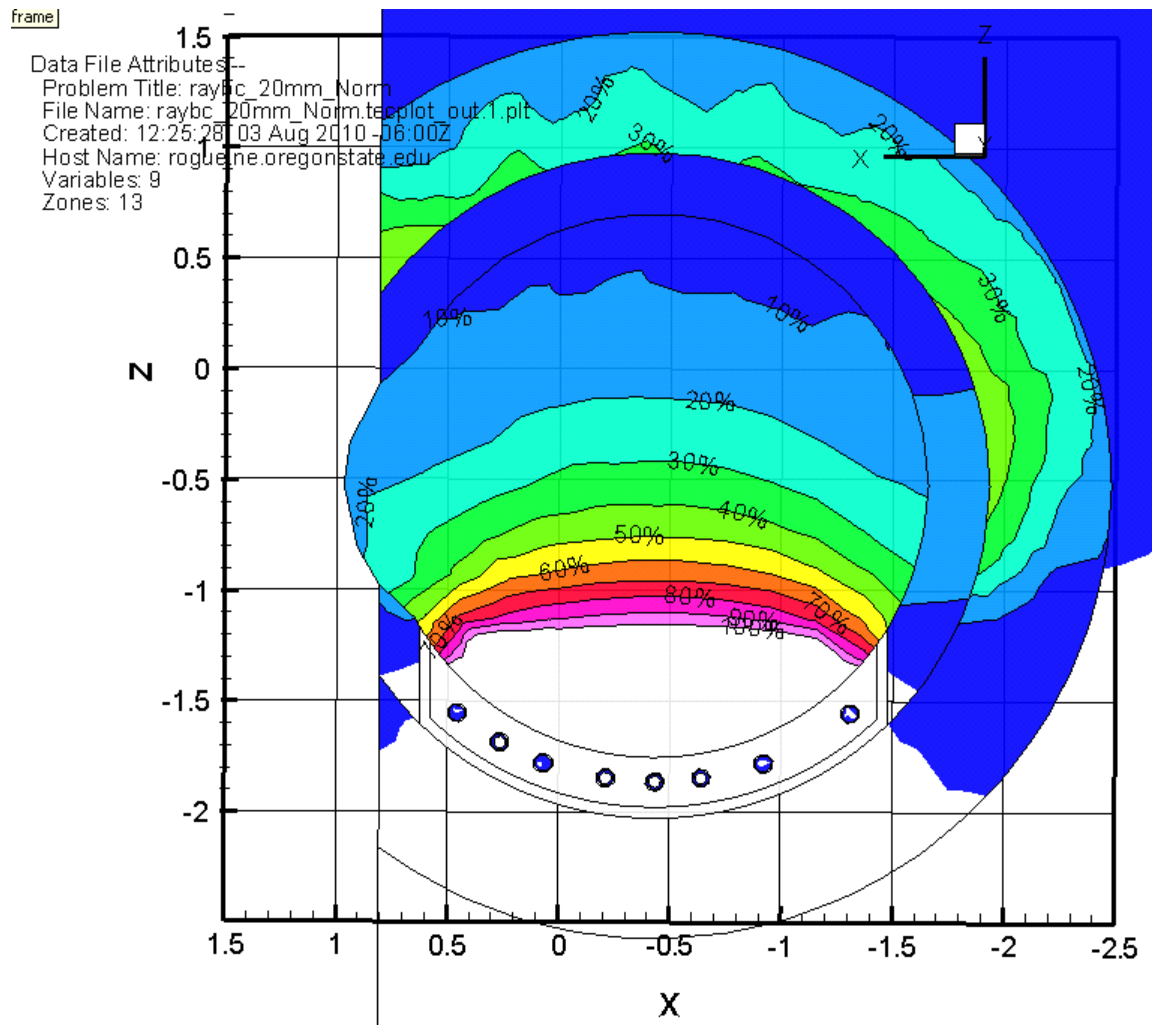


Figure 29: Y-plane 20mm plaque isodose lines from Attila, 100% at tumor apex

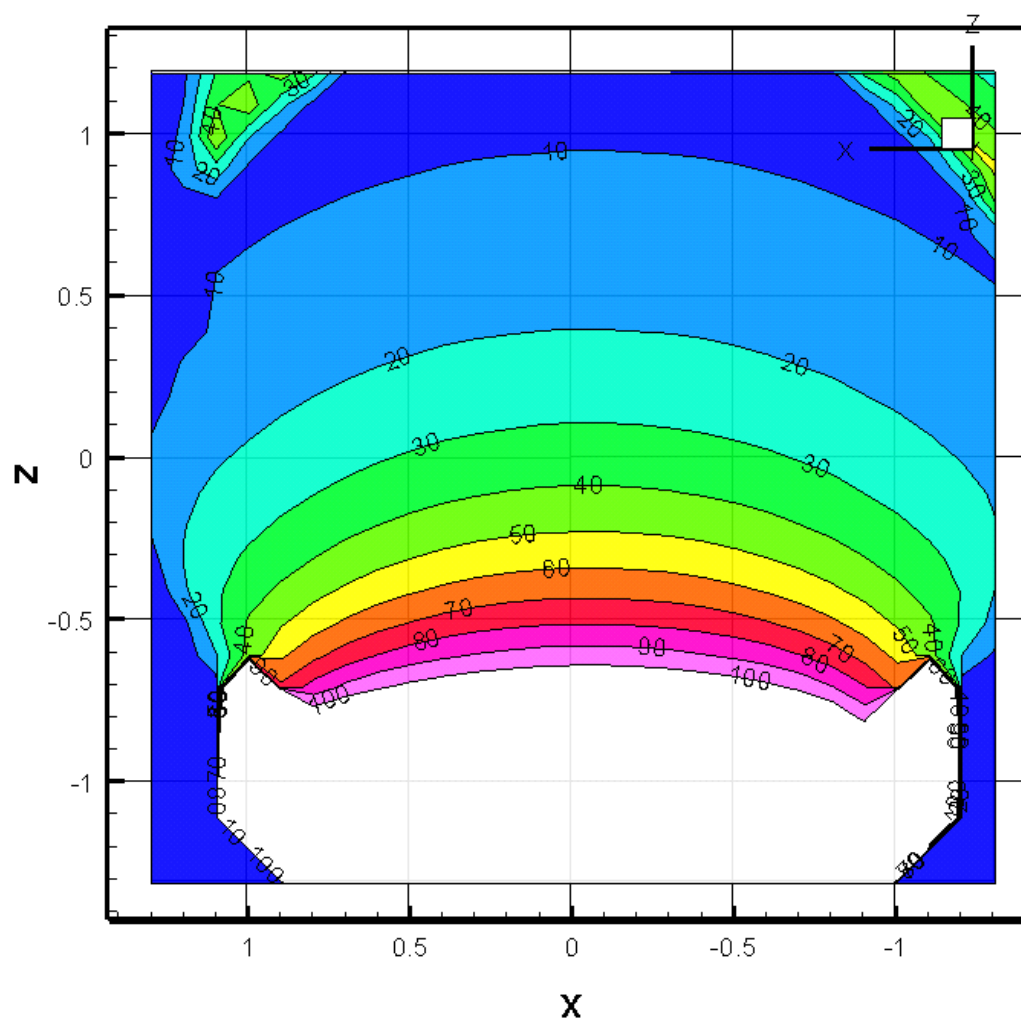


Figure 30: Y-plane 20mm plaque isodose lines from MCNPX, 100% at tumor apex

The comparison of percent depth isodose lines from the 16mm and 20mm COMS eye plaques in Figures 19-30 indicate differences unapparent in the 12mm COMS eye plaques. A notable difference appears between the Plaque Simulator percent depth isodose lines and those from MCNPX and Attila in the higher isodose lines. The 70% to 100% isodose lines in the Plaque Simulator are convex from the lip of the plaque. These same lines in the MCNPX and Attila calculations are concave from the lip of the plaque, following the curve of the insert.

20mm Isodose Line over 100%

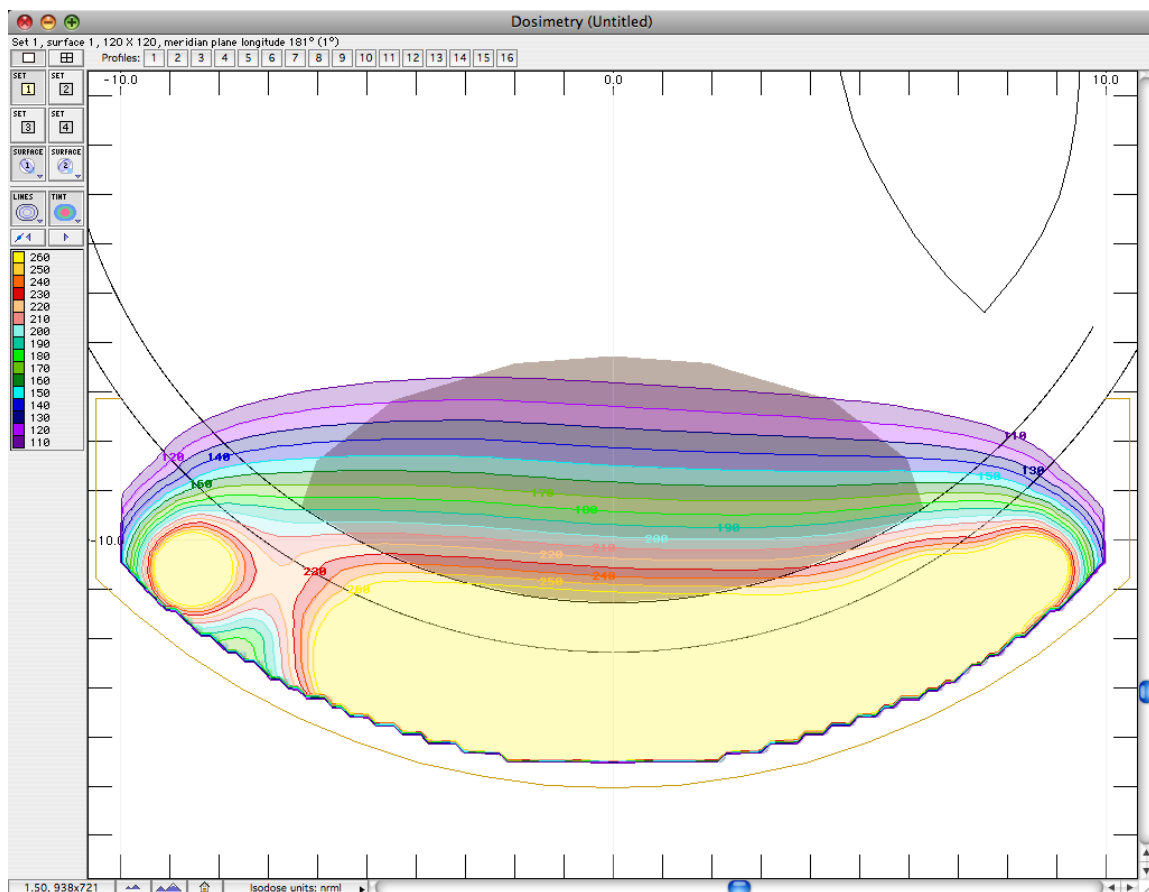


Figure 31: +100% Isodose lines of a 20mm plaque from the Plaque Simulator

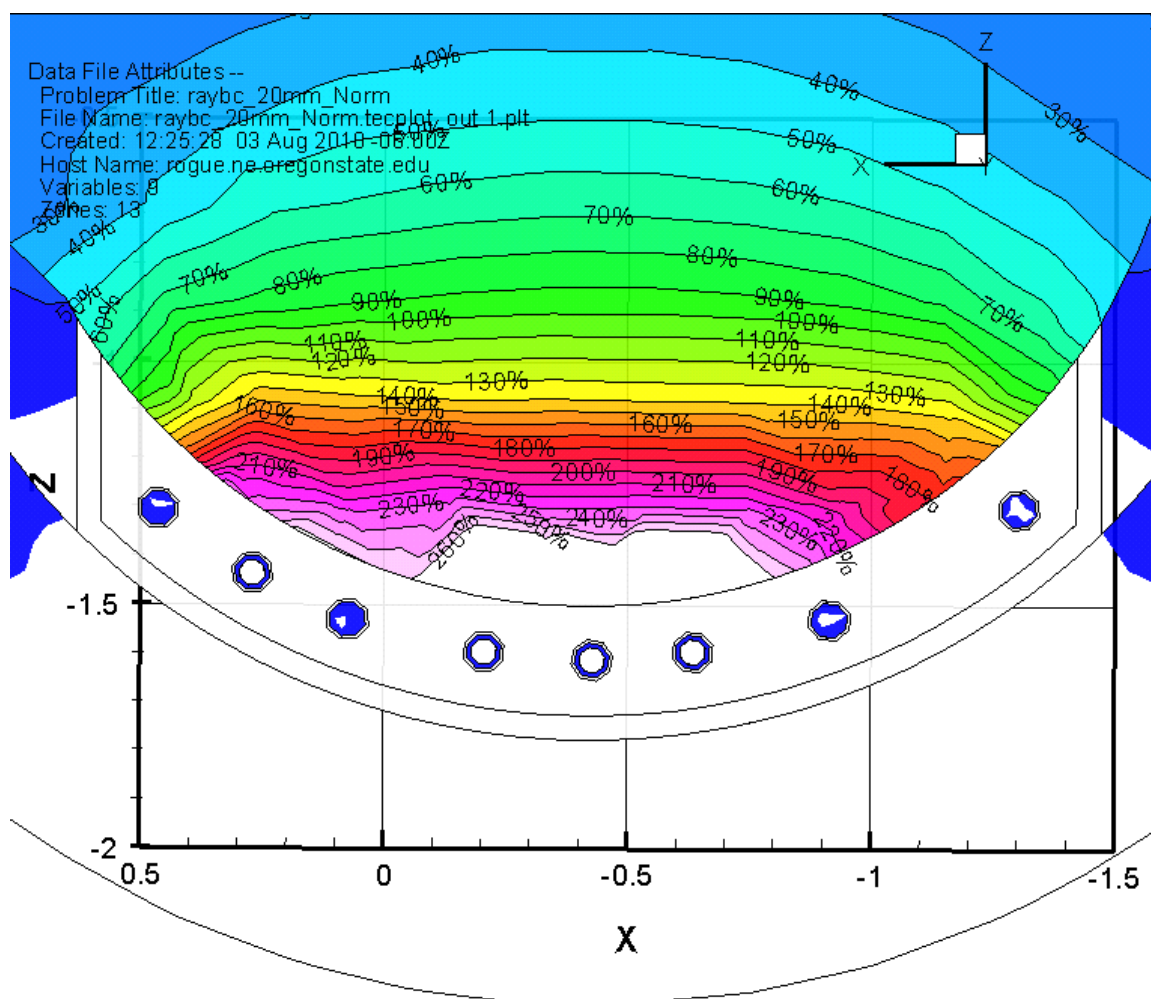


Figure 32: +100% Isodose lines of a 20mm plaque from Attila

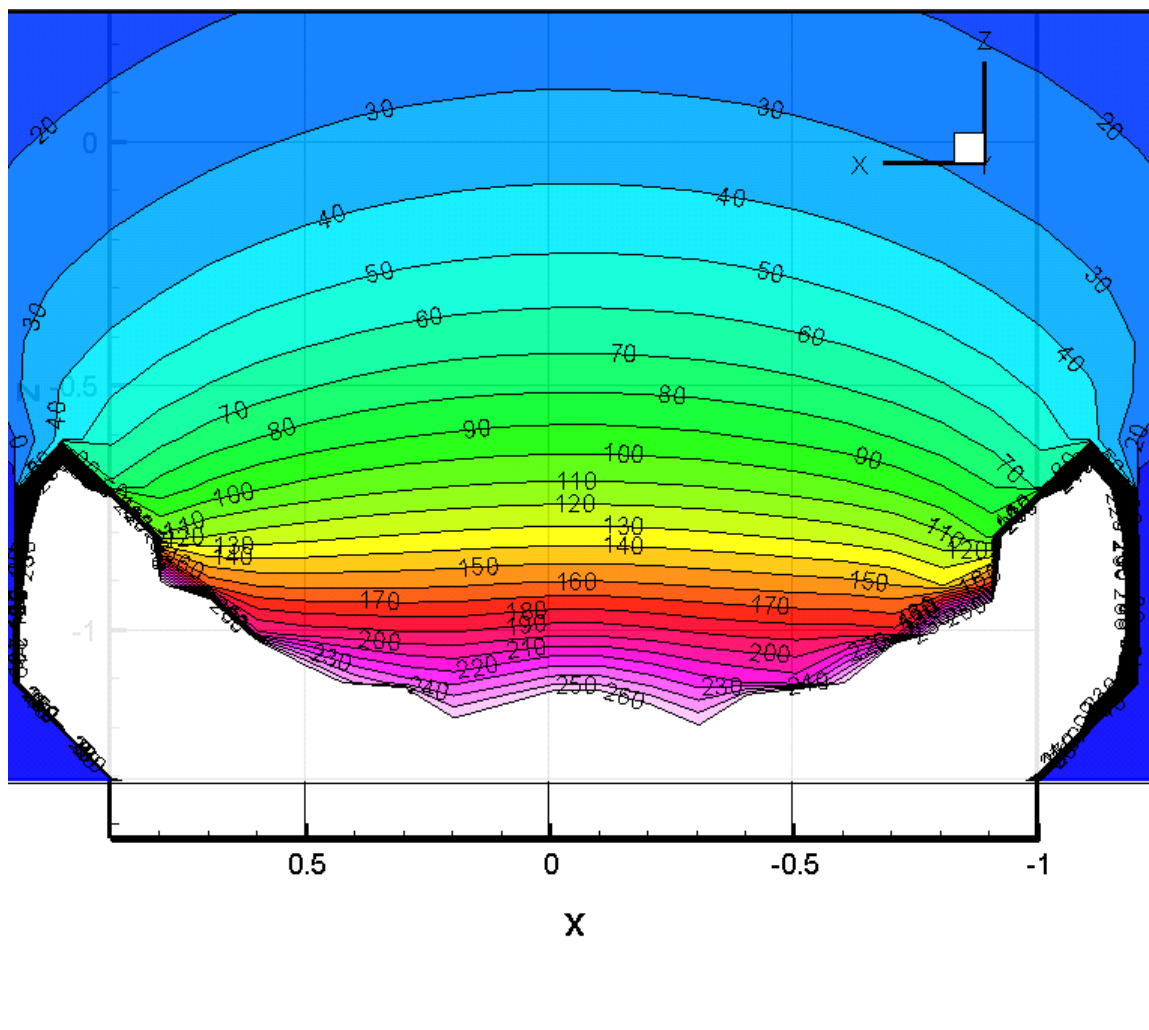


Figure 33: +100% Isodose lines of a 20mm plaque from the MCNPX

Figures 31-33 show a lack in detail from the Plaque Simulator at the regions of high dose near the surface of the plaque insert. The three programs were used here to demonstrate the depth along the plaque central axis a percent of the prescription dose will be absorbed. When looking at the distribution of the isodose lines it is clear that the Plaque Simulator doesn't calculate these dose distributions accurately.

Plaque's Central Axis & the Optic Axis Comparison

Figures 35-46 depict the extracted data values along the Optic axis of the eye and the central axis of the plaque. The data in Tables 6-11 from which these graphs were made of can be found in the Appendix. Figure 34 shows the location of the plaque relative to the eye, as well as indicating the axis used in the following graphs.

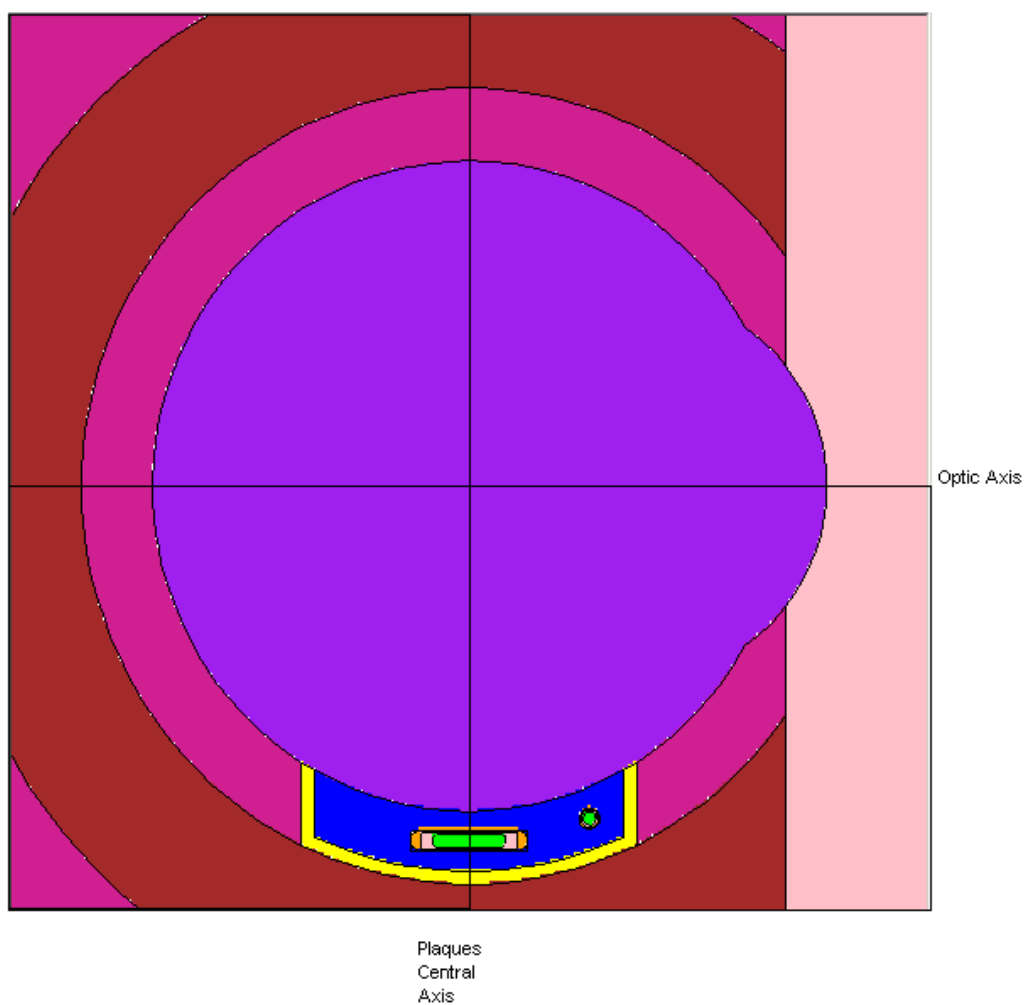


Figure 34: MCNPX phantom with the optic axis and the plaque central axis

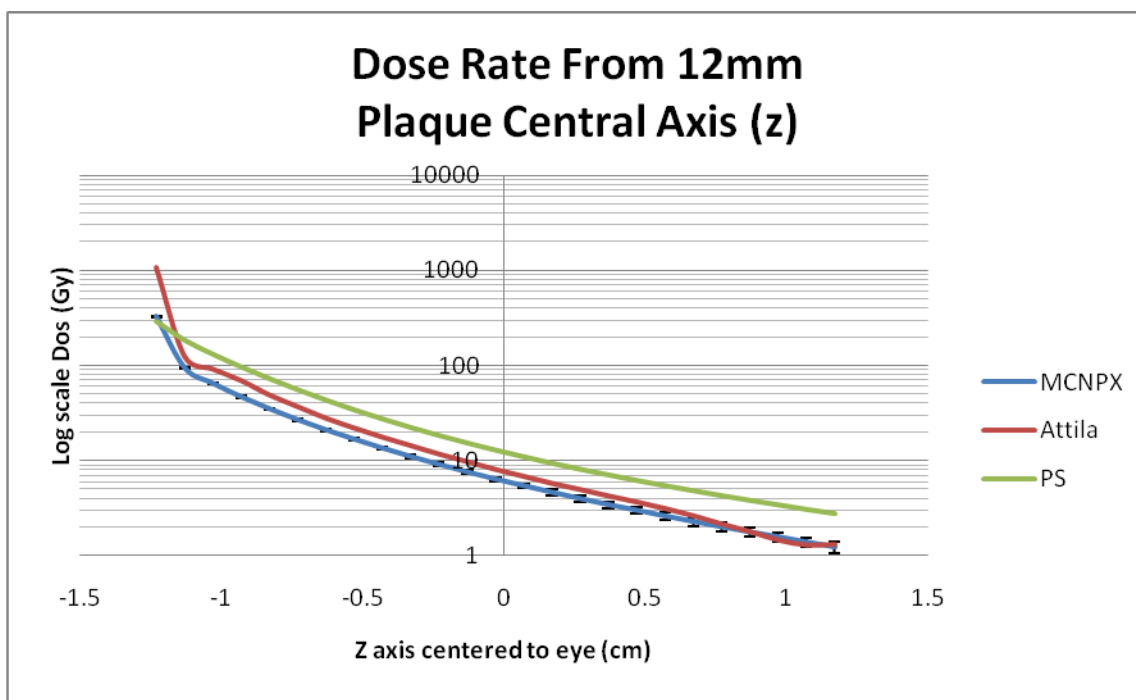


Figure 35: Plaques central axis dose comparison of the 12mm plaque

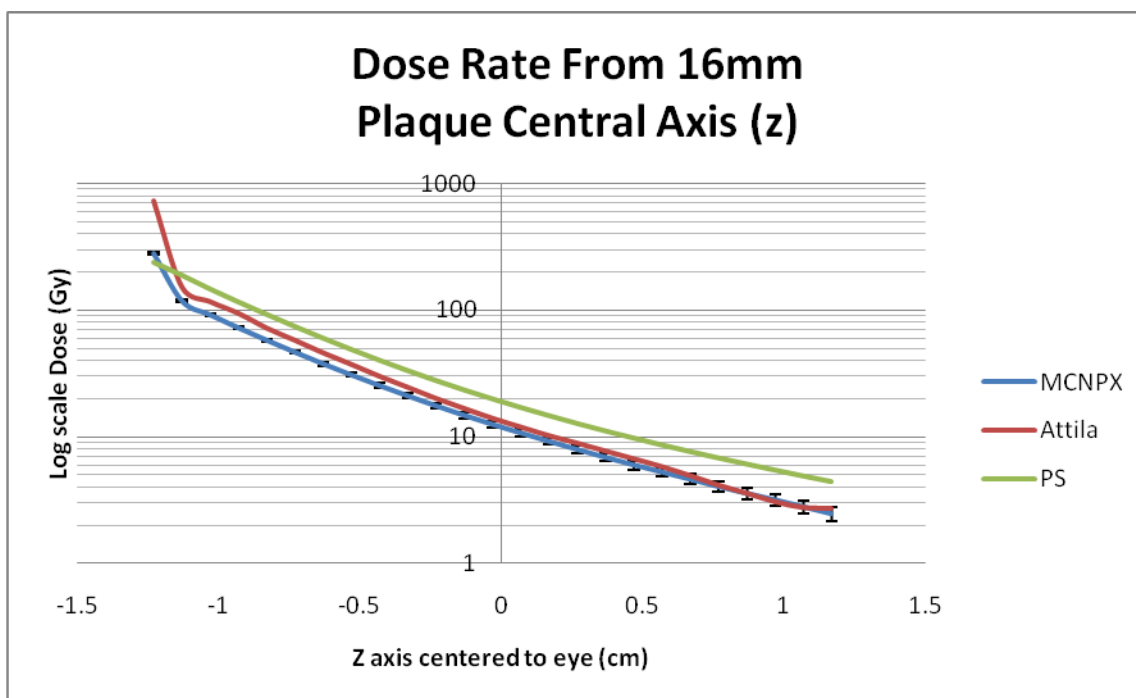


Figure 36: Plaques central axis dose comparison of the 16mm plaque

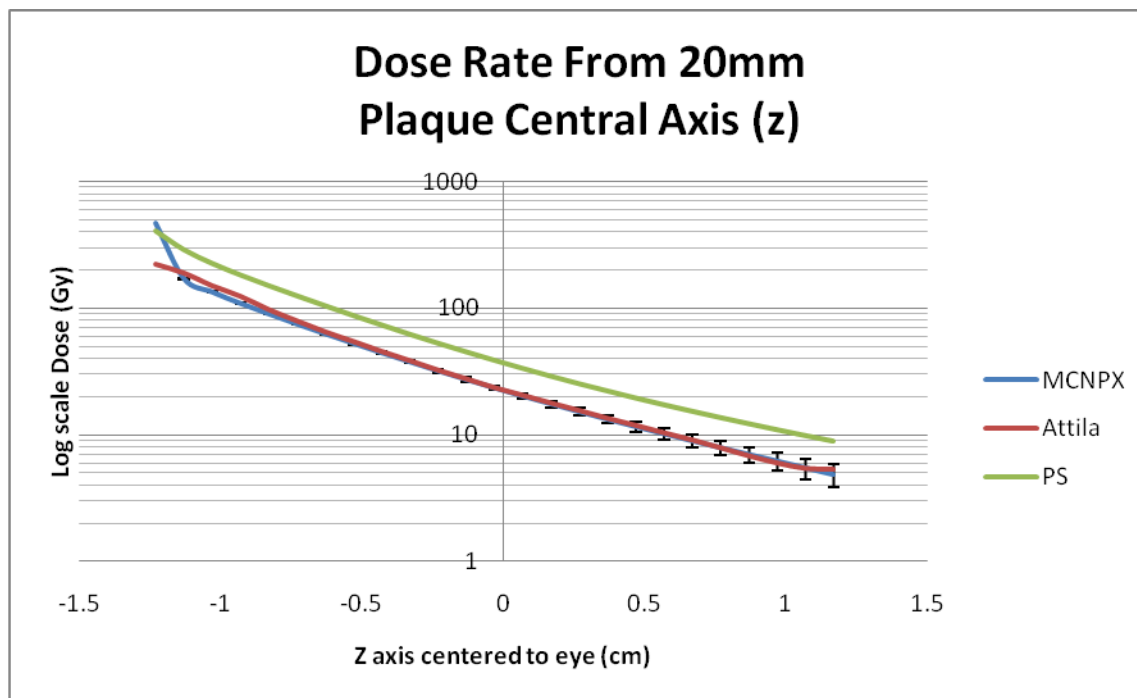


Figure 37: Plaques central axis dose comparison of the 20mm plaque

Figures 35-37 show that the Plaque Simulator's dose distributions are higher than those of both MCNPX and Attila. The difference in dose values between the Plaque Simulator and the other two programs could be in part due to the difference in the source's photon spectrum. The Plaque Simulator uses source specifications defined by AAMP's TG-43U1 for the ^{125}I Onco-seed model 6711. The MCNPX and Attila simulations used the photon spectrum of ICRP-38 for the decay of ^{125}I to ^{125}Te . The TG-43U1 photon spectrum is a simplified spectrum of photons emitted from the Onco-seed, and therefore is a hardened version of the actual ^{125}I spectrum. In both Attila and MCNPX the complete Onco-seed was modeled with the source as a thin coating of silver iodine inside the seed. Therefore the photon spectrum is attenuated through the titanium capsule of the seed. To accurately model the photon spectrum emitted from the seed, the source needed to be the complete photon spectrum from ^{125}I . The difference in source spectra may cause a small difference in the dose distributions.

Close to the plaque, MCNPX and Attila tend to disagree more than at distances further from the plaque. The dose gradient from all three programs seems to agree fairly well, with the Plaque Simulator underestimating the reduction near the opposite side of the eye.

Figures 38-40 show the dose from the three programs along the Optic axis with zero at the center of the eye, and along the plaque's central axis. The error bars on the MCNPX line indicate the 68% confidence interval of the MCNPX data.

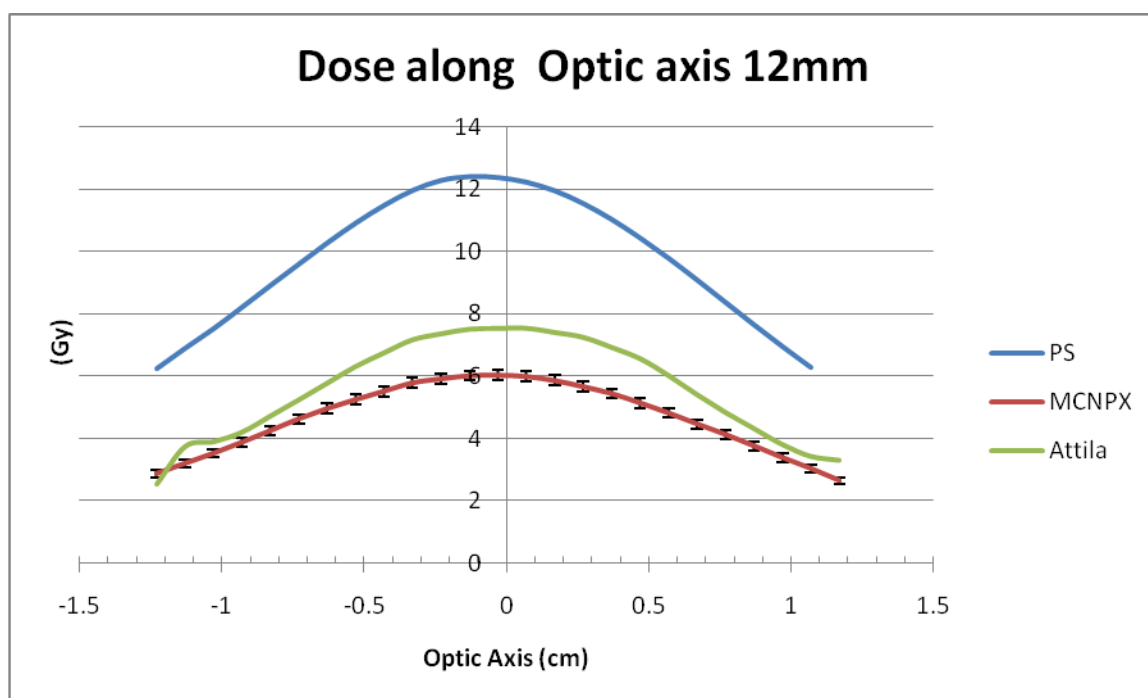


Figure 38: Optic axis dose comparison of the 12mm plaque

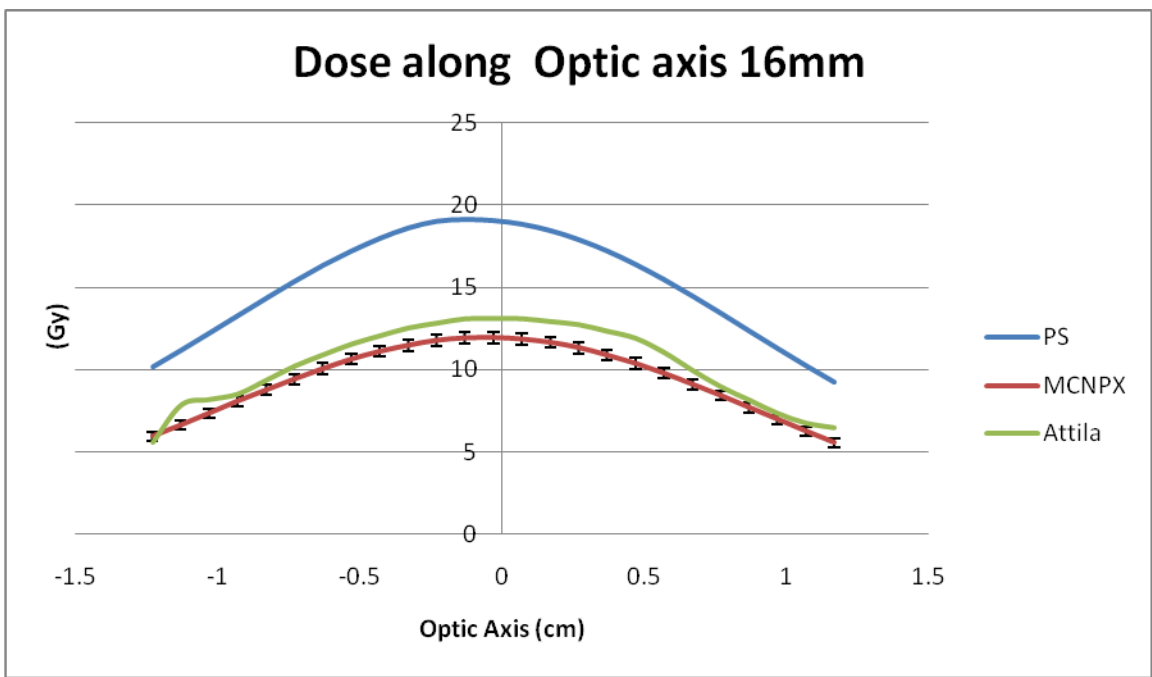


Figure 39: Optic axis dose comparison of the 16mm plaque

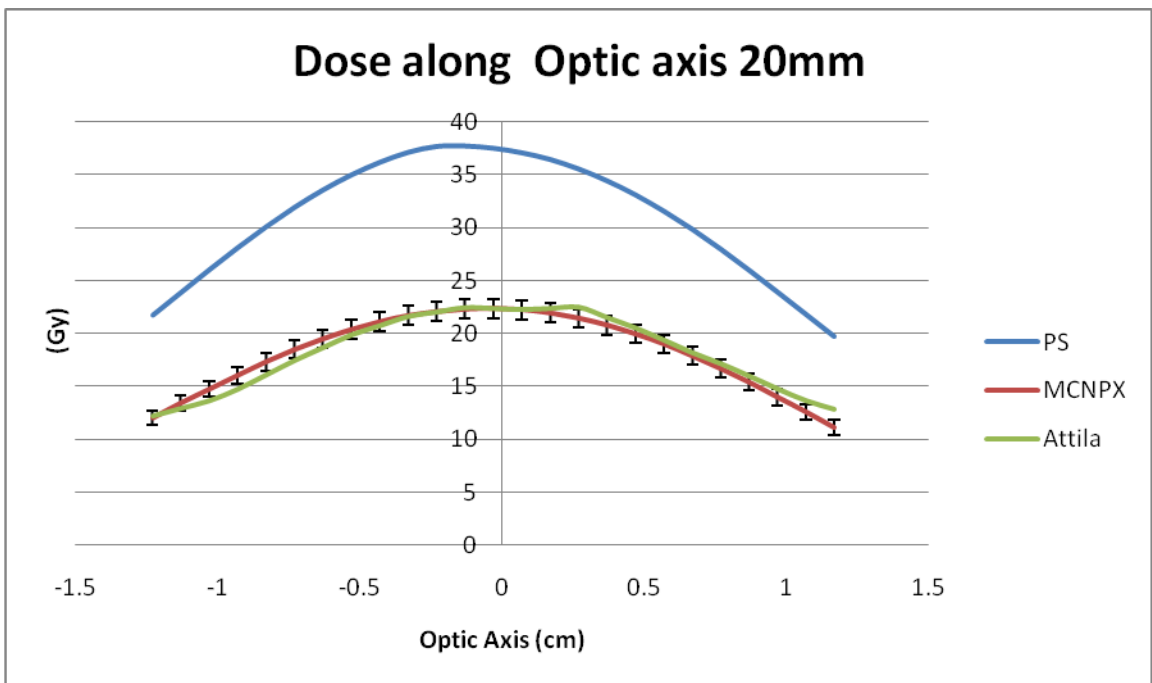


Figure 40: Optic axis dose comparison of the 20mm plaque

Figures 38-40 show that the dose estimate from the Plaque simulator is much higher than the other two programs – by nearly a factor of 2. Using the error bars that indicate the 68% confidence interval of the MCNPX data, both the 16mm and 20mm plaque distributions from Attila agree well with MCNPX. The 68% confidence error bars from the MCNPX dose values along optic axis of the 12mm plaque indicate that Attila is calculating different dose values than MCNPX.

Figures 41-43 are of the same data points along the optic axis only normalized to the center-of-eye dose value. The error bars on the MCNPX line indicate the 68% confidence interval of the MCNPX data.

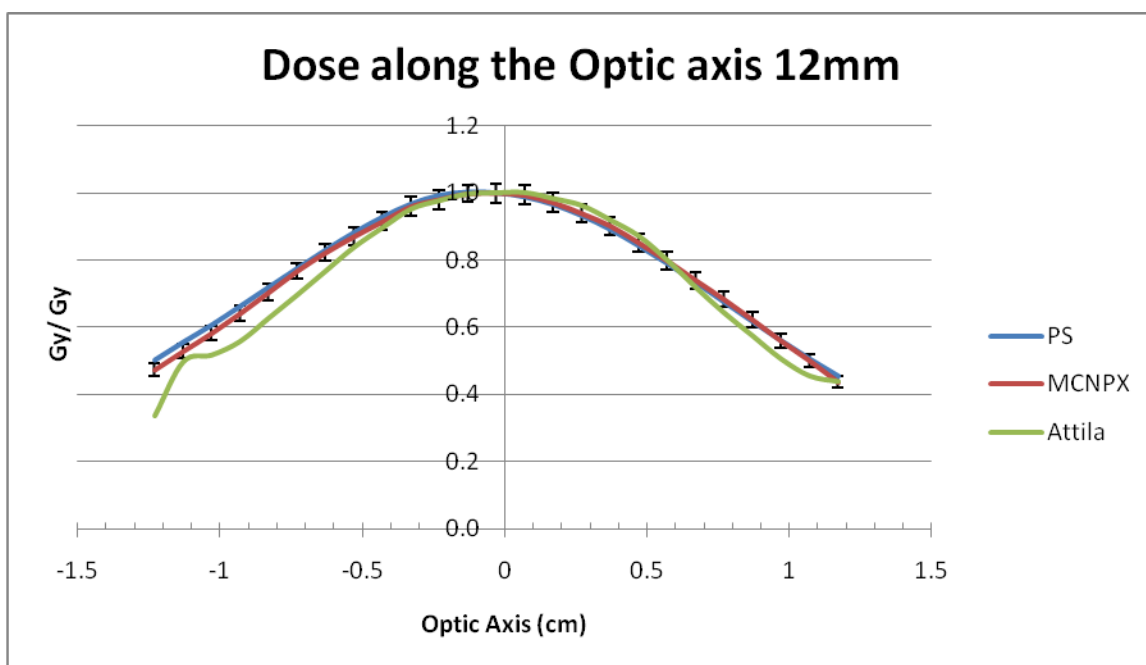


Figure 41: Optic axis normalized dose comparison of the 12mm plaque

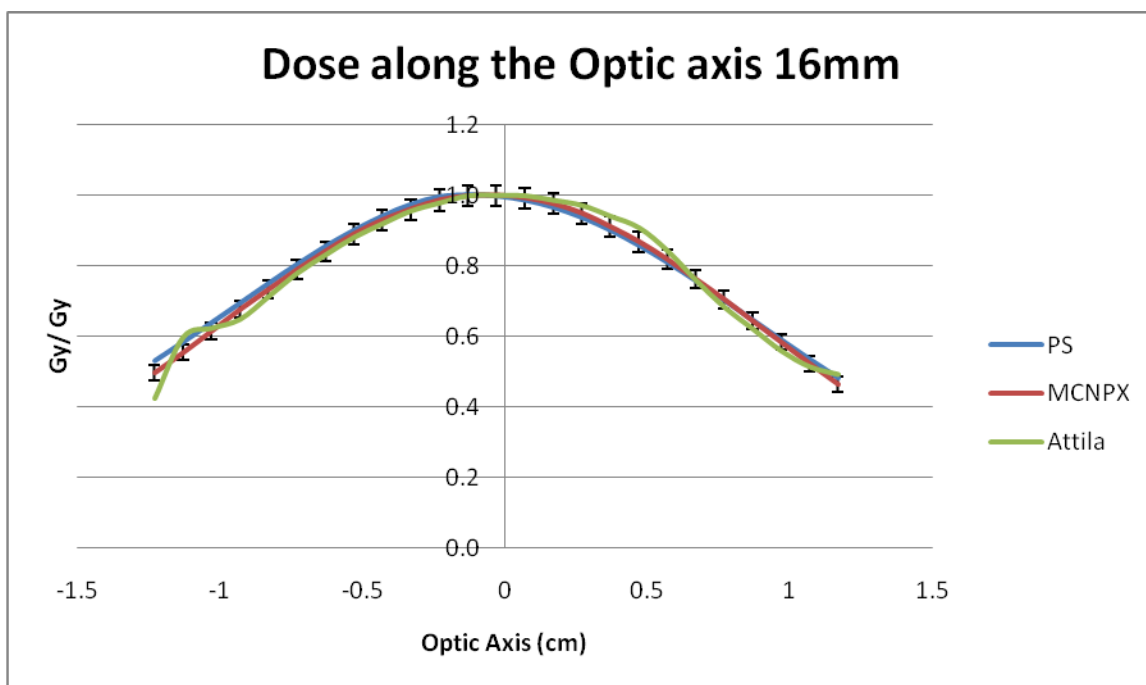


Figure 42: Optic axis normalized dose comparison of the 16mm plaque

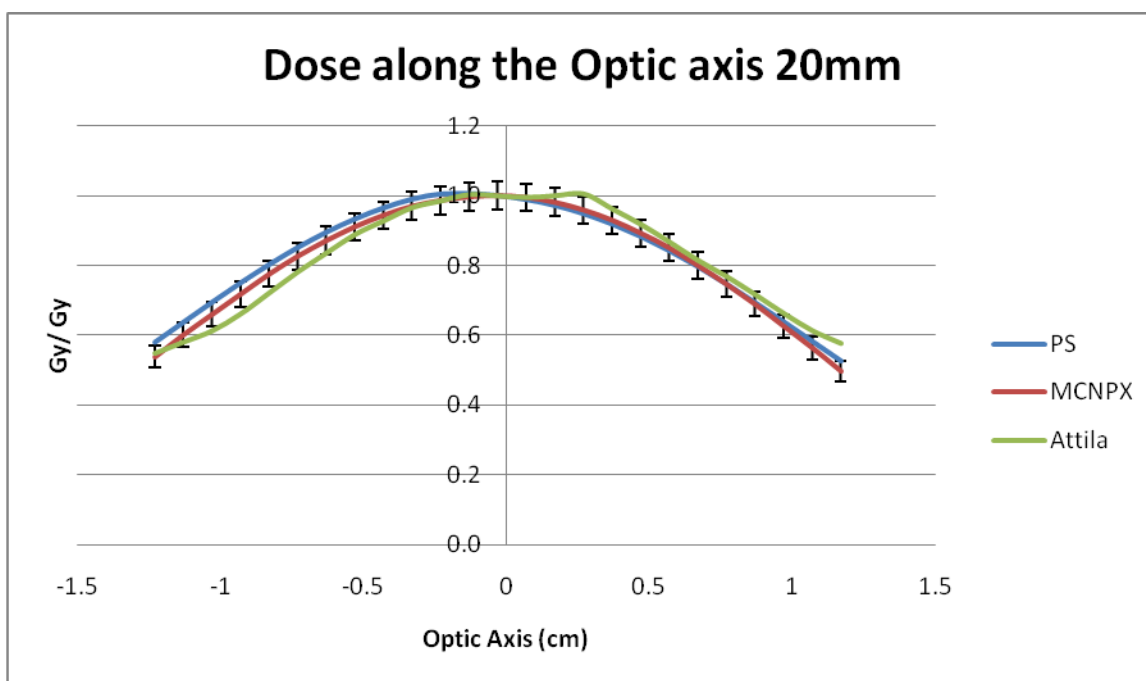


Figure 43: Optic axis normalized dose comparison of the 20mm plaque

The graphs of normalized dose distribution along the optic axis suggest that all three programs calculate nearly the same dose gradient away from the center of the eye.

Points of Interest

Tables 3-5 compare data points from locations of interest to oncologists from the three simulation tools. The simulated dose values have been manipulated to show the percent difference of the Plaque Simulator and Attila results compared to the MCNPX results. The differences are also displayed in percent depth dose with the dose at the Sclera equal to 100%. Tables 12-14 have the simulated dose values for each program at the points of interest, and can be found in the Appendix.

Table 3: Points of Interest dose difference and percent dose of 12mm plaque

12mm Eye Plaque					
Point of Interest	% diff. PS/ MCNPX	% diff. Attila/ MCNPX	% Dose PS	% Dose MCNPX	% Dose Attila
Macula	115%	17%	3.70%	3.38%	3.01%
Optical Disk	119%	26%	3.70%	3.32%	3.17%
Center of Lens	103%	18%	4.66%	4.50%	4.05%
Sclera	96%	32%	100.00%	100.00%	100.00%
Opposite side	127%	1%	1.57%	1.36%	1.04%
Tumor Apex	107%	33%	23.46%	22.24%	22.38%

Table 4: Points of Interest dose difference and percent dose of 16mm plaque

16mm Eye Plaque					
Point of Interest	% diff.	% diff.	% Dose	% Dose	% Dose
	PS/ MCNPX	Attila/ MCNPX	PS	MCNPX	Attila
Macula	68%	18%	5.87%	5.61%	5.18%
Optical Disk	72%	15%	5.90%	5.51%	4.95%
Center of Lens	59%	7%	7.27%	7.35%	6.14%
Sclera	61%	28%	100.00%	100.00%	100.00%
Opposite side	76%	3%	2.42%	2.21%	1.78%
Tumor Apex	60%	21%	31.72%	31.90%	30.22%

Table 5: Points of Interest dose difference and percent dose of 20mm plaque

20mm Eye Plaque					
Point of Interest	% diff.	% diff.	% Dose	% Dose	% Dose
	PS/ MCNPX	Attila/ MCNPX	PS	MCNPX	Attila
Macula	78%	-9%	8.23%	7.88%	6.51%
Optical Disk	83%	-3%	8.28%	7.68%	6.72%
Center of Lens	68%	2%	9.90%	10.05%	9.29%
Sclera	70%	10%	100.00%	100.00%	100.00%
Opposite side	85%	4%	3.24%	2.99%	2.82%
Tumor Apex	68%	3%	36.21%	36.79%	34.42%

These tables clearly show some variation between all three programs at these points of interest regardless of the plaque size. The percent dose difference between MCNPX and Attila is much smaller than those from the Plaque Simulator. When looking at the percent dose at the points of interest all three programs compare fairly well.

Speed and ease of using Attila vs. MCNPX and Plaque Simulator

In this project, Attila was able to perform most of the dose distribution calculation within 45 minutes while the same problem took approximately 14hrs in MCNPX. The Plaque Simulator may be faster at producing dose distributions than Attila; however, the accuracy of its results are limited by the dosimetric assumptions used for the calculation, and the availability only of eye dosimetry - no surrounding tissue. Dosimetric problems can also be quickly setup in Attila after the source spectrum, cross-section and geometry files have been loaded into the program. The geometry files can be easily created and loaded into Attila with SolidWorks export files. With these setup features and its solution speed, Attila could have potential in the clinical setting. However, due to the wide range of applications for Attila, there are many ways a user could run a simulation and get answers that are misleading. This is also true for the Plaque Simulator, which has a surprisingly large range of user definable parameters for the dose distribution calculations. These parameters allow a user to produce dose calculations consistent with their unique protocols. The problem with this large number of definable parameters is that two users can run similar versions of an identical treatment plan, and the Plaque Simulator could give significantly different dose distributions.

Areas for Improvement

This project could be expanded to look more closely at the source specification used for the Plaque Simulator, and determining the effects of the simplified source spectrum from AAPM. As indicated by the consistent dose increase by a factor of 2, there is some discrepancy between the source specifications used in the MCNPX and Attila simulations and source specifications used in the Plaque Simulator. The MCNPX data could be improved by using more histories, reducing the statistical error, if more computer time were available. This reduction in error would be important if the researcher wanted to prove either of the other programs simulation data disagreed with MCNPX. The input parameters of the Attila simulation could be adjusted to remove the unphysical oscillations in the percent depth dose lines.

Conclusion

The data from this project indicates that the Plaque Simulator, MCNPX, and Attila can all be used with reasonable success to estimate dose distributions from COMS eye plaques loaded with the ^{125}I Onco-seed model 6711. Plaque Simulator does not provide accurate details of the dose distribution near the surface of the plaque insert, or in the tissue and bone surrounding the eye. This lack of detail could be important when trying to estimate areas of the sclera that will receive high doses during the treatment. The dosimetric modeling provided by Attila offers greater resolution of the dose distribution near the plaque insert. The benefit of using Attila for dosimetric modeling can also be seen in the detail provided at tissue interfaces as well as the dose distribution outside the eye. The level of detail Attila offers compares well to that of MCNPX. The source strength specification used in this project may be suspect due to the average factor of 2 increases in calculated dose from the Plaque Simulator over the other two programs. The dose values from Attila and MCNPX along both the optic axis and the plaque's central axis compared well for all three plaque sizes. The variation in dose at the points of interest was outside the expected range. However when these dose values were normalized to the dose at the sclera, they agreed within 2%. All three programs studied here can be used to estimate the dose distribution of the COMS eye plaques loaded with ^{125}I Onco-seeds model 6711. The source parameters used in each program should be more closely studied to determine the source of the difference in estimate dose values.

Bibliography

1. Astrahan, Melvin A. "An Interactive Treatment Planning System for Ophthalmic Plaque Radiotherapy." *Int. J. of Radiation Oncology Bio. Phys* 18 (1990): 679-87.
2. Astrahan, Melvin A., Andrzej Szechter, and Paul T. Finger. "Design and Dosimetric Considerations of a Modified COMS Plaque: The Reusable Seed-Guide Insert." *Medical Physics* 32 (2005): 2706-16.
3. Astrahan, Melvin A. "A Patch Source model for Treatment Planning of Ruthenium Ophthalmic Applicators." *Medical Physics Journal* 30 (2003): 889-98.
4. Astrahan, Melvin A., Ph.D. "Improved Treatment Planning for COMS Eye Plaques." *Int. J. Radiation Oncology Biol. Phys* 61 (2005): 1227-42.
5. Beard, Charles H., M.D. *Ophthalmic surgery*. Philadelphia: P. Blakiston's Son & Co., 1910.
6. Chiu-Tsao, Sou-Tung, et al. "Dosimetry for I-125 seed (model 6711) in eye plaques." *Medical Physics* 20 (1993): 383-9.
7. Collaborative Ocular Melanoma Study Group. "Comparison of Clinical, Echographic, and Histopathological Measurements from Eyes with Medium-Sized Choroidal Melanoma in the Collaborative Ocular Melanoma Study: COMS Report No. 21." *Archive Ophthalmology* 121 (2003): 1163-71.
8. Collaborative Ocular Melanoma Study Group. "Quality of Life after Iodine 125 Brachytherapy versus Enucleation for Choroidal Melanoma: 5-Year Results From the Collaborative Ocular Melanoma Study: COMS QOLS Report No. 3." *Archive Ophthalmology* 124 (2006): 226-38.
9. Collaborative Ocular Melanoma Study Group. "Selection of Iodine 125 for the Collaborative Ocular Melanoma Study." *Archive Ophthalmology* 105 (1987): 763-4.
10. Collaborative Ocular Melanoma Study Group. "The COMS Randomized Trial of Iodine 125 Brachytherapy for Choroidal Melanoma, V. Twelve-Year Mortality Rates and Prognostic Factors: COMS Report No.28." *Archive Ophthalmology* 124 (2006): 1684-93.
11. Collaborative Ocular Melanoma Study Group, *Johns Hopkins University*. 21 June 1996. The National Eye Institute and the National Cancer Institute of the National Institutes of Health: U.S. Department of Health and Human Services. 11 Jan. 2010
<http://www.jhu.edu/wctb/coms/manual/coms_chap12.pdf>.

12. Cygler, Joanna , Janos Szanto, and Mazen Soubra. "Effect of gold and silver backings on the dose rate around an I-125 seed." *Medical Physics* 17 (1990): 172-8.
13. Dolan, James, Zuofeng Li, and Jeffery F. Williamson. "Monte Carlo and experimental dosimetry of an I-125 brachytherapy seed." *Medical Physics* 33 (2006): 4675-3684.
14. Knutsen, Stig, M.Sc., et al. "Dosimetric Verification of a Dedicated 3D Treatment Planning System for Apiscleral Plaque Therapy." *Int. J. of Radiation Oncology, Bio. Phys* 51 (2001): 1159-66.
15. Krintz, Amanda L., M.S., et al. "A Reanalysis of the Collaborative Ocular Melanoma Study Medium Tumor Trial Eye Plaque Dosimetry." *Int. J. of Radiation Oncology, Bio. Phys* 56 (2003): 889-98.
16. Luxton, Gary, Melvin A. Astrahan, and Zbigniew Petrovich. "Backscatter measurements from a single seed of I-125 for ophthalmic plaque dosimetry." *Medical Physics* 15 (1988): 397-400.
17. Melhus, Christopher S., Mark J. Rivard. "COMS eye plaque brachytherapy dosimetry simulations for ^{103}Pd , ^{125}I , and ^{131}Cs ." *Medical Physics* 35 (2008): 3364-71
18. Meli, Jerome A., and Kazi A. Motakabbir. "The effect of lead, gold, and silver backings on dose near I-125 seeds." *Medical Physics* 20 (1993): 1251-6.
19. Moore, R. F. "Choroidal sarcoma treated by the intraocular insertion of radon seeds." *British journal of ophthalmology* 14 (1930): 145-52.
20. Moshfeghi, Darius M., M.D., Andrew A. Moshfeghi, M.D., and Paul T. Finger, M.D. "Enucleation." *Survey of Ophthalmology* 44 (2000): 277-301.
21. Nag, Subir, M.D., et al. "The American Brachytherapy Society Recommendations for Brachytherapy of Uveal Melanomas." *Int. J. Radiation Oncology Biol. Phys* 56 (2003): 544-55.
22. Nath, Ravinder, et al. "Dosimetry of Interstitial Brachytherapy Sources: Recommendations of the AAPM Radiation Therapy Committee Task Group No. 43." *Medical Physics* 22 (1995): 209-34.
23. Packer, Kate. "Verification of Ophthalmic Brachytherapy Treatment Planning." *Australian Physical & Engineering Sciences in Medicine* 24 (2001): 177-80.
24. Rivard, Mark J., et al. "Update of AAPM Task Group No. 43 Report: A revised AAPM protocol for brachytherapy dose calculations." *Medical Physics* 31 (2004): 633-74.

25. Shultis, J. Kenneth, and Richard E. Faw. Radiation Shielding. La Grange Park, Illinois 60526 USA: American Nuclear Society, Inc, 2000.
26. Stallard, H. B. "Radiotherapy for malignant melanoma of the choroid." *British Journal of Ophthalmology* 50 (1966): 147-55.
27. Taylor, R P., and D O. Roger. Canada. University. Education. *Carleton University*. Aug. 2009. 16 Feb. 2010 <http://www.physics.carleton.ca/clrp/seed_database/i125/oncoseed_6711/>.
28. Thomson, R M., R E. Taylor, and D O. Rogers. "Monte Carlo dosimetry for I-125 and Pd-103 eye plaque brachytherapy." *Medical Physics* 35 (2008): 5530-43.
29. Weaver, Keith A. "The dosimetry of I-125 seed eye plaques." *Medical Physics* 13 (1986): 78-83.
30. Wu, Andrew, E. S. Sternick, and D J. Muise. "Effect of gold shielding on the dosimetry of an I-125 seed at close range." *Medical Physics* 15 (1988): 627-8.
31. Zerda, Alberto de la, Sou-Tung Chiu-Tsao, Jun Lin, Leslie L. Boulay, Ilham Kana, Jae Ho Kim. "I-125 eye plaque dose distribution including penumbra characteristics." *Medical Physics* 23 (1996): 407-18

Appendix

Appendix A: Dose Values from the plaque's Central Axis and the Optic Axis

Table 6: Plaque's central axis dose values for the 12mm plaque

Loc. Z-axis	Dst. z-axis	PS	MCNPX	Attila
		12mm	12mm	12mm
		Gy	Gy	GY
-1.23	0	291.02	328.116	1071.314
-1.13	0.1	185.37	94.484	124.570
-1.03	0.2	131.64	64.764	91.436
-0.93	0.3	97.01	46.780	69.379
-0.83	0.4	72.99	34.951	48.865
-0.73	0.5	55.88	26.819	36.859
-0.63	0.6	43.5	21.010	27.870
-0.53	0.7	34.36	16.718	21.929
-0.43	0.8	27.58	13.477	17.569
-0.33	0.9	22.44	11.002	14.350
-0.23	1	18.48	9.085	11.665
-0.13	1.1	15.41	7.558	9.714
-0.03	1.2	12.98	6.356	8.048
0.07	1.3	11.04	5.412	6.790
0.17	1.4	9.45	4.622	5.732
0.27	1.5	8.17	3.961	4.941
0.37	1.6	7.12	3.418	4.233
0.47	1.7	6.23	2.985	3.648
0.57	1.8	5.49	2.602	3.118
0.67	1.9	4.86	2.275	2.612
0.77	2	4.32	2.001	2.144
0.87	2.1	3.86	1.768	1.781
0.97	2.2	3.46	1.571	1.453
1.07	2.3	3.1	1.385	1.290
1.17	2.4	2.8	1.226	1.309

Table 7: Plaque's central axis dose values for the 16mm plaque

Loc. Z-axis	Dst. z-axis	PS	MCNPX	Attila
		16mm	16mm	16mm
		Gy	Gy	Gy
-1.23	0	240.72	280.374	728.525
-1.13	0.1	190.48	118.392	151.729
-1.03	0.2	148.17	91.891	116.330
-0.93	0.3	117.03	72.602	94.172
-0.83	0.4	93.3	58.001	71.981
-0.73	0.5	74.86	46.654	57.633
-0.63	0.6	60.48	37.762	45.859
-0.53	0.7	49.21	30.881	37.169
-0.43	0.8	40.38	25.441	29.906
-0.33	0.9	33.44	21.101	24.513
-0.23	1	27.91	17.613	19.995
-0.13	1.1	23.51	14.813	16.656
-0.03	1.2	19.97	12.580	13.931
0.07	1.3	17.08	10.761	11.881
0.17	1.4	14.72	9.248	10.152
0.27	1.5	12.76	7.970	8.867
0.37	1.6	11.14	6.911	7.688
0.47	1.7	9.78	6.019	6.671
0.57	1.8	8.63	5.289	5.783
0.67	1.9	7.65	4.642	4.914
0.77	2	6.81	4.064	4.131
0.87	2.1	6.09	3.597	3.566
0.97	2.2	5.46	3.194	3.052
1.07	2.3	4.9	2.818	2.751
1.17	2.4	4.42	2.484	2.702

Table 8: Plaque's central axis dose values for the 20mm plaque

Loc. Z-axis	Dst. z-axis	PS	MCNPX	Attila
		20mm	20mm	20mm
		Gy	Gy	Gy
-1.23	0	408.87	466.690	221.239
-1.13	0.1	290.95	170.692	188.552
-1.03	0.2	226.94	133.911	149.646
-0.93	0.3	184.05	108.901	123.667
-0.83	0.4	151.74	90.016	97.313
-0.73	0.5	126.08	74.972	79.075
-0.63	0.6	105.26	62.789	64.908
-0.53	0.7	88.22	52.768	54.401
-0.43	0.8	74.26	44.470	45.456
-0.33	0.9	62.8	37.695	38.437
-0.23	1	53.35	32.004	32.338
-0.13	1.1	45.57	27.340	27.610
-0.03	1.2	39.14	23.465	23.545
0.07	1.3	33.79	20.233	20.507
0.17	1.4	29.33	17.535	17.805
0.27	1.5	25.57	15.218	15.553
0.37	1.6	22.43	13.253	13.506
0.47	1.7	19.76	11.595	11.855
0.57	1.8	17.48	10.185	10.370
0.67	1.9	15.54	8.978	9.104
0.77	2	13.86	7.918	7.904
0.87	2.1	12.4	7.003	6.831
0.97	2.2	11.13	6.201	6.000
1.07	2.3	10.01	5.485	5.437
1.17	2.4	9.03	4.861	5.334

Table 9: Optic axis dose values for the 12mm plaque

Loc. x-axis	Dst. x-axis	PS	MCNPX	Attila
		12mm	12mm	12mm
-1.23	0	6.23	2.86	2.53
-1.13	0.1	6.89	3.19	3.74
-1.03	0.2	7.52	3.52	3.89
-0.93	0.3	8.21	3.87	4.20
-0.83	0.4	8.91	4.25	4.72
-0.73	0.5	9.6	4.63	5.24
-0.63	0.6	10.28	4.96	5.78
-0.53	0.7	10.92	5.25	6.32
-0.43	0.8	11.49	5.52	6.75
-0.33	0.9	11.97	5.79	7.17
-0.23	1	12.29	5.91	7.36
-0.13	1.1	12.41	6.02	7.51
-0.03	1.2	12.38	6.03	7.54
0.07	1.3	12.23	5.99	7.54
0.17	1.4	11.95	5.86	7.41
0.27	1.5	11.54	5.66	7.25
0.37	1.6	11.03	5.44	6.92
0.47	1.7	10.43	5.14	6.56
0.57	1.8	9.78	4.81	6.02
0.67	1.9	9.08	4.46	5.41
0.77	2	8.36	4.12	4.84
0.87	2.1	7.64	3.75	4.32
0.97	2.2	6.94	3.38	3.80
1.07	2.3	6.27	3.02	3.42
1.17	2.4	5.64	2.64	3.30

Table 10: Optic axis dose values for the 16mm plaque

Loc.	Dst.	PS	MCNPX	Attila
x-axis	x-axis	16mm	16mm	16mm
-1.23	0	10.16	5.95	5.57
-1.13	0.1	11.18	6.64	7.86
-1.03	0.2	12.23	7.36	8.19
-0.93	0.3	13.29	8.10	8.52
-0.83	0.4	14.35	8.77	9.37
-0.73	0.5	15.39	9.44	10.23
-0.63	0.6	16.36	10.06	10.93
-0.53	0.7	17.23	10.64	11.58
-0.43	0.8	18	11.12	12.08
-0.33	0.9	18.63	11.48	12.56
-0.23	1	19.04	11.79	12.86
-0.13	1.1	19.15	11.93	13.12
-0.03	1.2	19.08	11.96	13.14
0.07	1.3	18.86	11.86	13.13
0.17	1.4	18.47	11.66	12.96
0.27	1.5	17.92	11.34	12.76
0.37	1.6	17.23	10.88	12.36
0.47	1.7	16.41	10.38	11.94
0.57	1.8	15.49	9.78	11.08
0.67	1.9	14.49	9.11	9.98
0.77	2	13.44	8.43	8.98
0.87	2.1	12.36	7.70	8.16
0.97	2.2	11.29	6.98	7.35
1.07	2.3	10.24	6.26	6.75
1.17	2.4	9.23	5.56	6.47

Table 11: Optic axis dose values for the 20mm plaque

Loc.	Dst.	PS	MCNPX	Attila
x-axis	x-axis	20mm	20mm	20mm
-1.23	0	21.76	12.03	12.27
-1.13	0.1	23.92	13.45	12.99
-1.03	0.2	26.07	14.76	13.71
-0.93	0.3	28.15	16.06	14.80
-0.83	0.4	30.13	17.34	16.15
-0.73	0.5	31.96	18.49	17.50
-0.63	0.6	33.6	19.49	18.71
-0.53	0.7	35.02	20.38	19.90
-0.43	0.8	36.21	21.11	20.77
-0.33	0.9	37.15	21.68	21.63
-0.23	1	37.7	22.06	22.05
-0.13	1.1	37.74	22.29	22.46
-0.03	1.2	37.53	22.36	22.38
0.07	1.3	37.1	22.25	22.28
0.17	1.4	36.46	21.93	22.39
0.27	1.5	35.57	21.44	22.50
0.37	1.6	34.45	20.78	21.53
0.47	1.7	33.12	19.95	20.55
0.57	1.8	31.58	19.01	19.41
0.67	1.9	29.87	17.88	18.23
0.77	2	28	16.69	17.20
0.87	2.1	26.01	15.40	16.04
0.97	2.2	23.94	13.99	14.83
1.07	2.3	21.84	12.61	13.72
1.17	2.4	19.74	11.12	12.90

Appendix B: Points of Interest Dose Values

Table 12: Points of Interest dose values for the 12mm plaque

Dose for 12mm Plaque (Gy)				
Point of Interest	Plaque Simulator	MCNPX		Attila
Macula	6.859	3.192	3.87%	3.743
Optical Disk	6.859	3.138	3.85%	3.947
Center of Lens	8.647	4.253	3.37%	5.040
Sclera	185.400	94.484	0.72%	124.542
Opposite side	2.914	1.285	6.27%	1.300
Tumor Apex	43.500	21.010	1.49%	27.866

Table 13: Points of Interest dose values for the 16mm plaque

Dose for 16mm Plaque (Gy)				
Point of Interest	Plaque Simulator	MCNPX		Attila
Macula	11.180	6.636	4.11%	7.858
Optical Disk	11.250	6.523	4.14%	7.508
Center of Lens	13.860	8.701	3.56%	9.320
Sclera	190.600	118.392	1.13%	151.729
Opposite side	4.606	2.612	6.28%	2.702
Tumor Apex	60.460	37.762	1.68%	45.859

Table 14: Points of Interest dose values for the 20mm plaque

Dose for 20mm Plaque (Gy)				
Point of Interest	Plaque Simulator	MCNPX		Attila
Macula	23.920	13.454	5.59%	12.268
Optical Disk	24.050	13.115	5.65%	12.675
Center of Lens	28.760	17.159	4.84%	17.521
Sclera	290.500	170.692	1.96%	188.552
Opposite side	9.409	5.099	8.33%	5.323
Tumor Apex	105.200	62.789	2.43%	64.908

Appendix C: MCNPX 12 mm Input Deck:

```

12mm Eye Plaque with 8 seeds: mode p source type 2
c
c Cell Cards
c
  1      9   -1.03 (-24 :-21 ) $cell of the phantom eye
  2      2   -1.12 (21 -22 -35 )37 137 237 337 437 537 637 &
$silastic insert
          737
  3      3   -15.8 (21 -22 -36 35 ):(22 -23 -36 ) $cell of Gold
alloy plaque
c
c Cells of Seed 1
c
  4      5   -10.5 (-31 :-41 :-42 ) $Silver rod seed 1
  5      6   -6.425 (-32 :-43 :-44 )#4 $AgI/AgBr coating seed 1
  6      8  -0.00120479 -33 #4 #5 $Air inside seed 1
  7      7   -4.54 (-34 :-25 :-26 )#4 #5 #6 $Titanium capsule
seed 1
  8      2   -1.12 -37 #4 #5 #6 #7 $cylinder containing the
seed 1
c
c Cells of Skull Bone, Phantom Head, and Air interface
c
  9      10  -1.60 (23 -17 -10) $skull bone around eye
  10     1   -1.0  (11 -10)(15 -14)(13 -12) 17 $Phantom head
outside skull bone
  11     1   -1.0  (21 24 -23 36 -10) $tissue between skull and
eye
  12     8   -0.00120479 (10 -16 15 -14 13 -12 24) $air
interface
c
c Cells of seed 2

```

c

14 5 -10.5 (-131 :-141 :-142) \$Silver rod seed 2
 15 6 -6.425 (-132 :-143 :-144)#14 \$AgI/AgBr coating
 seed 2
 16 8 -0.00120479 -133 #14 #15 \$Air inside seed 2
 17 7 -4.54 (-134 :-125 :-126)#14 #15 #16 \$Titanium
 capsule seed 2
 18 2 -1.12 -137 #14 #15 #16 #17 \$cylinder containing
 the seed 2

c

c Cells of seed 3

c

24 5 -10.5 (-231 :-241 :-242) \$Silver rod seed 3
 25 6 -6.425 (-232 :-243 :-244)#24 \$AgI/AgBr coating
 seed 3
 26 8 -0.00120479 -233 #24 #25 \$Air inside seed 3
 27 7 -4.54 (-234 :-225 :-226)#24 #25 #26 \$Titanium
 capsule seed 3
 28 2 -1.12 -237 #24 #25 #26 #27 \$cylinder containing
 the seed 3

c

c Cells of Seed 4

c

34 5 -10.5 (-331 :-341 :-342) \$Silver rod seed 4
 35 6 -6.425 (-332 :-343 :-344)#34 \$AgI/AgBr coating
 seed 4
 36 8 -0.00120479 -333 #34 #35 \$Air inside seed 4
 37 7 -4.54 (-334 :-325 :-326)#34 #35 #36 \$Titanium
 capsule seed 4
 38 2 -1.12 -337 #34 #35 #36 #37 \$cylinder containing
 the seed 4

c

c Cells of Seed 5

c

44 5 -10.5 (-431 :-441 :-442) \$Silver rod seed 5
 45 6 -6.425 (-432 :-443 :-444)#44 \$AgI/AgBr coating
 seed 5
 46 8 -0.00120479 -433 #44 #45 \$Air inside seed 5
 47 7 -4.54 (-434 :-425 :-426)#44 #45 #46 \$Titanium
 capsule seed 5
 48 2 -1.12 -437 #44 #45 #46 #47 \$cylinder containing
 the seed 5

c

c Cells of Seed 6

c

54 5 -10.5 (-531 :-541 :-542) \$Silver rod seed 6
 55 6 -6.425 (-532 :-543 :-544)#54 \$AgI/AgBr coating
 seed 6
 56 8 -0.00120479 -533 #54 #55 \$Air inside seed 6
 57 7 -4.54 (-534 :-525 :-526)#54 #55 #56 \$Titanium
 capsule seed 6
 58 2 -1.12 -537 #54 #55 #56 #57 \$cylinder containing
 the seed 6

c

c Cells of Seed 7

c

64 5 -10.5 (-631 :-641 :-642) \$Silver rod seed 7
 65 6 -6.425 (-632 :-643 :-644)#64 \$AgI/AgBr coating
 seed 7
 66 8 -0.00120479 -633 #64 #65 \$Air inside seed 7
 67 7 -4.54 (-634 :-625 :-626)#64 #65 #66 \$Titanium
 capsule seed 7
 68 2 -1.12 -637 #64 #65 #66 #67 \$cylinder containing
 the see

c

c Cells of Seed 8

c

74 5 -10.5 (-731 :-741 :-742) \$Silver rod seed 8

```

75      6  -6.425 (-732 :-743 :-744 )#74  $AgI/AgBr coating
seed 8
76      8  -0.00120479 -733 #74 #75  $Air inside seed 8
77      7  -4.54 (-734 :-725 :-726 )#74 #75 #76  $Titanium
capsule seed 8
78      2  -1.12 -737 #74 #75 #76 #77  $cylinder containing
the see
999     0  14: -15: 12: -13: 16: -11 $Void

```

c

c Surface Cards

c

```

10      px  1.23  $ outer plane of water head
11      px -28.77 $ outer plane of water head
12      py  15.0  $ outer plane of water head
13      py -15.0  $ outer plane of water head
14      pz  15.0  $ outer plane of water head
15      pz -15.0  $ outer plane of water head
16      px  15.0  $ outer plane of air interface
17      sph 0 0 0 2.05  $ outer sphere of skull bone
21      sph 0 0 0 1.23  $lateral sphere of eye
22      sph 0 0 0 1.455  $inner surface of plaque
23      sph 0 0 0 1.505  $outer surface of plaque
24      sph 0.663 0 0 0.727  $cornea
25      sph -0.1875 0 -1.34 0.04  $titanium cap weld
26      sph 0.1875 0 -1.34 0.04  $titanium cap weld

```

c

c Onco Seed 6711 surfaces #1

c

```

31      rcc -0.12975 0 -1.34 0.2595 0 0 0.02475  $Ag cylinder
32      rcc -0.13 0 -1.34 0.26 0 0 0.025  $AgI/AgBr cylinder
33      rcc -0.1875 0 -1.34 0.375 0 0 0.034  $Air cylinder
34      rcc -0.1875 0 -1.34 0.375 0 0 0.04  $Titanium capsule

```

```

35      rcc 0 0 -0.97 0 0 $cylinder defining the inner radius
of plaque
          -0.54 0.6
36      rcc 0 0 -0.97 0 0 $cylinder defining the outer radius
of plaqu
          -0.54 0.65
37      rcc -0.22755 0 -1.34 0.4551 0 0 0.0401 $cylinder
cantaining seed
41      trc -0.12975 0 -1.34 -0.0099 0 0 0.02475 0.01485 $Ag
bevel @ origin
42      trc 0.12975 0 -1.34 0.0099 0 0 0.02475 0.01485 $Ag
bevel op. origin
43      trc -0.13 0 -1.34 -0.01 0 0 0.025 0.015 $AgI bevel @
origin
44      trc 0.13 0 -1.34 0.01 0 0 0.025 0.015 $AgI bevel op.
origin
c
c Onco Seed 6711 surfaces #2
c
125     sph -0.1875 0.285 -1.31 0.04 $titanium cap weld
126     sph 0.1875 0.285 -1.31 0.04 $titanium cap weld
131     rcc -0.12975 0.285 -1.31 0.2595 0 0 0.02475 $Ag
cylinder
132     rcc -0.13 0.285 -1.31 0.26 0 0 0.025 $AgI/AgBr
cylinder
133     rcc -0.1875 0.285 -1.31 0.375 0 0 0.034 $Air
cylinder
134     rcc -0.1875 0.285 -1.31 0.375 0 0 0.04 $Titanium
capsule
137     rcc -0.22755 0.285 -1.31 0.4551 0 0 $cylinder
cantaining seed
          0.0401
141     trc -0.12975 0.285 -1.31 -0.0099 0 0 0.02475 $Ag
bevel @ origin

```

```

                0.01485
142          trc 0.12975 0.285 -1.31 0.0099 0 0 0.02475 $Ag bevel
op. origin
                0.01485
143          trc -0.13 0.285 -1.31 -0.01 0 0 0.025 0.015 $AgI
bevel @ origin
144          trc 0.13 0.285 -1.31 0.01 0 0 0.025 0.015 $AgI bevel
op. origin
c
c Onco Seed 6711 surfaces #3
c
225          sph -0.1875 -0.285 -1.31 0.04 $titanium cap weld
226          sph 0.1875 -0.285 -1.31 0.04 $titanium cap weld
231          rcc -0.12975 -0.285 -1.31 0.2595 0 0 0.02475 $Ag
cylinder
232          rcc -0.13 -0.285 -1.31 0.26 0 0 0.025 $AgI/AgBr
cylinder
233          rcc -0.1875 -0.285 -1.31 0.375 0 0 0.034 $Air
cylinder
234          rcc -0.1875 -0.285 -1.31 0.375 0 0 0.04 $Titanium
capsule
237          rcc -0.22755 -0.285 -1.31 0.4551 0 0 $cylendar
cantaining seed
                0.0401
241          trc -0.12975 -0.285 -1.31 -0.0099 0 0 0.02475 $Ag
bevel @ origin
                0.01485
242          trc 0.12975 -0.285 -1.31 0.0099 0 0 0.02475 $Ag bevel
op. origin
                0.01485
243          trc -0.13 -0.285 -1.31 -0.01 0 0 0.025 0.015 $AgI
bevel @ origin
244          trc 0.13 -0.285 -1.31 0.01 0 0 0.025 0.015 $AgI
bevel op. origin

```

```

c
c Onco Seed 6711 surfaces #4
c
325      sph 0.469 -0.1875 -1.257 0.04  $titanium cap weld
326      sph 0.469 0.1875 -1.257 0.04  $titanium cap weld
331      rcc 0.469 -0.12975 -1.257 0 0.2595 0 0.02475  $Ag
cylinder
332      rcc 0.469 -0.13 -1.257 0 0.26 0 0.025  $AgI/AgBr
cylinder
333      rcc 0.469 -0.1875 -1.257 0 0.375 0 0.034  $Air
cylinder
334      rcc 0.469 -0.1875 -1.257 0 0.375 0 0.04  $Titanium
capsule
337      rcc 0.469 -0.22755 -1.257 0 0.4551 0 $cylendar
cantaining seed
          0.0401
341      trc 0.469 -0.12975 -1.257 0 -0.0099 0 0.02475 $Ag
bevel @ origin
          0.01485
342      trc 0.469 0.12975 -1.257 0 0.0099 0 0.02475 $Ag bevel
op. origin
          0.01485
343      trc 0.469 -0.13 -1.257 0 -0.01 0 0.025 0.015  $AgI
bevel @ origin
344      trc 0.469 0.13 -1.257 0 0.01 0 0.025 0.015  $AgI
bevel op. origin
c
c Onco Seed 6711 surfaces #5
c
425      sph 0.323306 0.388032 -1.257 0.04  $titanium cap weld
dis
426      sph -0.033305 0.503971 -1.257 0.04  $titanium cap
weld prox

```

431 rcc 0.268387 0.405886 -1.257 -0.24677 0.080229 0 \$Ag
 cylinder
 0.02475
 432 rcc 0.268625 0.405809 -1.257 -0.24725 0.080384 0
 \$AgI/AgBr cylinde
 0.025
 433 rcc 0.323306 0.388032 -1.257 -0.35661 0.115939 0 \$Air
 cylinder
 0.034
 434 rcc 0.323306 0.388032 -1.257 -0.35661 0.115939 0
 \$Titanium capsule
 0.04
 437 rcc 0.361392 0.37565 -1.257 -0.432784 0.140703 0
 \$cylendar conta
 0.0401
 441 trc 0.268387 0.405886 -1.257 0.0094145 -0.0030607 0
 0.02475 \$Ag b
 0.01485
 442 trc 0.021613 0.486115 -1.257 -0.0094145 0.0030607 0
 0.02475 \$Ag
 0.01485
 443 trc 0.268625 0.405809 -1.257 0.00951 -0.003092 0
 0.025 \$AgI bev
 0.015
 444 trc 0.021375 0.486193 -1.257 -0.00951 0.003092 0
 0.025 0.015 \$AgI b
 c
 c Onco Seed 6711 surfaces #6
 c
 525 sph -0.269089 0.426567 -1.257 0.04 \$titanium cap
 weld dis
 526 sph -0.488997 0.123495 -1.257 0.04 \$titanium cap
 weld prox

531 rcc -0.302938 0.379873 -1.257 -0.152168 -0.209715 0
 \$Ag cylinde
 0.02475
 532 rcc -0.302791 0.380075 -1.257 -0.152461 -0.210119 0
 \$AgI/AgBr cyl
 0.025
 533 rcc -0.269089 0.426567 -1.257 -0.219908 -0.303073 0
 \$Air cylinder
 0.034
 534 rcc -0.269089 0.426567 -1.257 -0.219908 -0.303073 0
 \$Titanium caps
 0.04
 537 rcc -0.245614 0.458957 -1.257 -0.266892 -0.367826 0
 \$cylendar co
 0.0401
 541 trc -0.302938 0.379873 -1.257 0.0058027 0.008004 0
 0.02475 \$Ag
 0.01485
 542 trc -0.455106 0.170158 -1.257 -0.0058092 -0.0079993 0
 0.02475 \$Ag
 0.01485
 543 trc -0.302791 0.380075 -1.257 0.005861 0.008085 0
 0.025 \$AgI be
 0.015
 544 trc -0.455252 0.169956 -1.257 -0.005861 -0.008085 0
 0.025 \$AgI be
 0.015
 c
 c Onco Seed 6711 surfaces #7
 c
 625 sph -0.488997 -0.123495 -1.257 0.04 \$titanium cap
 weld dis
 626 sph -0.269089 -0.426567 -1.257 0.04 \$titanium cap
 weld prox

631 rcc -0.455106 -0.170158 -1.257 0.152168 -0.209715 0
 \$Ag cylinder
 0.02475
 632 rcc -0.455252 -0.169956 -1.257 0.152461 -0.210119
 \$AgI/AgBr cylind
 0 0.025
 633 rcc -0.488997 -0.123495 -1.257 0.219908 -0.303073 0
 \$Air cylinder
 0.034
 634 rcc -0.488997 -0.123495 -1.257 0.219908 -0.303073
 \$Titanium capsule
 0 0.04
 637 rcc -0.512506 -0.091131 -1.257 0.266892 -0.367826 0
 \$cylendar canta
 0.0401
 641 trc -0.455106 -0.170158 -1.257 -0.005809 0.007999 0
 0.02475 \$Ag be
 0.01485
 642 trc -0.302938 -0.379873 -1.257 0.0058027 -0.008004 0
 0.02475 \$Ag b
 0.01485
 643 trc -0.455106 -0.170158 -1.257 -0.005868 0.00808 0
 0.025 \$AgI bevel
 0.015
 644 trc -0.302791 -0.380075 -1.257 0.005861 -0.008085 0
 \$AgI bevel
 0.025 0.015
 c
 c Onco Seed 6711 surfaces #8
 c
 725 sph -0.03305 -0.503971 -1.257 0.04 \$titanium cap
 weld dis
 726 sph 0.323306 -0.388032 -1.257 0.04 \$titanium cap
 weld prox

```

731      rcc 0.021613 -0.486115 -1.257 0.246774 0.080229 0 $Ag
cylinder
          0.02475
732      rcc 0.021375 -0.486193 -1.257 0.24725 0.080384 0
$AgI/AgBr cylinder
          0.025
733      rcc -0.03305 -0.503971 -1.257 0.356611 0.115939 0
$Air cylinder
          0.034
734      rcc -0.03305 -0.503971 -1.257 0.356611 0.115939 0
$Titanium capsule
          0.04
737      rcc -0.071391 -0.516354 -1.257 0.432784 0.140703 0
$scylendar cantai
          0.0401
741      trc 0.021613 -0.486115 -1.257 -0.0094146 -0.0030607 0
0.02475 $Ag
          0.01485
742      trc 0.268387 -0.405886 -1.257 0.0094146 0.0030607 0
0.02475 $Ag be
          0.01485
743      trc 0.021375 -0.486193 -1.257 -0.00951 -0.003092 0
0.025 $AgI bevel
          0.015
744      trc 0.268625 -0.405809 -1.257 0.00951 0.003092 0 $AgI
bevel pr
          0.025 0.015

mode p $e
c water for phantom head
m1      8000.04p      -0.888099
          1000.04p      -0.111901 $Water weight fractions
c silastic insert
m2      1000.04p      -0.06 $MAT

```

6000.04p -0.25 8000.04p -0.29 14000.04p
 -0.39995
 78000.04p -5e-005
 c COM plaque cover
 m3 79000.04p -0.77 \$MAT
 47000.04p -0.14 29000.04p -0.08 46000.04p
 -0.01
 c silver wire
 m5 47000.04p -1 \$MAT
 c radioactive coating on wire
 m6 47000.04p -0.54 \$MAT
 35000.04p -0.28 53000.04p -0.18
 c titanium capsule and end welds
 m7 22000.04p -1 \$MAT
 c NIST Air, Dry (near sea level)
 m8 6000.04p -0.00012425 \$MAT
 7000.04p -0.7552673 8000.04p -0.2317812 18000.04p
 -0.01282725
 c Homogenized eye (Thomaon, 2008 MP.35)
 m9 1000.04p -0.107 \$MAT
 6000.04p -0.038 7000.04p -0.012 8000.04p
 -0.843
 c Skull bone (Thomaon, 2008 MP.35)
 m10 1000.04p -0.05 \$MAT
 6000.04p -0.212 7000.04p -0.04 8000.04p
 -0.435
 11000.04p -0.001 12000.04p -0.002 15000.04p
 -0.081
 16000.04p -0.003 20000.04p -0.176
 c cut:p j 0.010
 imp:p 1 46r 0 \$ 1, 999
 c imp:e 1 46r 0
 vol 4J 0.0000119 8J 0.0000119 4J 0.0000119 4J 0.0000119 &
 4j 0.0000119 4J 0.0000119 4J 0.0000119 4J 0.0000119 4J

```

e0  0 1e-5 0.51 1.024
sdef erg=d1 pos=-0.12999 0 -1.34 rad=d2 axs=0.2 0 0 ext=d3 par=2
    eff=0.01
#   si1      spl
    L        d
0.0268746   3.16341E-05
0.0041731   0.000418578
0.004829    0.00107944
0.003606    0.00114638
0.0312373   0.00144465
0.0033354   0.00176708
0.004829    0.00184814
0.0045722   0.00454971
0.00406949  0.0049638
0.0037589   0.00614614
0.0041205   0.0081776
0.00430159  0.00993986
0.00402949  0.0358245
0.0317101   0.0429691
0.0037693   0.0552214
0.0354919   0.0666816
0.0309441   0.0720103
0.0309951   0.14002
0.0272018   0.397834
0.0274724   0.740847
si2 0.0246 0.02499
si3 L 0 0.25998
c Rectangular mesh tally:
c cora: describes the planes perpendicular to x axis
c corb: describes the planes perpendicular to y axis
c corc: describes the planes perpendicular to z axis
c "i" data input notation even divides dif. by n
tmesh
rmesh3 total

```

```
cora3 -1.3 26i 1.4
corb3 -1.3 25i 1.3
corc3 -1.3 25i 1.3
endmd
nps 100000000
dbcn 12j 703687
prdmp 1000000 1000000 2 2 1000000
```

Appendix D: MCNPX 16 mm Input Deck:

```

16mm Eye Plaque with 16 seeds source seed 1: mode p source type
2
c
c Cell Cards
c
1 9 -1.03 (-24 :-21) $cell of the phantom
eye
2 2 -1.12 (21 -22 -35) 37 137 237 337 437 537 & $silastic insert
637 737 837 937 1037 1137 1237
3 3 -15.8 (21 -22 -36 35):(22 -23 -36) $cell of Gold
alloy plaque
c
c Cells of Seed 1
c
4 5 -10.5 (-31:-41:-42) $Silver rod seed 1
5 6 -6.425 (-32:-43:-44) #4 $AgI/AgBr coating
seed 1
6 8 -0.00120479 -33 #4 #5 $Air inside seed 1
7 7 -4.54 (-34:-25:-26) #4 #5 #6 $Titanium capsule
seed 1
8 2 -1.12 -37 #4 #5 #6 #7 $cylinder
containing the seed 1
c
c Cells of Skull Bone, Phantom Head, and Air interface
c
9 10 -1.60 (23 -17 -10) $skull bone around eye
10 1 -1.0 (11 -10) (15 -14) (13 -12) 17 $Phantom head outside
skull bone
11 1 -1.0 (21 24 -23 36 -10) $tissue between skull and eye
12 8 -0.00120479 (10 -16 15 -14 13 -12 24) $air interface
c
c Cells of seed 2

```

c

14 5 -10.5 (-131:-141:-142)	\$Silver rod seed 2
15 6 -6.425 (-132:-143:-144) #14 seed 2	\$AgI/AgBr coating
16 8 -0.00120479 -133 #14 #15	\$Air inside seed 2
17 7 -4.54 (-134:-125:-126) #14 #15 #16 seed 2	\$Titanium capsule
18 2 -1.12 -137 #14 #15 #16 #17 containing the seed 2	\$cylinder

c

c Cells of seed 3

c

24 5 -10.5 (-231:-241:-242)	\$Silver rod seed 3
25 6 -6.425 (-232:-243:-244) #24 seed 3	\$AgI/AgBr coating
26 8 -0.00120479 -233 #24 #25	\$Air inside seed 3
27 7 -4.54 (-234:-225:-226) #24 #25 #26 seed 3	\$Titanium capsule
28 2 -1.12 -237 #24 #25 #26 #27 containing the seed 3	\$cylinder

c

c Cells of Seed 4

c

34 5 -10.5 (-331:-341:-342) 4	\$Silver rod seed
35 6 -6.425 (-332:-343:-344) #34 seed 4	\$AgI/AgBr coating
36 8 -0.00120479 -333 #34 #35 4	\$Air inside seed
37 7 -4.54 (-334:-325:-326) #34 #35 #36 seed 4	\$Titanium capsule
38 2 -1.12 -337 #34 #35 #36 #37 containing the seed 4	\$cylinder

c

c Cells of Seed 5

c

44 5 -10.5 (-431:-441:-442) \$Silver rod seed

5

45 6 -6.425 (-432:-443:-444) #44 \$AgI/AgBr coating

seed 5

46 8 -0.00120479 -433 #44 #45 \$Air inside seed

5

47 7 -4.54 (-434:-425:-426) #44 #45 #46 \$Titanium capsule

seed 5

48 2 -1.12 -437 #44 #45 #46 #47 \$cylinder

containing the seed 5

c

c Cells of Seed 6

c

54 5 -10.5 (-531:-541:-542) \$Silver rod seed

6

55 6 -6.425 (-532:-543:-544) #54 \$AgI/AgBr coating

seed 6

56 8 -0.00120479 -533 #54 #55 \$Air inside seed

6

57 7 -4.54 (-534:-525:-526) #54 #55 #56 \$Titanium capsule

seed 6

58 2 -1.12 -537 #54 #55 #56 #57 \$cylinder

containing the seed 6

c

c Cells of Seed 7

c

64 5 -10.5 (-631:-641:-642) \$Silver rod seed

7

65 6 -6.425 (-632:-643:-644) #64 \$AgI/AgBr coating

seed 7

66 8 -0.00120479 -633 #64 #65 \$Air inside seed

7

67 7 -4.54 (-634:-625:-626) #64 #65 #66 \$Titanium capsule
seed 7

68 2 -1.12 -637 #64 #65 #66 #67 \$cylinder
containing the seed 7

c
c Cells of Seed 8

c

74 5 -10.5 (-731:-741:-742) \$Silver rod seed
8

75 6 -6.425 (-732:-743:-744) #74 \$AgI/AgBr coating
seed 8

76 8 -0.00120479 -733 #74 #75 \$Air inside seed
8

77 7 -4.54 (-734:-725:-726) #74 #75 #76 \$Titanium capsule
seed 8

78 2 -1.12 -737 #74 #75 #76 #77 \$cylinder
containing the seed 8

c
c Cells of Seed 9

c

84 5 -10.5 (-831:-841:-842) \$Silver rod seed
1

85 6 -6.425 (-832:-843:-844) #84 \$AgI/AgBr coating
seed 1

86 8 -0.00120479 -833 #84 #85 \$Air inside seed
1

87 7 -4.54 (-834:-825:-826) #84 #85 #86 \$Titanium capsule
seed 1

88 2 -1.12 -837 #84 #85 #86 #87 \$cylinder
containing the seed 1

c
c Cells of Seed 10

c

94 5 -10.5 (-931:-941:-942)	\$Silver rod seed
1	
95 6 -6.425 (-932:-943:-944) #94	\$AgI/AgBr coating
seed 1	
96 8 -0.00120479 -933 #94 #95	\$Air inside seed
1	
97 7 -4.54 (-934:-925:-926) #94 #95 #96	\$Titanium capsule
seed 1	
98 2 -1.12 -937 #94 #95 #96 #97	\$cylinder
containing the seed 1	
c	
c Cells of Seed 11	
c	
104 5 -10.5 (-1031:-1041:-1042)	\$Silver rod
seed 1	
105 6 -6.425 (-1032:-1043:-1044) #104	\$AgI/AgBr
coating seed 1	
106 8 -0.00120479 -1033 #104 #105	\$Air inside
seed 1	
107 7 -4.54 (-1034:-1025:-1026) #104 #105 #106	\$Titanium
capsule seed 1	
108 2 -1.12 -1037 #104 #105 #106 #107	\$cylinder
containing the seed 1	
c	
c Cells of Seed 12	
c	
114 5 -10.5 (-1131:-1141:-1142)	\$Silver rod
seed 1	
115 6 -6.425 (-1132:-1143:-1144) #114	\$AgI/AgBr
coating seed 1	
116 8 -0.00120479 -1133 #114 #115	\$Air inside
seed 1	
117 7 -4.54 (-1134:-1125:-1126) #114 #115 #116	\$Titanium
capsule seed 1	

```

118 2 -1.12 -1137 #114 #115 #116 #117          $cylinder
containing the seed 1
c
c Cells of Seed 13
c
124 5 -10.5 (-1231:-1241:-1242)             $Silver rod
seed 1
125 6 -6.425 (-1232:-1243:-1244) #124       $AgI/AgBr
coating seed 1
126 8 -0.00120479 -1233 #124 #125           $Air inside
seed 1
127 7 -4.54 (-1234:-1225:-1226) #124 #125 #126 $Titanium
capsule seed 1
128 2 -1.12 -1237 #124 #125 #126 #127       $cylinder
containing the seed 1
999      0   14: -15: 12: -13: 16: -11 $Void

c
c Surface Cards
c
10 px  1.23   $ outer plane of water head
11 px -28.77 $ outer plane of water head
12 py  15.0   $ outer plane of water head
13 py -15.0   $ outer plane of water head
14 pz  15.0   $ outer plane of water head
15 pz -15.0   $ outer plane of water head
16 px  15.0   $ outer plane of air interface
17 sph   0 0 0   2.05                $ outer sphere of skull bone
21 SPH   0 0 0   1.23                $lateral sphere of eye
22 SPH   0 0 0   1.455               $inner sphere of plaque
23 SPH   0 0 0   1.505               $outer sphere of plaque
24 SPH   0.663 0 0   0.727           $cornea

c
c Onco Seed 6711 surfaces #1

```

c

25 SPH	-0.1875	0.167	-1.33	0.04					\$titanium
cap welds									
26 SPH	0.1875	0.167	-1.33	0.04					\$titanium
cap welds									
31 RCC	-0.12975	0.167	-1.33	0.2595	0	0	0.02475		\$Ag cylinder
32 RCC	-0.13	0.167	-1.33	0.26	0	0	0.025		\$AgI/AgBr
cylinder									
33 RCC	-0.1875	0.167	-1.33	0.375	0	0	0.034		\$Air
cylinder									
34 RCC	-0.1875	0.167	-1.33	0.375	0	0	0.04		\$Titanium
capsule									
35 RCC	0	0	-0.88	0	0	-0.63	0.8		\$cylinder of
inner lip									
36 RCC	0	0	-0.88	0	0	-0.63	0.85		\$cylendar of
outer lip									
37 RCC	-0.22755	0.167	-1.33	0.4551	0	0	0.0401		\$cylinder containing seed
41 TRC	-0.12975	0.167	-1.33	-0.0099	0	0	0.02475	0.01485	\$Ag
bevel @ dis									
42 TRC	0.12975	0.167	-1.33	0.0099	0	0	0.02475	0.01485	\$Ag
bevel @ prox									
43 TRC	-0.13	0.167	-1.33	-0.01	0	0	0.025	0.015	\$AgI
bevel @ dis									
44 TRC	0.13	0.167	-1.33	0.01	0	0	0.025	0.015	\$AgI
bevel @ prox									

c

c Onco Seed 6711 surfaces #2

c

125 SPH	-0.1875	-0.167	-1.33	0.04					\$titanium cap welds
126 SPH	0.1875	-0.167	-1.33	0.04					\$titanium cap welds

237 RCC 0.446 -0.22755 -1.265 0 0.4551 0 0.0401
 \$cylinder containing seed
 241 TRC 0.446 -0.12975 -1.265 0 -0.0099 0 0.02475 0.01485 \$Ag
 bevel @ dis
 242 TRC 0.446 0.12975 -1.265 0 0.0099 0 0.02475 0.01485 \$Ag
 bevel @ prox
 243 TRC 0.446 -0.13 -1.265 0 -0.01 0 0.025 0.015
 \$AgI bevel @ dis
 244 TRC 0.446 0.13 -1.265 0 0.01 0 0.025 0.015
 \$AgI bevel @ prox
 c
 c Onco Seed 6711 surfaces #4
 c
 325 SPH -0.1875 0.446 -1.265 0.04
 \$titanium cap welds
 326 SPH 0.1875 0.446 -1.265 0.04
 \$titanium cap welds
 331 RCC -0.12975 0.446 -1.265 0.2595 0 0 0.02475 \$Ag
 cylinder
 332 RCC -0.13 0.446 -1.265 0.26 0 0 0.025
 \$AgI/AgBr cylinder
 333 RCC -0.1875 0.446 -1.265 0.375 0 0 0.034
 \$Air cylinder
 334 RCC -0.1875 0.446 -1.265 0.375 0 0 0.04
 \$Titanium capsule
 337 RCC -0.22755 0.446 -1.265 0.4551 0 0 0.0401
 \$cylinder containing seed
 341 TRC -0.12975 0.446 -1.265 -0.0099 0 0 0.02475 0.01485 \$Ag
 bevel @ dis
 342 TRC 0.12975 0.446 -1.265 0.0099 0 0 0.02475 0.01485 \$Ag
 bevel @ prox
 343 TRC -0.13 0.446 -1.265 -0.01 0 0 0.025 0.015
 \$AgI bevel @ dis

344 TRC 0.13 0.446 -1.265 0.01 0 0 0.025 0.015
 \$AgI bevel @ prox
 c
 c Onco Seed 6711 surfaces #5
 c
 425 SPH -0.446 -0.1875 -1.265 0.04
 \$titanium cap welds
 426 SPH -0.446 0.1875 -1.265 0.04
 \$titanium cap welds
 431 RCC -0.446 -0.12975 -1.265 0 0.2595 0 0.02475
 \$Ag cylinder
 432 RCC -0.446 -0.13 -1.265 0 0.26 0 0.025
 \$AgI/AgBr cylinder
 433 RCC -0.446 -0.1875 -1.265 0 0.375 0 0.034
 \$Air cylinder
 434 RCC -0.446 -0.1875 -1.265 0 0.375 0 0.04
 \$Titanium capsule
 437 RCC -0.446 -0.22755 -1.265 0 0.4551 0 0.0401
 \$cylinder containing seed
 441 TRC -0.446 -0.12975 -1.265 0 -0.0099 0 0.02475 0.01485
 \$Ag bevel @ dis
 442 TRC -0.446 0.12975 -1.265 0 0.0099 0 0.02475 0.01485
 \$Ag bevel @ prox
 443 TRC -0.446 -0.13 -1.265 0 -0.01 0 0.025 0.015
 \$AgI bevel @ dis
 444 TRC -0.446 0.13 -1.265 0 0.01 0 0.025 0.015
 \$AgI bevel @ prox
 c
 c Onco Seed 6711 surfaces #6
 c
 525 SPH -0.1875 -0.446 -1.265 0.04
 \$titanium cap welds
 526 SPH 0.1875 -0.446 -1.265 0.04
 \$titanium cap welds

531 RCC -0.12975 -0.446 -1.265 0.2595 0 0 0.02475
 \$Ag cylinder
 532 RCC -0.13 -0.446 -1.265 0.26 0 0 0.025
 \$AgI/AgBr cylinder
 533 RCC -0.1875 -0.446 -1.265 0.375 0 0 0.034
 \$Air cylinder
 534 RCC -0.1875 -0.446 -1.265 0.375 0 0 0.04
 \$Titanium capsule
 537 RCC -0.22755 -0.446 -1.265 0.4551 0 0 0.0401
 \$cylinder containing seed
 541 TRC -0.12975 -0.446 -1.265 -0.0099 0 0 0.02475 0.01485
 \$Ag bevel @ dis
 542 TRC 0.12975 -0.446 -1.265 0.0099 0 0 0.02475 0.01485
 \$Ag bevel @ prox
 543 TRC -0.13 -0.446 -1.265 -0.01 0 0 0.025 0.015
 \$AgI bevel @ dis
 544 TRC 0.13 -0.446 -1.265 0.01 0 0 0.025 0.015
 \$AgI bevel @ prox
 c
 c Onco Seed 6711 surfaces #7
 c
 625 SPH 0.643 -0.1875 -1.18 0.04
 \$titanium cap welds
 626 SPH 0.643 0.1875 -1.18 0.04
 \$titanium cap welds
 631 RCC 0.643 -0.12975 -1.18 0 0.2595 0 0.02475
 \$Ag cylinder
 632 RCC 0.643 -0.13 -1.18 0 0.26 0 0.025
 \$AgI/AgBr cylinder
 633 RCC 0.643 -0.1875 -1.18 0 0.375 0 0.034
 \$Air cylinder
 634 RCC 0.643 -0.1875 -1.18 0 0.375 0 0.04
 \$Titanium capsule

637 RCC 0.643 -0.22755 -1.18 0 0.4551 0 0.0401
 \$cylinder containing seed
 641 TRC 0.643 -0.12975 -1.18 0 -0.0099 0 0.02475 0.01485
 \$Ag bevel @ dis
 642 TRC 0.643 0.12975 -1.18 0 0.0099 0 0.02475 0.01485
 \$Ag bevel @ prox
 643 TRC 0.643 -0.13 -1.18 0 -0.01 0 0.025 0.015
 \$AgI bevel @ dis
 644 TRC 0.643 0.13 -1.18 0 0.01 0 0.025 0.015
 \$AgI bevel @ prox
 c
 c Onco Seed 6711 surfaces #8
 c
 725 SPH 0.550786 0.381891 -1.18 0.04
 \$titanium cap welds
 726 SPH 0.259192 0.618082 -1.18 0.04
 \$titanium cap welds
 731 RCC 0.505887 0.418270 -1.18 -0.201786 0.163446 0 0.02475
 \$Ag cylinder
 732 RCC 0.506082 0.418112 -1.18 -0.202175 0.163761 0 0.025
 \$AgI/AgBr cylinder
 733 RCC 0.550786 0.381891 -1.18 -0.291594 0.236191 0 0.034
 \$Air cylinder
 734 RCC 0.550786 0.381891 -1.18 -0.291594 0.236191 0 0.04
 \$Titanium capsule
 737 RCC 0.581921 0.356661 -1.18 -0.353874 0.286638 0 0.0401
 \$cylinder containing seed
 741 TRC 0.505887 0.418270 -1.18 0.007697 -0.006236 0 0.02475
 0.01485 \$Ag bevel @ dis
 742 TRC 0.304102 0.581716 -1.18 -0.007699 0.006234 0 0.02475
 0.01485 \$Ag bevel @ prox
 743 TRC 0.506082 0.418112 -1.18 0.007775 -0.006297 0 0.025
 0.015 \$AgI bevel @ dis

744 TRC 0.303907 0.581874 -1.18 -0.007775 0.006297 0 0.025
 0.015 \$AgI bevel @ prox
 c
 c Onco Seed 6711 surfaces #9
 c
 825 SPH 0.037833 0.669259 -1.18 0.04
 \$titanium cap welds
 826 SPH -0.327823 0.584698 -1.18 0.04
 \$titanium cap welds
 831 RCC -0.018478 0.656248 -1.18 -0.253039 -0.058518 0 0.02475
 \$Ag cylinder
 832 RCC -0.018235 0.656305 -1.18 -0.253526 -0.058630 0 0.025
 \$AgI/AgBr cylinder
 833 RCC 0.037833 0.669259 -1.18 -0.365656 -0.084562 0 0.034
 \$Air cylinder
 834 RCC 0.037833 0.669259 -1.18 -0.365656 -0.084562 0 0.04
 \$Titanium capsule
 837 RCC 0.076884 0.678281 -1.18 -0.443754 -0.102623 0 0.0401
 \$cylinder containing seed
 841 TRC -0.018478 0.656248 -1.18 0.009654 0.002231 0 0.02475
 0.01485 \$Ag bevel @ dis
 842 TRC -0.271517 0.597731 -1.18 -0.009653 -0.002234 0 0.02475
 0.01485 \$Ag bevel @ prox
 843 TRC -0.018235 0.656305 -1.18 0.009751 0.002253 0 0.025
 0.015 \$AgI bevel @ dis
 844 TRC -0.271761 0.597674 -1.18 -0.009751 0.002253 0 0.025
 0.015 \$AgI bevel @ prox
 c
 c Onco Seed 6711 surfaces #10
 c
 925 SPH -0.495764 0.450542 -1.18 0.04
 \$titanium cap welds
 926 SPH -0.660227 0.113453 -1.18 0.04
 \$titanium cap welds

931 RCC -0.521094 0.398632 -1.18 -0.113808 -0.233267 0 0.02475
 \$Ag cylinder
 932 RCC -0.520984 0.398857 -1.18 -0.114028 -0.233716 0 0.025
 \$AgI/AgBr cylinder
 933 RCC -0.495764 0.450542 -1.18 -0.164462 -0.337089 0 0.034
 \$Air cylinder
 934 RCC -0.495764 0.450542 -1.18 -0.164462 -0.337089 0 0.04
 \$Titanium capsule
 937 RCC -0.478198 0.486542 -1.18 -0.199591 -0.409090 0 0.0401
 \$cylinder containing seed
 941 TRC -0.521094 0.398632 -1.18 0.004342 0.008899 0 0.02475
 0.01485 \$Ag bevel @ dis
 942 TRC -0.634902 0.165366 -1.18 -0.004341 -0.008899 0 0.02475
 0.01485 \$Ag bevel @ prox
 943 TRC -0.520984 0.398857 -1.18 0.004386 0.008989 0 0.025
 0.015 \$AgI bevel @ dis
 944 TRC -0.635012 0.165141 -1.18 -0.004386 -0.008989 0 0.025
 0.015 \$AgI bevel @ prox
 c
 c Onco Seed 6711 surfaces #11
 c
 1025 SPH -0.660227 -0.113453 -1.18 0.04
 \$titanium cap welds
 1026 SPH -0.495764 -0.450542 -1.18 0.04
 \$titanium cap welds
 1031 RCC -0.634902 -0.165366 -1.18 0.113808 -0.233267 0
 0.02475 \$Ag cylinder
 1032 RCC -0.635012 -0.165141 -1.18 0.114028 -0.233716 0 0.025
 \$AgI/AgBr cylinder
 1033 RCC -0.660227 -0.113453 -1.18 0.164462 -0.337089 0 0.034
 \$Air cylinder
 1034 RCC -0.660227 -0.113453 -1.18 0.164462 -0.337089 0 0.04
 \$Titanium capsule

1037 RCC -0.677789 -0.077452 -1.18 0.199591 -0.409090 0 0.0401
 \$cylinder containing seed
 1041 TRC -0.634902 -0.165366 -1.18 -0.004341 0.008899 0
 0.02475 0.01485 \$Ag bevel @ dis
 1042 TRC -0.521094 -0.398632 -1.18 0.004342 -0.008899 0
 0.02475 0.01485 \$Ag bevel @ prox
 1043 TRC -0.635012 -0.165141 -1.18 -0.004386 0.008989 0 0.025
 0.015 \$AgI bevel @ dis
 1044 TRC -0.520984 -0.398857 -1.18 0.004386 -0.008989 0 0.025
 0.015 \$AgI bevel @ prox
 c
 c Onco Seed 6711 surfaces #12
 c
 1125 SPH -0.327823 -0.584698 -1.18 0.04
 \$titanium cap welds
 1126 SPH 0.037833 -0.669259 -1.18 0.04
 \$titanium cap welds
 1131 RCC -0.271517 -0.597731 -1.18 0.253039 -0.058518 0
 0.02475 \$Ag cylinder
 1132 RCC -0.271761 -0.597674 -1.18 0.253526 -0.058630 0 0.025
 \$AgI/AgBr cylinder
 1133 RCC -0.327823 -0.584698 -1.18 0.365656 -0.084562 0 0.034
 \$Air cylinder
 1134 RCC -0.327823 -0.584698 -1.18 0.365656 -0.084562 0 0.04
 \$Titanium capsule
 1137 RCC -0.366870 -0.575658 -1.18 0.443754 -0.102623 0 0.0401
 \$cylinder containing seed
 1141 TRC -0.271517 -0.597731 -1.18 -0.009653 0.002234 0
 0.02475 0.01485 \$Ag bevel @ dis
 1142 TRC -0.018478 -0.656248 -1.18 0.009654 -0.002231 0
 0.02475 0.01485 \$Ag bevel @ prox
 1143 TRC -0.271761 -0.597674 -1.18 -0.009751 0.002257 0 0.025
 0.015 \$AgI bevel @ dis

1144 TRC -0.018235 -0.656305 -1.18 0.009751 -0.002257 0 0.025
 0.015 \$AgI bevel @ prox
 c
 c Onco Seed 6711 surfaces #13
 c
 1225 SPH 0.259192 -0.618082 -1.18 0.04
 \$titanium cap welds
 1226 SPH 0.550786 -0.381891 -1.18 0.04
 \$titanium cap welds
 1231 RCC 0.304102 -0.581716 -1.18 0.201786 0.163446 0 0.02475
 \$Ag cylinder
 1232 RCC 0.303907 -0.581874 -1.18 0.202175 0.163761 0 0.025
 \$AgI/AgBr cylinder
 1233 RCC 0.259192 -0.618082 -1.18 0.291594 0.236191 0 0.034
 \$Air cylinder
 1234 RCC 0.259192 -0.618082 -1.18 0.291594 0.236191 0 0.04
 \$Titanium capsule
 1237 RCC 0.228047 -0.643299 -1.18 0.353874 0.286638 0 0.0401
 \$cylinder containing seed
 1241 TRC 0.304102 -0.581716 -1.18 -0.007699 -0.006234 0 0.02475
 0.01485 \$Ag bevel @ dis
 1242 TRC 0.505887 -0.418270 -1.18 0.007697 0.006236 0 0.02475
 0.01485 \$Ag bevel @ prox
 1243 TRC 0.303907 -0.581874 -1.18 -0.007775 -0.006299 0 0.025
 0.015 \$AgI bevel @ dis
 1244 TRC 0.506082 -0.418112 -1.18 0.007775 0.006299 0 0.025
 0.015 \$AgI bevel @ prox

 c Data Cards
 c
 c
 Mode P \$E
 cut:p j 0.0010
 imp:p 1 71r 0

```

c imp:e 1 126r 0
c water for phantom head
m1      8000.04p      -0.888099
        1000.04p      -0.111901 $Water weight fractions
c silastic insert
m2      1000.04p      -0.06  $MAT
        6000.04p      -0.25 8000.04p      -0.29 14000.04p
-0.39995
        78000.04p     -5e-005
c COM plaque cover
m3      79000.04p     -0.77  $MAT
        47000.04p     -0.14 29000.04p     -0.08 46000.04p
-0.01
c silver wire
m5      47000.04p      -1  $MAT
c radioactive coating on wire
m6      47000.04p      -0.54  $MAT
        35000.04p     -0.28 53000.04p     -0.18
c titanium capsole and end welds
m7      22000.04p      -1  $MAT
c NIST Air, Dry (near sea level)
m8      6000.04p      -0.00012425  $MAT
        7000.04p      -0.7552673 8000.04p     -0.2317812 18000.04p
-0.01282725
c Homogenized eye (Thomaon, 2008 MP.35)
m9      1000.04p      -0.107  $MAT
        6000.04p      -0.038 7000.04p     -0.012 8000.04p
-0.843
c Skull bone (Thomaon, 2008 MP.35)
m10     1000.04p      -0.05  $MAT
        6000.04p      -0.212 7000.04p     -0.04 8000.04p
-0.435
        11000.04p     -0.001 12000.04p     -0.002 15000.04p
-0.081

```

```

16000.04p          -0.003 20000.04p          -0.176
VOL 4J 0.0000119 8J 0.0000119 4J 0.0000119 4J 0.0000119 &
4J 0.0000119 4J 0.0000119 4J 0.0000119 4J 0.0000119 &
4J 0.0000119 4J 0.0000119 4J 0.0000119 4J 0.0000119 4J
0.0000119 4J
E0 0 1e-5 0.51 1.024
sdef erg=d1 pos=-0.13 0.167 -1.33 rad=d2 axs=0.13 0 0 &
ext=d3 par=2 eff=0.01
#  si1      spl
   L        d
0.0268746  3.16341E-05
0.0041731  0.000418578
0.004829   0.00107944
0.003606   0.00114638
0.0312373  0.00144465
0.0033354  0.00176708
0.004829   0.00184814
0.0045722  0.00454971
0.00406949 0.0049638
0.0037589  0.00614614
0.0041205  0.0081776
0.00430159 0.00993986
0.00402949 0.0358245
0.0317101  0.0429691
0.0037693  0.0552214
0.0354919  0.0666816
0.0309441  0.0720103
0.0309951  0.14002
0.0272018  0.397834
0.0274724  0.740847
si2 0.02476 0.02499
si3 L 0 0.25998
c Rectangular mesh tally:
c cora: describes the planes perpendicular to x axis

```

```
c corb: describes the planes perpendicular to y axis
c corc: describes the planes perpendicular to z axis
c "i" data input notation even divides dif. by n
tmesh
Rmesh3 total
cora3 -1.3 26i 1.4
corb3 -1.3 25i 1.3
corc3 -1.3 25i 1.3
endmd
nps 100000000
dbcn 12j 703687
prdmp 1000000 1000000 2 2 1000000
```

Appendix E: MCNPX 20 mm Input Deck

```

20mm Eye Plaque with 24 seeds source seed 1: mode p source type
2
c
c Cell Cards
c
1 9 -1.03 (-24 :-21) $cell of the
phantom eye
2 2 -1.12 (21 -22 -35) 37 137 237 337 437 537 637 737 837 937
1037 &
1137 1237 1337 1437 1537 1637 1737 1837 1937 2037 2137 2237
2337
3 3 -15.8 (21 -22 -36 35):(22 -23 -36) $cell of Gold
alloy plaque
c
c Cells of Seed 1
c
4 5 -10.5 (-31:-41:-42) $Silver rod seed 1
5 6 -6.425 (-32:-43:-44) #4 $AgI/AgBr coating
seed 1
6 8 -0.00120479 -33 #4 #5 $Air inside seed 1
7 7 -4.54 (-34:-25:-26) #4 #5 #6 $Titanium capsule
seed 1
8 2 -1.12 -37 #4 #5 #6 #7 $cylinder
containing the seed 1
c
c Cells of Skull Bone, Phantom Head, and Air interface
c
9 10 -1.60 (23 -17 -10) $skull bone around eye
10 1 -1.0 (11 -10) (15 -14) (13 -12) 17 $Phantom head outside
skull bone
11 1 -1.0 (21 24 -23 36 -10) $tissue between skull and eye

```

```

12 8 -0.00120479 (10 -16 15 -14 13 -12 24) $air interface
c
c Cells of seed 2
c
14 5 -10.5 (-131:-141:-142) $Silver rod seed 2
15 6 -6.425 (-132:-143:-144) #14 $AgI/AgBr coating
seed 2
16 8 -0.00120479 -133 #14 #15 $Air inside seed 2
17 7 -4.54 (-134:-125:-126) #14 #15 #16 $Titanium capsule
seed 2
18 2 -1.12 -137 #14 #15 #16 #17 $cylinder
containing the seed 2
c
c Cells of seed 3
c
24 5 -10.5 (-231:-241:-242) $Silver rod seed 3
25 6 -6.425 (-232:-243:-244) #24 $AgI/AgBr coating
seed 3
26 8 -0.00120479 -233 #24 #25 $Air inside seed 3
27 7 -4.54 (-234:-225:-226) #24 #25 #26 $Titanium capsule
seed 3
28 2 -1.12 -237 #24 #25 #26 #27 $cylinder
containing the seed 3
c
c Cells of Seed 4
c
34 5 -10.5 (-331:-341:-342) $Silver rod seed
4
35 6 -6.425 (-332:-343:-344) #34 $AgI/AgBr coating
seed 4
36 8 -0.00120479 -333 #34 #35 $Air inside seed
4
37 7 -4.54 (-334:-325:-326) #34 #35 #36 $Titanium capsule
seed 4

```

38 2 -1.12 -337 #34 #35 #36 #37	\$cylinder
containing the seed 4	
c	
c Cells of Seed 5	
c	
44 5 -10.5 (-431:-441:-442)	\$Silver rod seed
5	
45 6 -6.425 (-432:-443:-444) #44	\$AgI/AgBr coating
seed 5	
46 8 -0.00120479 -433 #44 #45	\$Air inside seed
5	
47 7 -4.54 (-434:-425:-426) #44 #45 #46	\$Titanium capsule
seed 5	
48 2 -1.12 -437 #44 #45 #46 #47	\$cylinder
containing the seed 5	
c	
c Cells of Seed 6	
c	
54 5 -10.5 (-531:-541:-542)	\$Silver rod seed
6	
55 6 -6.425 (-532:-543:-544) #54	\$AgI/AgBr coating
seed 6	
56 8 -0.00120479 -533 #54 #55	\$Air inside seed
6	
57 7 -4.54 (-534:-525:-526) #54 #55 #56	\$Titanium capsule
seed 6	
58 2 -1.12 -537 #54 #55 #56 #57	\$cylinder
containing the seed 6	
c	
c Cells of Seed 7	
c	
64 5 -10.5 (-631:-641:-642)	\$Silver rod seed
7	

65 6 -6.425 (-632:-643:-644) #64 seed 7	\$AgI/AgBr coating
66 8 -0.00120479 -633 #64 #65 7	\$Air inside seed
67 7 -4.54 (-634:-625:-626) #64 #65 #66 seed 7	\$Titanium capsule
68 2 -1.12 -637 #64 #65 #66 #67 containing the seed 7 c c Cells of Seed 8 c	\$cylinder
74 5 -10.5 (-731:-741:-742) 8	\$Silver rod seed
75 6 -6.425 (-732:-743:-744) #74 seed 8	\$AgI/AgBr coating
76 8 -0.00120479 -733 #74 #75 8	\$Air inside seed
77 7 -4.54 (-734:-725:-726) #74 #75 #76 seed 8	\$Titanium capsule
78 2 -1.12 -737 #74 #75 #76 #77 containing the seed 8 c c Cells of Seed 9 c	\$cylinder
84 5 -10.5 (-831:-841:-842) 1	\$Silver rod seed
85 6 -6.425 (-832:-843:-844) #84 seed 1	\$AgI/AgBr coating
86 8 -0.00120479 -833 #84 #85 1	\$Air inside seed
87 7 -4.54 (-834:-825:-826) #84 #85 #86 seed 1	\$Titanium capsule
88 2 -1.12 -837 #84 #85 #86 #87 containing the seed 1	\$cylinder

c
 c Cells of Seed 10
 c
 94 5 -10.5 (-931:-941:-942) \$Silver rod seed
 1
 95 6 -6.425 (-932:-943:-944) #94 \$AgI/AgBr coating
 seed 1
 96 8 -0.00120479 -933 #94 #95 \$Air inside seed
 1
 97 7 -4.54 (-934:-925:-926) #94 #95 #96 \$Titanium capsule
 seed 1
 98 2 -1.12 -937 #94 #95 #96 #97 \$cylinder
 containing the seed 1
 c
 c Cells of Seed 11
 c
 104 5 -10.5 (-1031:-1041:-1042) \$Silver rod
 seed 1
 105 6 -6.425 (-1032:-1043:-1044) #104 \$AgI/AgBr
 coating seed 1
 106 8 -0.00120479 -1033 #104 #105 \$Air inside
 seed 1
 107 7 -4.54 (-1034:-1025:-1026) #104 #105 #106 \$Titanium
 capsule seed 1
 108 2 -1.12 -1037 #104 #105 #106 #107 \$cylinder
 containing the seed 1
 c
 c Cells of Seed 12
 c
 114 5 -10.5 (-1131:-1141:-1142) \$Silver rod
 seed 1
 115 6 -6.425 (-1132:-1143:-1144) #114 \$AgI/AgBr
 coating seed 1

116 8 -0.00120479 -1133 #114 #115 \$Air inside
 seed 1
 117 7 -4.54 (-1134:-1125:-1126) #114 #115 #116 \$Titanium
 capsule seed 1
 118 2 -1.12 -1137 #114 #115 #116 #117 \$cylinder
 containing the seed 1
 c
 c Cells of Seed 13
 c
 124 5 -10.5 (-1231:-1241:-1242) \$Silver rod
 seed 1
 125 6 -6.425 (-1232:-1243:-1244) #124 \$AgI/AgBr
 coating seed 1
 126 8 -0.00120479 -1233 #124 #125 \$Air inside
 seed 1
 127 7 -4.54 (-1234:-1225:-1226) #124 #125 #126 \$Titanium
 capsule seed 1
 128 2 -1.12 -1237 #124 #125 #126 #127 \$cylinder
 containing the seed 1
 c
 c Cells of Seed 14
 c
 134 5 -10.5 (-1331:-1341:-1342) \$Silver rod
 seed 1
 135 6 -6.425 (-1332:-1343:-1344) #134 \$AgI/AgBr
 coating seed 1
 136 8 -0.00120479 -1333 #134 #135 \$Air inside
 seed 1
 137 7 -4.54 (-1334:-1325:-1326) #134 #135 #136 \$Titanium capsule seed 1
 138 2 -1.12 -1337 #134 #135 #136 #137 \$cylinder containing the seed 1
 c
 c Cells of Seed 15

c
 144 5 -10.5 (-1431:-1441:-1442) \$Silver rod
 seed 1
 145 6 -6.425 (-1432:-1443:-1444) #144 \$AgI/AgBr
 coating seed 1
 146 8 -0.00120479 -1433 #144 #145 \$Air inside
 seed 1
 147 7 -4.54 (-1434:-1425:-1426) #144 #145 #146
 \$Titanium capsule seed 1
 148 2 -1.12 -1437 #144 #145 #146 #147
 \$cylinder containing the seed 1
 c
 c Cells of Seed 16
 c
 154 5 -10.5 (-1531:-1541:-1542) \$Silver rod
 seed 1
 155 6 -6.425 (-1532:-1543:-1544) #154 \$AgI/AgBr
 coating seed 1
 156 8 -0.00120479 -1533 #154 #155 \$Air inside
 seed 1
 157 7 -4.54 (-1534:-1525:-1526) #154 #155 #156
 \$Titanium capsule seed 1
 158 2 -1.12 -1537 #154 #155 #156 #157
 \$cylinder containing the seed 1
 c
 c Cells of Seed 17
 c
 164 5 -10.5 (-1631:-1641:-1642) \$Silver rod
 seed 1
 165 6 -6.425 (-1632:-1643:-1644) #164 \$AgI/AgBr
 coating seed 1
 166 8 -0.00120479 -1633 #164 #165 \$Air inside
 seed 1

167 7 -4.54 (-1634:-1625:-1626) #164 #165 #166
 \$Titanium capsule seed 1
 168 2 -1.12 -1637 #164 #165 #166 #167
 \$cylinder containing the seed 1
 c
 c Cells of Seed 18
 c
 174 5 -10.5 (-1731:-1741:-1742) \$Silver rod
 seed 1
 175 6 -6.425 (-1732:-1743:-1744) #174 \$AgI/AgBr
 coating seed 1
 176 8 -0.00120479 -1733 #174 #175 \$Air inside
 seed 1
 177 7 -4.54 (-1734:-1725:-1726) #174 #175 #176
 \$Titanium capsule seed 1
 178 2 -1.12 -1737 #174 #175 #176 #177
 \$cylinder containing the seed 1
 c
 c Cells of Seed 19
 c
 184 5 -10.5 (-1831:-1841:-1842) \$Silver rod
 seed 1
 185 6 -6.425 (-1832:-1843:-1844) #184 \$AgI/AgBr
 coating seed 1
 186 8 -0.00120479 -1833 #184 #185 \$Air inside
 seed 1
 187 7 -4.54 (-1834:-1825:-1826) #184 #185 #186
 \$Titanium capsule seed 1
 188 2 -1.12 -1837 #184 #185 #186 #187
 \$cylinder containing the seed 1
 c
 c Cells of Seed 20
 c

194 5 -10.5 (-1931:-1941:-1942) \$Silver rod
 seed 1
 195 6 -6.425 (-1932:-1943:-1944) #194 \$AgI/AgBr
 coating seed 1
 196 8 -0.00120479 -1933 #194 #195 \$Air inside
 seed 1
 197 7 -4.54 (-1934:-1925:-1926) #194 #195 #196
 \$Titanium capsule seed 1
 198 2 -1.12 -1937 #194 #195 #196 #197
 \$cylinder containing the seed 1
 c
 c Cells of Seed 21
 c
 204 5 -10.5 (-2031:-2041:-2042) \$Silver rod
 seed 1
 205 6 -6.425 (-2032:-2043:-2044) #204 \$AgI/AgBr
 coating seed 1
 206 8 -0.00120479 -2033 #204 #205 \$Air inside
 seed 1
 207 7 -4.54 (-2034:-2025:-2026) #204 #205 #206 \$Titanium
 capsule seed 1
 208 2 -1.12 -2037 #204 #205 #206 #207 \$cylinder
 containing the seed 1
 c
 c Cells of Seed 22
 c
 214 5 -10.5 (-2131:-2141:-2142) \$Silver rod
 seed 1
 215 6 -6.425 (-2132:-2143:-2144) #214 \$AgI/AgBr
 coating seed 1
 216 8 -0.00120479 -2133 #214 #215 \$Air inside
 seed 1
 217 7 -4.54 (-2134:-2125:-2126) #214 #215 #216 \$Titanium
 capsule seed 1

218 2 -1.12 -2137 #214 #215 #216 #217 \$cylinder
 containing the seed 1
 c
 c Cells of Seed 23
 c
 224 5 -10.5 (-2231:-2241:-2242) \$Silver rod
 seed 1
 225 6 -6.425 (-2232:-2243:-2244) #224 \$AgI/AgBr
 coating seed 1
 226 8 -0.00120479 -2233 #224 #225 \$Air inside
 seed 1
 227 7 -4.54 (-2234:-2225:-2226) #224 #225 #226 \$Titanium
 capsule seed 1
 228 2 -1.12 -2237 #224 #225 #226 #227 \$cylinder
 containing the seed 1
 c
 c Cells of Seed 24
 c
 234 5 -10.5 (-2331:-2341:-2342) \$Silver rod
 seed 1
 235 6 -6.425 (-2332:-2343:-2344) #234 \$AgI/AgBr
 coating seed 1
 236 8 -0.00120479 -2333 #234 #235 \$Air inside
 seed 1
 237 7 -4.54 (-2334:-2325:-2326) #234 #235 #236 \$Titanium
 capsule seed 1
 238 2 -1.12 -2337 #234 #235 #236 #237 \$cylinder
 containing the seed 1
 999 0 14: -15: 12: -13: 16: -11 \$Void

 c
 c Surface Cards
 c
 10 px 1.23 \$ outer plane of water head

11 px -28.77 \$ outer plane of water head
 12 py 15.0 \$ outer plane of water head
 13 py -15.0 \$ outer plane of water head
 14 pz 15.0 \$ outer plane of water head
 15 pz -15.0 \$ outer plane of water head
 16 px 15.0 \$ outer plane of air interface
 17 sph 0 0 0 2.05 \$ outer sphere of skull bone
 21 SPH 0 0 0 1.23 \$lateral sphere of eye
 22 SPH 0 0 0 1.455 \$inner sphere of plaque
 23 SPH 0 0 0 1.505 \$outer sphere of plaque
 24 SPH 0.663 0 0 0.727 \$cornea
 35 RCC 0 0 -0.64 0 0 -0.865 1 \$cylinder of inner lip
 36 RCC 0 0 -0.64 0 0 -0.865 1.05 \$cylendar of outer lip
 c
 c Onco Seed 6711 surfaces #1
 c
 25 SPH -0.1875 0 -1.34 0.04 \$titanium cap welds
 26 SPH 0.1875 0 -1.34 0.04 \$titanium cap welds
 31 RCC -0.12975 0 -1.34 0.2595 0 0 0.02475 \$Ag cylinder
 32 RCC -0.13 0 -1.34 0.26 0 0 0.025 \$AgI/AgBr cylinder
 33 RCC -0.1875 0 -1.34 0.375 0 0 0.034 \$Air cylinder
 34 RCC -0.1875 0 -1.34 0.375 0 0 0.04 \$Titanium capsule
 37 RCC -0.22755 0 -1.34 0.4551 0 0 0.0401 \$cylinder containing
 seed
 41 TRC -0.12975 0 -1.34 -0.0099 0 0 0.02475 0.01485 \$Ag bevel @
 dis
 42 TRC 0.12975 0 -1.34 0.0099 0 0 0.02475 0.01485 \$Ag bevel @
 prox
 43 TRC -0.13 0 -1.34 -0.01 0 0 0.025 0.015 \$AgI bevel @
 dis
 44 TRC 0.13 0 -1.34 0.01 0 0 0.025 0.015 \$AgI bevel @
 prox
 c
 c Onco Seed 6711 surfaces #2

c

125	SPH	-0.1875	0.214	-1.323	0.04	\$titanium	cap welds
126	SPH	0.1875	0.214	-1.323	0.04	\$titanium	cap welds
131	RCC	-0.12975	0.214	-1.323	0.2595	0 0	0.02475 \$Ag cylinder
132	RCC	-0.13	0.214	-1.323	0.26	0 0	0.025 \$AgI/AgBr cylinder
133	RCC	-0.1875	0.214	-1.323	0.375	0 0	0.034 \$Air cylinder
134	RCC	-0.1875	0.214	-1.323	0.375	0 0	0.04 \$Titanium capsule
137	RCC	-0.22755	0.214	-1.323	0.4551	0 0	0.0401 \$cylinder containing seed
141	TRC	-0.12975	0.214	-1.323	-0.0099	0 0	0.02475 0.01485 \$Ag bevel @ dis
142	TRC	0.12975	0.214	-1.323	0.0099	0 0	0.02475 0.01485 \$Ag bevel @ prox
143	TRC	-0.13	0.214	-1.323	-0.01	0 0	0.025 0.015 \$AgI bevel @ dis
144	TRC	0.13	0.214	-1.323	0.01	0 0	0.025 0.015 \$AgI bevel @ prox

c

c Onco Seed 6711 surfaces #3

c

225	SPH	-0.1875	-0.214	-1.323	0.04	\$titanium	cap welds
226	SPH	0.1875	-0.214	-1.323	0.04	\$titanium	cap welds
231	RCC	-0.12975	-0.214	-1.323	0.2595	0 0	0.02475 \$Ag cylinder
232	RCC	-0.13	-0.214	-1.323	0.26	0 0	0.025 \$AgI/AgBr cylinder
233	RCC	-0.1875	-0.214	-1.323	0.375	0 0	0.034 \$Air cylinder
234	RCC	-0.1875	-0.214	-1.323	0.375	0 0	0.04 \$Titanium capsule
237	RCC	-0.22755	-0.214	-1.323	0.4551	0 0	0.0401 \$cylinder containing seed
241	TRC	-0.12975	-0.214	-1.323	-0.0099	0 0	0.02475 0.01485 \$Ag bevel @ dis

242 TRC 0.12975 -0.214 -1.323 0.0099 0 0 0.02475 0.01485 \$Ag
 bevel @ prox
 243 TRC -0.13 -0.214 -1.323 -0.01 0 0 0.025 0.015 \$AgI
 bevel @ dis
 244 TRC 0.13 -0.214 -1.323 0.01 0 0 0.025 0.015 \$AgI
 bevel @ prox
 c
 c Onco Seed 6711 surfaces #4
 c
 325 SPH 0.469 -0.1875 -1.257 0.04 \$titanium cap welds
 326 SPH 0.469 0.1875 -1.257 0.04 \$titanium cap welds
 331 RCC 0.469 -0.12975 -1.257 0 0.2595 0 0.02475 \$Ag cylinder
 332 RCC 0.469 -0.13 -1.257 0 0.26 0 0.025 \$AgI/AgBr
 cylinder
 333 RCC 0.469 -0.1875 -1.257 0 0.375 0 0.034 \$Air cylinder
 334 RCC 0.469 -0.1875 -1.257 0 0.375 0 0.04 \$Titanium
 capsule
 337 RCC 0.469 -0.22755 -1.257 0 0.4551 0 0.0401 \$cylinder
 containing seed
 341 TRC 0.469 -0.12975 -1.257 0 -0.0099 0 0.02475 0.01485 \$Ag
 bevel @ dis
 342 TRC 0.469 0.12975 -1.257 0 0.0099 0 0.02475 0.01485 \$Ag
 bevel @ prox
 343 TRC 0.469 -0.13 -1.257 0 -0.01 0 0.025 0.015 \$AgI
 bevel @ dis
 344 TRC 0.469 0.13 -1.257 0 0.01 0 0.025 0.015 \$AgI
 bevel @ prox
 c
 c Onco Seed 6711 surfaces #5
 c
 425 SPH 0.323306 0.388032 -1.257 0.04 \$titanium cap welds
 426 SPH -0.033305 0.503971 -1.257 0.04 \$titanium cap welds
 431 RCC 0.268387 0.405886 -1.257 -0.246774 0.080229 0 0.02475
 \$Ag cylinder

432 RCC 0.268625 0.405809 -1.257 -0.247250 0.080384 0 0.025
 \$AgI/AgBr cylinder
 433 RCC 0.323306 0.388032 -1.257 -0.356611 0.115939 0 0.034
 \$Air cylinder
 434 RCC 0.323306 0.388032 -1.257 -0.356611 0.115939 0 0.04
 \$Titanium capsule
 437 RCC 0.361392 0.375650 -1.257 -0.432784 0.140703 0 0.0401
 \$cylinder containing seed
 441 TRC 0.268387 0.405886 -1.257 0.009415 -0.003061 0 0.02475
 0.01485 \$Ag bevel @ dis
 442 TRC 0.021613 0.486115 -1.257 -0.009415 0.003061 0 0.02475
 0.01485 \$Ag bevel @ prox
 443 TRC 0.268625 0.405809 -1.257 0.009510 -0.003092 0 0.025
 0.015 \$AgI bevel @ dis
 444 TRC 0.021375 0.486193 -1.257 -0.009510 0.003092 0 0.025
 0.015 \$AgI bevel @ prox
 c
 c Onco Seed 6711 surfaces #6
 c
 525 SPH -0.269089 0.426567 -1.257 0.04 \$titanium cap welds
 526 SPH -0.488997 0.123495 -1.257 0.04 \$titanium cap welds
 531 RCC -0.302938 0.379873 -1.257 -0.152168 -0.209715 0 0.02475
 \$Ag cylinder
 532 RCC -0.302791 0.380075 -1.257 -0.152461 -0.210119 0 0.025
 \$AgI/AgBr cylinder
 533 RCC -0.269089 0.426567 -1.257 -0.219908 -0.303073 0 0.034
 \$Air cylinder
 534 RCC -0.269089 0.426567 -1.257 -0.219908 -0.303073 0 0.04
 \$Titanium capsule
 537 RCC -0.245614 0.458957 -1.257 -0.266892 -0.367826 0 0.0401
 \$cylinder containing seed
 541 TRC -0.302938 0.379873 -1.257 0.005803 0.008004 0 0.02475
 0.01485 \$Ag bevel @ dis

542 TRC -0.455106 0.170158 -1.257 -0.005809 -0.007999 0 0.02475

0.01485 \$Ag bevel @ prox

543 TRC -0.302791 0.380075 -1.257 0.005861 0.008085 0 0.025

0.015 \$AgI bevel @ dis

544 TRC -0.455252 0.169956 -1.257 -0.005868 -0.008080 0 0.025

0.015 \$AgI bevel @ prox

c

c Onco Seed 6711 surfaces #7

c

625 SPH -0.488997 -0.123495 -1.257 0.04 \$titanium cap welds

626 SPH -0.269089 -0.426567 -1.257 0.04 \$titanium cap welds

631 RCC -0.455106 -0.170158 -1.257 0.152168 -0.209715 0 0.02475

\$Ag cylinder

632 RCC -0.455252 -0.169956 -1.257 0.152461 -0.210119 0 0.025

\$AgI/AgBr cylinder

633 RCC -0.488997 -0.123495 -1.257 0.219908 -0.303073 0 0.034

\$Air cylinder

634 RCC -0.488997 -0.123495 -1.257 0.219908 -0.303073 0 0.04

\$Titanium capsule

637 RCC -0.512506 -0.091131 -1.257 0.266892 -0.367826 0 0.0401

\$cylinder containing seed

641 TRC -0.455106 -0.170158 -1.257 -0.005809 0.007999 0 0.02475

0.01485 \$Ag bevel @ dis

642 TRC -0.302938 -0.379873 -1.257 0.005803 -0.008004 0 0.02475

0.01485 \$Ag bevel @ prox

643 TRC -0.455252 -0.169956 -1.257 -0.005868 0.008080 0 0.025

0.015 \$AgI bevel @ dis

644 TRC -0.302791 -0.380075 -1.257 0.005861 -0.008085 0 0.025

0.015 \$AgI bevel @ prox

c

c Onco Seed 6711 surfaces #8

c

725 SPH -0.033305 -0.503971 -1.257 0.04 \$titanium cap welds

726 SPH 0.323306 -0.388032 -1.257 0.04 \$titanium cap welds

731 RCC 0.021613 -0.486115 -1.257 0.246774 0.080229 0
 0.02475 \$Ag cylinder
 732 RCC 0.021375 -0.486193 -1.257 0.247250 0.080384 0 0.025
 \$AgI/AgBr cylinder
 733 RCC -0.033305 -0.503971 -1.257 0.356611 0.115939 0 0.034
 \$Air cylinder
 734 RCC -0.033305 -0.503971 -1.257 0.356611 0.115939 0 0.04
 \$Titanium capsule
 737 RCC -0.071391 -0.516354 -1.257 0.432784 0.140703 0 0.0401
 \$cylinder containing seed
 741 TRC 0.021613 -0.486115 -1.257 -0.009415 -0.003061 0
 0.02475 0.01485 \$Ag bevel @ dis
 742 TRC 0.268387 -0.405886 -1.257 0.009415 0.003061 0
 0.02475 0.01485 \$Ag bevel @ prox
 743 TRC 0.021375 -0.486193 -1.257 -0.009510 -0.003092 0 0.025
 0.015 \$AgI bevel @ dis
 744 TRC 0.268625 -0.405809 -1.257 0.009510 0.003092 0 0.025
 0.015 \$AgI bevel @ prox
 c
 c Onco Seed 6711 surfaces #9
 c
 825 SPH 0.655982 0.245143 -1.162 0.04 \$titanium cap welds
 826 SPH 0.435450 0.548444 -1.162 0.04 \$titanium cap welds
 831 RCC 0.622020 0.291852 -1.162 -0.152608 0.209884 0 0.02475
 \$Ag cylinder
 832 RCC 0.622167 0.291649 -1.162 -0.152902 0.210288 0 0.025
 \$AgI/AgBr cylinder
 833 RCC 0.655982 0.245143 -1.162 -0.220531 0.303300 0 0.034
 \$Air cylinder
 834 RCC 0.655982 0.245143 -1.162 -0.220531 0.303300 0 0.04
 \$Titanium capsule
 837 RCC 0.679534 0.212751 -1.162 -0.267637 0.368085 0 0.0401
 \$cylinder containing seed

841 TRC 0.622020 0.291852 -1.162 0.005822 -0.008007 0 0.02475
 0.01485 \$Ag bevel @ dis
 842 TRC 0.469412 0.501735 -1.162 -0.005822 0.008007 0 0.02475
 0.01485 \$Ag bevel @ prox
 843 TRC 0.622167 0.291649 -1.162 0.005881 -0.008088 0 0.025
 0.015 \$AgI bevel @ dis
 844 TRC 0.469265 0.501938 -1.162 -0.005881 0.008088 0 0.025
 0.015 \$AgI bevel @ prox
 c
 c Onco Seed 6711 surfaces #10
 c
 925 SPH 0.211302 0.667341 -1.162 0.04 \$titanium cap welds
 926 SPH -0.163302 0.680680 -1.162 0.04 \$titanium cap welds
 931 RCC 0.153612 0.669390 -1.162 -0.259224 0.009231 0 0.02475
 \$Ag cylinder
 932 RCC 0.153862 0.669381 -1.162 -0.259723 0.009248 0 0.025
 \$AgI/AgBr cylinder
 933 RCC 0.211302 0.667341 -1.162 -0.374604 0.013339 0 0.034
 \$Air cylinder
 934 RCC 0.211302 0.667341 -1.162 -0.374604 0.013339 0 0.04
 \$Titanium capsule
 937 RCC 0.251312 0.665921 -1.162 -0.454623 0.016188 0 0.0401
 \$cylinder containing seed
 941 TRC 0.153612 0.669390 -1.162 0.009890 -0.000351 0 0.02475
 0.01485 \$Ag bevel @ dis
 942 TRC -0.105612 0.678621 -1.162 -0.009890 0.000353 0 0.02475
 0.01485 \$Ag bevel @ prox
 943 TRC 0.153862 0.669381 -1.162 0.009990 -0.000355 0 0.025
 0.015 \$AgI bevel @ dis
 944 TRC -0.105862 0.678629 -1.162 -0.009990 0.000357 0 0.025
 0.015 \$AgI bevel @ prox
 c
 c Onco Seed 6711 surfaces #11
 c

1025 SPH -0.385893 0.584445 -1.162 0.04 \$titanium cap welds
 1026 SPH -0.632104 0.301552 -1.162 0.04 \$titanium cap welds
 1031 RCC -0.423810 0.540880 -1.162 -0.170379 -0.195762 0
 0.02475 \$Ag cylinder
 1032 RCC -0.423646 0.541069 -1.162 -0.170707 -0.196139 0 0.025
 \$AgI/AgBr cylinder
 1033 RCC -0.385893 0.584445 -1.162 -0.246211 -0.282893 0 0.034
 \$Air cylinder
 1034 RCC -0.385893 0.584445 -1.162 -0.246211 -0.282893 0 0.04
 \$Titanium capsule
 1037 RCC -0.359597 0.614657 -1.162 -0.298802 -0.343318 0 0.0401
 \$cylinder containing seed
 1041 TRC -0.423810 0.540880 -1.162 0.006500 0.007468 0
 0.02475 0.01485 \$Ag bevel @ dis
 1042 TRC -0.594188 0.345118 -1.162 -0.006500 -0.007468 0
 0.02475 0.01485 \$Ag bevel @ prox
 1043 TRC -0.423646 0.541069 -1.162 0.006566 0.007544 0 0.025
 0.015 \$AgI bevel @ dis
 1044 TRC -0.594353 0.344930 -1.162 -0.006566 -0.007544 0 0.025
 0.015 \$AgI bevel @ prox
 c
 c Onco Seed 6711 surfaces #12
 c
 1125 SPH -0.697858 0.054965 -1.162 0.04 \$titanium cap welds
 1126 SPH -0.626161 -0.312969 -1.162 0.04 \$titanium cap welds
 1131 RCC -0.686812 -0.001697 -1.162 0.049614 -0.254609 0
 0.02475 \$Ag cylinder
 1132 RCC -0.686860 -0.001451 -1.162 0.049710 -0.255099 0 0.025
 \$AgI/AgBr cylinder
 1133 RCC -0.697858 0.054965 -1.162 0.071697 -0.367934 0 0.034
 \$Air cylinder
 1134 RCC -0.697858 0.054965 -1.162 0.071697 -0.367934 0 0.04
 \$Titanium capsule

1137 RCC -0.705520 0.094261 -1.162 0.087012 -0.446528 0 0.0401
 \$cylinder containing seed
 1141 TRC -0.686812 -0.001697 -1.162 -0.001894 0.009713 0
 0.02475 0.01485 \$Ag bevel @ dis
 1142 TRC -0.637198 -0.256305 -1.162 0.001892 -0.009714 0
 0.02475 0.01485 \$Ag bevel @ prox
 1143 TRC -0.686860 -0.001451 -1.162 -0.001913 0.009812 0 0.025
 0.015 \$AgI bevel @ dis
 1144 TRC -0.637150 -0.256551 -1.162 0.001911 -0.009812 0 0.025
 0.015 \$AgI bevel @ prox
 c
 c Onco Seed 6711 surfaces #13
 c
 1225 SPH -0.482615 -0.507899 -1.162 0.04 \$titanium cap welds
 1226 SPH -0.151374 -0.684079 -1.162 0.04 \$titanium cap welds
 1231 RCC -0.431608 -0.535036 -1.162 0.229221 -0.121918 0
 0.02475 \$Ag cylinder
 1232 RCC -0.431828 -0.534918 -1.162 0.229663 -0.122153 0 0.025
 \$AgI/AgBr cylinder
 1233 RCC -0.482615 -0.507899 -1.162 0.331241 -0.176180 0 0.034
 \$Air cylinder
 1234 RCC -0.482615 -0.507899 -1.162 0.331241 -0.176180 0 0.04
 \$Titanium capsule
 1237 RCC -0.517987 -0.489079 -1.162 0.401991 -0.213811 0 0.0401
 \$cylinder containing seed
 1241 TRC -0.431608 -0.535036 -1.162 -0.008744 0.004652 0
 0.02475 0.01485 \$Ag bevel @ dis
 1242 TRC -0.202387 -0.656954 -1.162 0.008745 -0.004650 0
 0.02475 0.01485 \$Ag bevel @ prox
 1243 TRC -0.431828 -0.534918 -1.162 -0.008833 0.004699 0 0.025
 0.015 \$AgI bevel @ dis
 1244 TRC -0.202166 -0.657071 -1.162 0.008833 -0.004697 0 0.025
 0.015 \$AgI bevel @ prox
 c

c Onco Seed 6711 surfaces #14

c

1325 SPH 0.102822 -0.692162 -1.162 0.04 \$titanium cap welds

1326 SPH 0.445194 -0.539873 -1.162 0.04 \$titanium cap welds

1331 RCC 0.155545 -0.668700 -1.162 0.236918 0.105383 0

0.02475 \$Ag cylinder

1332 RCC 0.155316 -0.668802 -1.162 0.237375 0.105586 0 0.025

\$AgI/AgBr cylinder

1333 RCC 0.102822 -0.692162 -1.162 0.342373 0.152289 0 0.034

\$Air cylinder

1334 RCC 0.102822 -0.692162 -1.162 0.342373 0.152289 0 0.04

\$Titanium capsule

1337 RCC 0.066257 -0.708436 -1.162 0.415509 0.184820 0 0.0401

\$cylinder containing seed

1341 TRC 0.155545 -0.668700 -1.162 -0.009038 -0.004022 0

0.02475 0.01485 \$Ag bevel @ dis

1342 TRC 0.392463 -0.563317 -1.162 0.009039 0.004019 0

0.02475 0.01485 \$Ag bevel @ prox

1343 TRC 0.155316 -0.668802 -1.162 -0.009129 -0.004062 0 0.025

0.015 \$AgI bevel @ dis

1344 TRC 0.392691 -0.563216 -1.162 0.009131 0.004060 0 0.025

0.015 \$AgI bevel @ prox

c

c Onco Seed 6711 surfaces #15

c

1425 SPH 0.603357 -0.356179 -1.162 0.04 \$titanium cap welds

1426 SPH 0.700618 0.006185 -1.162 0.04 \$titanium cap welds

1431 RCC 0.618341 -0.300378 -1.162 0.067305 0.250758 0

0.02475 \$Ag cylinder

1432 RCC 0.617961 -0.300466 -1.162 0.067400 0.251113 0 0.025

\$AgI/AgBr cylinder

1433 RCC 0.603357 -0.356179 -1.162 0.097260 0.362364 0 0.034

\$Air cylinder

1434 RCC 0.603357 -0.356179 -1.162 0.097260 0.362364 0 0.04
 \$Titanium capsule
 1437 RCC 0.592965 -0.394876 -1.162 0.118034 0.439761 0 0.0401
 \$cylinder containing seed
 1441 TRC 0.618341 -0.300378 -1.162 -0.002569 -0.009566 0
 0.02475 0.01485\$Ag bevel @ dis
 1442 TRC 0.685646 -0.049619 -1.162 0.002567 0.009567 0
 0.02475 0.01485 \$Ag bevel @ prox
 1443 TRC 0.617961 -0.300466 -1.162 -0.002279 -0.009816 0 0.025
 0.015 \$AgI bevel @ dis
 1444 TRC 0.685361 -0.049352 -1.162 0.002943 0.009638 0 0.025
 0.015 \$AgI bevel @ prox
 c
 c Onco Seed 6711 surfaces #16
 c
 1525 SPH 0.868000 -0.187500 -1.03 0.04 \$titanium cap welds
 1526 SPH 0.868000 0.187500 -1.03 0.04 \$titanium cap welds
 1531 RCC 0.868000 -0.129750 -1.03 0 0.2595 0 0.02475 \$Ag
 cylinder
 1532 RCC 0.868000 -0.130000 -1.03 0 0.26 0 0.025 \$AgI/AgBr
 cylinder
 1533 RCC 0.868000 -0.187500 -1.03 0 0.375 0 0.034 \$Air
 cylinder
 1534 RCC 0.868000 -0.187500 -1.03 0 0.375 0 0.04 \$Titanium
 capsule
 1537 RCC 0.868000 -0.227550 -1.03 0 0.4551 0 0.0401 \$cylinder
 containing seed
 1541 TRC 0.868000 -0.129750 -1.03 0 -0.0099 0 0.02475 0.01485
 \$Ag bevel @ dis
 1542 TRC 0.868000 0.129750 -1.03 0 0.0099 0 0.02475 0.01485
 \$Ag bevel @ prox
 1543 TRC 0.868000 -0.130000 -1.03 0 -0.01 0 0.025 0.015 \$AgI
 bevel @ dis

1544 TRC 0.868000 0.130000 -1.03 0 0.01 0 0.025 0.015 \$AgI
 bevel @ prox
 c
 c Onco Seed 6711 surfaces #17
 c
 1625 SPH 0.785534 0.414350 -1.03 0.04 \$titanium cap welds
 1626 SPH 0.544463 0.701647 -1.03 0.04 \$titanium cap welds
 1631 RCC 0.748410 0.458594 -1.03 -0.166821 0.198810 0 0.02475
 \$Ag cylinder
 1632 RCC 0.748571 0.458403 -1.03 -0.167143 0.199193 0 0.025
 \$AgI/AgBr cylinder
 1633 RCC 0.785534 0.414350 -1.03 -0.241071 0.287298 0 0.034
 \$Air cylinder
 1634 RCC 0.785534 0.414350 -1.03 -0.241071 0.287298 0 0.04
 \$Titanium capsule
 1637 RCC 0.811279 0.383666 -1.03 -0.292563 0.348664 0 0.0401
 \$cylinder containing seed
 1641 TRC 0.748410 0.458594 -1.03 0.006364 -0.007585 0 0.02475
 0.01485 \$Ag bevel @ dis
 1642 TRC 0.581589 0.657404 -1.03 -0.006364 0.007585 0 0.02475
 0.01485 \$Ag bevel @ prox
 1643 TRC 0.748571 0.458403 -1.03 0.006428 -0.007661 0 0.025
 0.015 \$AgI bevel @ dis
 1644 TRC 0.581428 0.657596 -1.03 -0.006429 0.007661 0 0.025
 0.015 \$AgI bevel @ prox
 c
 c Onco Seed 6711 surfaces #18
 c
 1725 SPH 0.335690 0.822377 -1.03 0.04 \$titanium cap welds
 1726 SPH -0.033692 0.887613 -1.03 0.04 \$titanium cap welds
 1731 RCC 0.278806 0.832426 -1.03 -0.255613 0.045143 0 0.02475
 \$Ag cylinder
 1732 RCC 0.279052 0.832382 -1.03 -0.256105 0.045230 0 0.025
 \$AgI/AgBr cylinder

1733	RCC	0.335690	0.822377	-1.03	-0.369381	0.065236	0	0.034
\$Air cylinder								
1734	RCC	0.335690	0.822377	-1.03	-0.369381	0.065236	0	0.04
\$Titanium capsule								
1737	RCC	0.375139	0.815408	-1.03	-0.448280	0.079170	0	0.0401
\$cylinder containing seed								
1741	TRC	0.278806	0.832426	-1.03	0.009752	-0.001723	0	0.02475
0.01485 \$Ag bevel @ dis								
1742	TRC	0.023193	0.877569	-1.03	-0.009752	0.001722	0	0.02475
0.01485 \$Ag bevel @ prox								
1743	TRC	0.279052	0.832382	-1.03	0.009850	-0.001740	0	0.025
0.015 \$AgI bevel @ dis								
1744	TRC	0.022947	0.877613	-1.03	-0.009850	0.001739	0	0.025
0.015 \$AgI bevel @ prox								
c								
c Onco Seed 6711 surfaces #19								
c								
1825	SPH	-0.271778	0.844764	-1.03	0.04	\$titanium cap welds		
1826	SPH	-0.596236	0.657261	-1.03	0.04	\$titanium cap welds		
1831	RCC	-0.321742	0.815881	-1.03	-0.224523	-0.129751	0	0.02475
\$Ag cylinder								
1832	RCC	-0.321526	0.816006	-1.03	-0.224956	-0.130001	0	0.025
\$AgI/AgBr cylinder								
1833	RCC	-0.271778	0.844764	-1.03	-0.324458	-0.187503	0	0.034
\$Air cylinder								
1834	RCC	-0.271778	0.844764	-1.03	-0.324458	-0.187503	0	0.04
\$Titanium capsule								
1837	RCC	-0.237128	0.864795	-1.03	-0.393765	-0.227555	0	0.0401
\$cylinder containing seed								
1841	TRC	-0.321742	0.815881	-1.03	0.008565	0.004951	0	0.02475
0.01485 \$Ag bevel @ dis								
1842	TRC	-0.546265	0.686130	-1.03	-0.008566	-0.004949	0	0.02475
0.01485 \$Ag bevel @ prox								

1843 TRC -0.321526 0.816006 -1.03 0.008652 0.005001 0 0.025
 0.015 \$AgI bevel @ dis
 1844 TRC -0.546481 0.686005 -1.03 -0.008653 -0.004999 0 0.025
 0.015 \$AgI bevel @ prox
 c
 c Onco Seed 6711 surfaces #20
 c
 1925 SPH -0.750855 0.473058 -1.03 0.04 \$titanium cap welds
 1926 SPH -0.879169 0.120951 -1.03 0.04 \$titanium cap welds
 1931 RCC -0.770610 0.418831 -1.03 -0.088793 -0.243657 0 0.02475
 \$Ag cylinder
 1932 RCC -0.770524 0.419065 -1.03 -0.088964 -0.244126 0 0.025
 \$AgI/AgBr cylinder
 1933 RCC -0.750855 0.473058 -1.03 -0.128314 -0.352108 0 0.034
 \$Air cylinder
 1934 RCC -0.750855 0.473058 -1.03 -0.128314 -0.352108 0 0.04
 \$Titanium capsule
 1937 RCC -0.737156 0.510667 -1.03 -0.155723 -0.427321 0 0.0401
 \$cylinder containing seed
 1941 TRC -0.770610 0.418831 -1.03 0.003387 0.009296 0 0.02475
 0.01485 \$Ag bevel @ dis
 1942 TRC -0.859402 0.175174 -1.03 -0.003388 -0.009295 0 0.02475
 0.01485 \$Ag bevel @ prox
 1943 TRC -0.770524 0.419065 -1.03 0.003421 0.009390 0 0.025
 0.015 \$AgI bevel @ dis
 1944 TRC -0.859488 0.174939 -1.03 -0.003423 -0.009389 0 0.025
 0.015 \$AgI bevel @ prox
 c
 c Onco Seed 6711 surfaces #21
 c
 2025 SPH -0.879169 -0.120951 -1.03 0.04 \$titanium cap welds
 2026 SPH -0.750855 -0.473058 -1.03 0.04 \$titanium cap welds
 2031 RCC -0.859402 -0.175174 -1.03 0.088793 -0.243657 0 0.02475
 \$Ag cylinder

2032	RCC	-0.859488	-0.174939	-1.03	0.088964	-0.244126	0	0.025
\$AgI/AgBr cylinder								
2033	RCC	-0.879169	-0.120951	-1.03	0.128314	-0.352108	0	0.034
\$Air cylinder								
2034	RCC	-0.879169	-0.120951	-1.03	0.128314	-0.352108	0	0.04
\$Titanium capsule								
2037	RCC	-0.892879	-0.083346	-1.03	0.155723	-0.427321	0	0.0401
\$cylinder containing seed								
2041	TRC	-0.859402	-0.175174	-1.03	-0.003388	0.009295	0	0.02475
0.01485 \$Ag bevel @ dis								
2042	TRC	-0.770610	-0.418831	-1.03	0.003387	-0.009296	0	0.02475
0.01485 \$Ag bevel @ prox								
2043	TRC	-0.859488	-0.174939	-1.03	-0.003423	0.009389	0	0.025
0.015 \$AgI bevel @ dis								
2044	TRC	-0.770524	-0.419065	-1.03	0.003421	-0.009390	0	0.025
0.015 \$AgI bevel @ prox								
c								
c Onco Seed 6711 surfaces #22								
c								
2125	SPH	-0.596236	-0.657261	-1.03	0.04	\$titanium cap welds		
2126	SPH	-0.271778	-0.844764	-1.03	0.04	\$titanium cap welds		
2131	RCC	-0.546265	-0.686130	-1.03	0.224523	-0.129751	0	0.02475
\$Ag cylinder								
2132	RCC	-0.546481	-0.686005	-1.03	0.224956	-0.130001	0	0.025
\$AgI/AgBr cylinder								
2133	RCC	-0.596236	-0.657261	-1.03	0.324458	-0.187503	0	0.034
\$Air cylinder								
2134	RCC	-0.596236	-0.657261	-1.03	0.324458	-0.187503	0	0.04
\$Titanium capsule								
2137	RCC	-0.630893	-0.637240	-1.03	0.393765	-0.227555	0	0.0401
\$cylinder containing seed								
2141	TRC	-0.546265	-0.686130	-1.03	-0.008566	0.004949	0	0.02475
0.01485 \$Ag bevel @ dis								

2142 TRC -0.321742 -0.815881 -1.03 0.008565 -0.004951 0 0.02475
 0.01485 \$Ag bevel @ prox
 2143 TRC -0.546481 -0.686005 -1.03 -0.008653 0.004999 0 0.025
 0.015 \$AgI bevel @ dis
 2144 TRC -0.321526 -0.816006 -1.03 0.008652 -0.005001 0 0.025
 0.015 \$AgI bevel @ prox
 c
 c Onco Seed 6711 surfaces #23
 c
 2225 SPH -0.033692 -0.887613 -1.03 0.04 \$titanium cap welds
 2226 SPH 0.335690 -0.822377 -1.03 0.04 \$titanium cap welds
 2231 RCC 0.023193 -0.877569 -1.03 0.255613 0.045143 0
 0.02475 \$Ag cylinder
 2232 RCC 0.022947 -0.877613 -1.03 0.256105 0.045230 0 0.025
 \$AgI/AgBr cylinder
 2233 RCC -0.033692 -0.887613 -1.03 0.369381 0.065236 0 0.034
 \$Air cylinder
 2234 RCC -0.033692 -0.887613 -1.03 0.369381 0.065236 0 0.04
 \$Titanium capsule
 2237 RCC -0.073141 -0.894578 -1.03 0.448280 0.079170 0 0.0401
 \$cylinder containing seed
 2241 TRC 0.023193 -0.877569 -1.03 -0.009752 -0.001722 0
 0.02475 0.01485 \$Ag bevel @ dis
 2242 TRC 0.278806 -0.832426 -1.03 0.009752 0.001723 0
 0.02475 0.01485 \$Ag bevel @ prox
 2243 TRC 0.022947 -0.877613 -1.03 -0.009850 -0.001739 0 0.025
 0.015 \$AgI bevel @ dis
 2244 TRC 0.279052 -0.832382 -1.03 0.009850 0.001740 0 0.025
 0.015 \$AgI bevel @ prox
 c
 c Onco Seed 6711 surfaces #24
 c
 2325 SPH 0.544463 -0.701647 -1.03 0.04 \$titanium cap welds
 2326 SPH 0.785534 -0.414350 -1.03 0.04 \$titanium cap welds

2331 RCC 0.581589 -0.657404 -1.03 0.166821 0.198810 0 0.02475
 \$Ag cylinder
 2332 RCC 0.581428 -0.657596 -1.03 0.167143 0.199193 0 0.025
 \$AgI/AgBr cylinder
 2333 RCC 0.544463 -0.701647 -1.03 0.241071 0.287298 0 0.034
 \$Air cylinder
 2334 RCC 0.544463 -0.701647 -1.03 0.241071 0.287298 0 0.04
 \$Titanium capsule
 2337 RCC 0.518716 -0.732330 -1.03 0.292563 0.348664 0 0.0401
 \$cylinder containing seed
 2341 TRC 0.581589 -0.657404 -1.03 -0.006364 -0.007585 0 0.02475
 0.01485 \$Ag bevel @ dis
 2342 TRC 0.748410 -0.458594 -1.03 0.006364 0.007585 0 0.02475
 0.01485 \$Ag bevel @ prox
 2343 TRC 0.581428 -0.657596 -1.03 -0.006429 -0.007661 0 0.025
 0.015 \$AgI bevel @ dis
 2344 TRC 0.748571 -0.458403 -1.03 0.006428 0.007661 0 0.025
 0.015 \$AgI bevel @ prox

c Data Cards

c

c

Mode P \$E

cut:p j 0.0010

imp:p 1 126r 0

c imp:e 1 126r 0

c water for phantom head

m1 8000.04p -0.888099

1000.04p -0.111901 \$Water weight fractions

c silastic insert

m2 1000.04p -0.06 \$MAT

6000.04p -0.25 8000.04p -0.29 14000.04p

-0.39995

78000.04p -5e-005

c COM plaque cover

m3 79000.04p -0.77 \$MAT
 47000.04p -0.14 29000.04p -0.08 46000.04p
 -0.01

c silver wire

m5 47000.04p -1 \$MAT

c radioactive coating on wire

m6 47000.04p -0.54 \$MAT
 35000.04p -0.28 53000.04p -0.18

c titanium capsule and end welds

m7 22000.04p -1 \$MAT

c NIST Air, Dry (near sea level)

m8 6000.04p -0.00012425 \$MAT
 7000.04p -0.7552673 8000.04p -0.2317812 18000.04p
 -0.01282725

c Homogenized eye (Thomaon, 2008 MP.35)

m9 1000.04p -0.107 \$MAT
 6000.04p -0.038 7000.04p -0.012 8000.04p
 -0.843

c Skull bone (Thomaon, 2008 MP.35)

m10 1000.04p -0.05 \$MAT
 6000.04p -0.212 7000.04p -0.04 8000.04p
 -0.435
 11000.04p -0.001 12000.04p -0.002 15000.04p
 -0.081
 16000.04p -0.003 20000.04p -0.176

VOL 4J 0.0000119 8J 0.0000119 4J 0.0000119 4J 0.0000119 4J

0.0000119 4J &

0.0000119 4J 0.0000119 4J 0.0000119 4J 0.0000119 4J 0.0000119

4J &

0.0000119 4J 0.0000119 4J 0.0000119 4J 0.0000119 4J 0.0000119

4J &

0.0000119 4J 0.0000119 4J 0.0000119 4J 0.0000119 4J 0.0000119

4J &

```

0.0000119 4J 0.0000119 4J 0.0000119 4J 0.0000119 4J
E0 0 1e-5 0.51 1.024
sdef erg=d1 pos=-0.13 0 -1.34 rad=d2 &
    axs=0.13 0 0 ext=d3 par=2 eff=0.01
#  si1      spl
    L      d
0.0268746  3.16341E-05
0.0041731  0.000418578
0.004829   0.00107944
0.003606   0.00114638
0.0312373  0.00144465
0.0033354  0.00176708
0.004829   0.00184814
0.0045722  0.00454971
0.00406949 0.0049638
0.0037589  0.00614614
0.0041205  0.0081776
0.00430159 0.00993986
0.00402949 0.0358245
0.0317101  0.0429691
0.0037693  0.0552214
0.0354919  0.0666816
0.0309441  0.0720103
0.0309951  0.14002
0.0272018  0.397834
0.0274724  0.740847
si2 0.02476 0.02499
si3 L 0 0.25998
c Rectangular mesh tally:
c cora: describes the planes perpendicular to x axis
c corb: describes the planes perpendicular to y axis
c corc: describes the planes perpendicular to z axis
c "i" data input notation even divides dif. by n
tmesh

```

```
Rmesh3 total  
cora3 -1.3 26i 1.4  
corb3 -1.3 25i 1.3  
corc3 -1.3 25i 1.3  
endmd  
nps 100000000  
dbcn 12j 703687  
prdmp 1000000 1000000 2 2 1000000
```